NASA CR144906

A LANDMARK RECOGNITION AND TRACKING EXPERIMENT FOR FLIGHT ON THE SHUTTLE/ADVANCED TECHNOLOGY LABORATORY (ATL)

FINAL REPORT

By J. D. Welch

Prepared under Contract No. NAS1-12550
General Electric/Space Division
Valley Forge, Pa.

for

NATIONAL AERONAUTICS AND SPACE ADMINISTRATION

NASA CR144906

A LANDMARK RECOGNITION AND TRACKING EXPERIMENT FOR FLIGHT ON THE SHUTTLE/ADVANCED TECHNOLOGY LABORATORY (ATL)

FINAL REPORT

By J. D. Welch

Prepared under Contract No. NAS1-12550
General Electric/Space Division
Valley Forge, Pa.

for

NATIONAL AERONAUTICS AND SPACE ADMINISTRATION

1. Report No.	2. Government Accession No.	3. Recipient's Catalog No.
NASA CR-144906		

4. Title and Subtitle	5. Report Date
A Landmark Recognition and Tracking Experiment for Flight on the Shuttle/Advanced Technology Laboratory (ATL)	December 9, 1975
	6. Performing Organization Code: IJLO
7. Author(s): J. D. Welch	8. Performing Organization Report No.
	10. Work Unit No.
9. Performing Organization Name and Address: General Electric Company, Space Systems/Valley Forge Space Center, P. O. Box 8555, Philadelphia, PA 19101	11. Contract or Grant No.: NAS1-12550
	13. Type of Report and Period Covered: Contractor Report - Final Report
12. Sponsoring Agency Name and Address: National Aeronautics and Space Administration, Washington, DC 20546	14. Sponsoring Agency Code

15. Supplementary Notes

16. Abstract

The preliminary design of an experiment for landmark recognition and tracking from the Shuttle/Advanced Technology Laboratory is described. It makes use of parallel coherent optical processing to perform correlation tests between landmarks observed passively with a telescope and previously made "holographic" matched filters. The experimental equipment including the optics, the low power laser, the random access file of matched filters and the electro-optical readout device are described. A real time optically excited liquid crystal device is recommended for performing the input non-coherent optical to coherent optical interface function.

A development program leading to a flight experiment in 1981 is outlined.

17. Key Words (Suggested by Author(s))	18. Distribution Statement
Landmark Tracking, Coherent Optical Correlation, (ATL) Flight Experiment	Unclassified - Unlimited

19. Security Classif. (of this report)	20. Security Classif. (of this page)	21. No. of Pages	22. Price*
Unclassified	Unclassified		

*For sale by the National Technical Information Service, Springfield, Virginia 22161

ACKNOWLEDGEMENT

The helpful suggestions of NASA LaRC people, especially W. E. Sivertson, R.G. Wilson and A. Hamer, are gratefully acknowledged.

TABLE OF CONTENTS

TABLE OF CONTENTS (Continued)

PREFACE

This report summarizes a preliminary design of an experimental plan for landmark recognition and tracking from the Advanced Technology Laboratory (ATL). The primary experimental approach is that of near-real-time pattern recognition by means of coherent optical techniques. An experiment development plan is outlined leading to a flight test in 1981. Although the experiment is designed for ATL flight, the design is appropriate for accommodation on a variety of STS payloads.

1.0 INTRODUCTION AND SUMMARY

This report addresses the preliminary design of an experiment to demonstrate and test a technique for automatically recognizing and tracking known Earth landmarks. This experiment is designed for Shuttle flight on board the Advanced Technology Laboratory (Ref.7). The utility of such an experiment can be of key significance for performing these functions for future space applications:

- Providing key fix data for an autonomous navigation system.
- Providing precision data for vehicle attitude determination and/or pointing control systems toward earth surface references.
- Providing "real time" interpretation of Ground Control Point (GCP) data for use with an Earth resources mission.

Potential benefits are to reduce requirements for ground-based processing of data, to simplify attitude determination techniques, to reduce dependence on Earth-based tracking stations, and to aid earth-resources studies, e.g., by classifying land areas by their spatial-frequency content.

Coherent optical data processing with matched spatial frequency filters is the basis of the proposed method for recognizing and tracking landmarks. The matched filters are pre-made transparencies on which the images of the selected landmarks are stored in the Fourier Transform (spatial frequency) domain. The filters will be selected in an earth-based laboratory prior to the flight experiment. Previous research efforts sponsored by the General Electric (GE) Company, as well as those through NASA/GE contracts, provide optimism for favoring this approach (See Appendix A and References 1 to 6 for a more complete discussion) to landmark tracking and its applicability to autonomous navigation. These analytic and experimental efforts have demonstrated the capability to uniquely recognize and track a variety of landmarks under a wide range of viewing conditions including some cases where more than 90% of the landmark was obscurred by simulated clouds. Other simulated experiments have shown that landmarks can be recognized and tracked when viewed at aspect (obliquity) angles which are angularly displaced by as much as 30 degrees from the direction from which the image was observed in making the matched filter. Simulated experiments have also shown that there is a wide tolerance for illumination conditions and that, for landmark areas having high contrast features, a matched filter can provide adequate correlation for input images obtained over a wide range of conditions from morning to evening.

The key components of the experimental package are a telescope, an optical-to-optical interface device, a low-power laser, the passive optical elements of the coherent optical processor, the file of matched spatial frequency filters and an electro-optical readout device. These are shown in the plan view of the experiment package of Figure 1-1. Key components and their characteristics are outlined in Table 1-1. The telescope transfers a focused candidate image to the interior of the ATL where all of the other experimental equipment will be located. The proposed arrangement permits the optimum participation by the crew in the experimental program. The candidate image is focused on the "real time" optical-to-optical interface device where it serves as an input image for the coherent optical process of matched filtering. Recent developments and evaluation of near real time optical-to-optical interface devices, especially a field effect liquid crystal device, provide encouragement in providing this single most critical component of the experiment. The passive optical elements provide Fourier transformations of the images. The electro-optical readout device provides a two-axes readout of the location of the correlation "spot".

The remainder of this report describes in more detail the design of the experimental program. Section 19 describes a plan leading to the flight experiment in 1981.

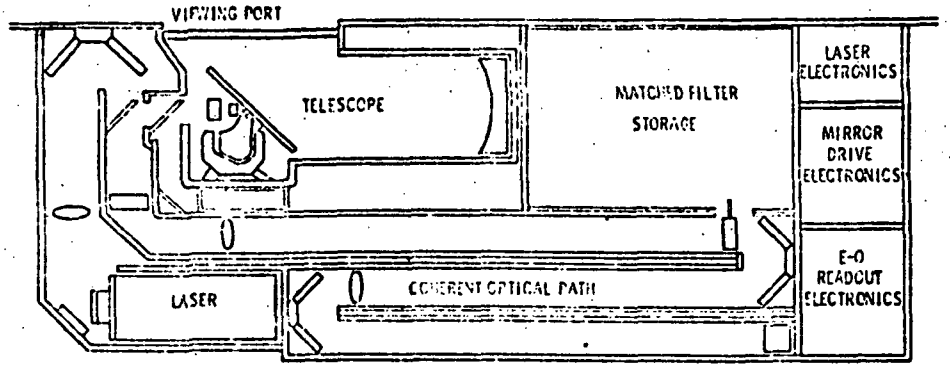

Figure 1-1. A Plan View of Experiment Package

Table 1-1. Key Components and Their Specifications for Flight Model

COMPONENT AND FUNCTION	KEY SPECIFICATION
• Tracking Mirror	• Diameter: 22 cm. • Flatness: 0.1 micrometer • Reflectivity (min): 95%
• Mirror Mount and Servo Drive	• Mounted with two gimbal axes • Gimbal freedom: Outer (Azimuth) Inner (Elevation) • Gimbal angular rates (min): 30°/sec • Gimbal angular acceleration (min): $100^{\circ}/sec^{2}$ • Angular Positioning Accuracy: 0.1° • Angular Readout: By 19 bit Optical Encoders in each axis.
• Telescope	• Focal Length: 44 cm. • Clear Aperture: 11 cm. • Relative Aperture: f/4 • Distortion (max. at edge of field): 1%
• Optical-to-Optical Interface Module	• Standardized Dimensions so as to accept any of these alternative near real time optical-to-optical interface devices: optically excited liquid crystal cell, Pockels cell devices, rapid process silver halide. • Module dimensions: 8 cm x 8 cm x 3 cm.
• TV Monitoring Cameras (2)	• Based on application of CID (Charge Injection Device) solid state detector array. • Elements in Array: 500 x 500 • Array Area: 18 mm x 24 mm
• Fourier Transform Optics	• Relative Aperture: f/20 • Focal Length: 800 mm • Effective Aperture: 40 mm
• Spatial Frequency Matched Filters, Storage and Retrieval Device	• 512 pre-made filters in 35 mm slide format • Stored in modified "Mast" random access slide device • Automatic or manual access to slides • Maximum time for any slide access - 5 sec. • Indexing precision (2 dimension): 12 micrometers
• Laser	• Type: CW HeNe • Power required: 0.1 m watt (min.) • A specific candidate: Hughes 3078H
• Electro-Optical Readout	• Solid state Detector array based on CID (Charge Injection Device) • Elements in Array: 1,000 x 1,000 • Array area: 36 mm x 48 mm

2.0 SUMMARY OF TECHNICAL OBJECTIVES

The primary objective of the planned experiment is to determine the feasibility of recognizing and obtaining vector direction from the spacecraft to preselected landmark areas by means of coherent optical matched spatial frequency filters. More specific objectives are:

a. To establish the feasibility of using pre-made matched spatial frequency filters for automatically recognizing and obtaining the vector direction to pre-selected landmark areas and for rejecting non-selected landmarks.

b. To achieve objective a for a wide range of landmark area types ranging from those with inherently high contrast characteristics, such as land-water boundaries, to those with much less well defined spatial features, such as desert areas.

c. To perform the recognition and tracking functions listed under objective b for selected landmarks over a wide range of angular viewing conditions relative to those for which the matched filter was made.

d. To perform recognition and tracking functions listed under objectives b and c for a range of illumination, obscuration and atmospheric conditions in order to determine the associated limits. (The evaluation of these effects will necessitate successive over-flights near the same landmark areas during different orbits.)

e. To evaluate the effectiveness of man's role in the coherent optical recognition and tracking operations.

f. To evaluate the feasibility of achieving fully automated coherent optical processing functions on-board a satellite. Although it is planned to make use of man's capability on board the ATL, the results of the experiments are expected to be meaningful in terms of feasibility evaluation of either a manually directed operational system or a fully automated system.

g. To evaluate the feasibility and techniques for fabricating matched spatial frequency filters on board a satellite.

h. To further evaluate the relative merits of several promising non-coherent to coherent optical conversion devices.

i. To evaluate the operation in space of all of the other key components of the system, including the electro-optical readout device, the matched filter storage and retrieval device, the laser and all of the passive optical elements of the system.

Although some of the objectives may be partially attained by experiments in a laboratory, with a physical simulator, or in an aircraft flight test, the full attainment of all these objectives can be achieved only in an orbital flight test. As the development of the experiment progresses, the specific experiments to achieve the above objectives will be scheduled for one or more specific ATL flights.

3.0 PERFORMANCE GOALS AND SYSTEMS ANALYSIS

3.1 Tracking Performance Goals

In order to be attractive for autonomous navigation and other applications automatic landmark tracking should provide constraints (or "fixes") which are considerably more accurate than those of other alternative on-board sensors, such as horizon trackers. Autonomous systems depending on landmark tracking should have performance which also compares favorably with that of non-autonomous systems.

State-of-the-art horizon sensors have predicted tracking accuracies ranging from 0.02° to 0.1°. Since positional constraints with them are obtained relative to the distance to earth center as base reference, these tracking accuracies correspond to primary[1] satellite position errors of 2 to 10 km for relatively low altitude orbits. In order for landmark tracking to be attractive it should provide primary constraints which are significantly better than those associated with horizon sensing, say by a factor of 10 or more. Non-autonomous radio tracking techniques can provide primary constraints which are typically in the 50 to 200 meter range. Therefore, a logical performance goal for the method under consideration would be one providing primary positional constraints having an uncertainty[2], due to the landmark tracking operation, of 100 meters (3 sigma). If we choose a 370 km circular orbit for performance evaluation purposes (Reference 7), this uncertainity corresponds to an angular tracking accuracy of 60 arc seconds (3 sigma), which will be established as an experiment performance goal. With regard to this goal, two points should be emphasized:

- This goal is not expected to represent an ultimate performance limit, which could be an order of magnitude less than 60 arc seconds. The 60 arc second goal, however, is a realistic objective for the initial orbital experiments.
- This goal is established for relatively well defined landmarks when tracked near the nadir (i.e., tracking angles no more than about 8°), from the nadir direction. However, tracking experiments at angles greater than 8° will be performed. Tracking at angles larger than 8° from nadir may result in errors greater than 60 arc seconds.

3.2 Field of View and Image Format Size

The upper limit on the field of view of the telescope is determined primarily by consideration of desired tracking accuracy. The lower limit is determined by the planned size of the landmarks and considerations of acquisition of the landmarks, as well as by consideration of telescope design. Previous analysis and experiments (Reference 8) indicate that tracking accuracies of 10^{-3} of the field of view is a realistic goal, and the error analysis of Section 10 substantiates this goal. For the selected 60 arc second accuracy goal this suggests an upper acceptable limit of 16° for the field of view. Setting a lower limit on the field of view requires certain considerations of landmark acquisition. We anticipate that the landmark tracking operation will be a precision, or "vernier", mode of operation, with less precise navigation determination as a starting point. If we assume that the navigation system is based on a horizon tracker, for example, an initial uncertainty in cross-track and in-track position of 20 km is realistic. In order to accommodate for this acquisition problem at the minimum altitude of 370 km, we require a total field of view of not less than 7°. With indicated needs for maximum and minimum fields of view of 16° and 7°, respectively, we select a field of view of 10° as sufficient. However this value should be regarded as subject to possible revision during the course of the development program.

The selection of the image format size is based on the resolution of the optical-to-optical interface device. The advanced optical-to-optical interface devices will typically have usable resolutions ranging between 25 and 50 lp/mm. In order to be consistent with the desired readout accuracies, the optical-to-optical interface device should be capable of recording over 1,000 total line pairs. A conservative appraisal suggests a minimum size of 50 mm x 50 mm for the optical-to-optical interface device.

(1) i.e., as obtained by sensor and not influenced by any short-period or long-period computational smoothing.

(2) i.e., in conical locus.

3.3 Systems Analysis

The following systems analysis is concerned primarily with the collection of energy at the front end, shutter speed, optical field of view and image motion. The analysis is intended as a basis for a preliminary design and preliminary sizing of the input optical system.

For extended objects, such as landmarks, the useful optical energy arriving at the image plane will be a function of input spectral radiance levels, f-number and transmissivity of the optics and spectral response of the optical-to-optical interface device. The input radiance will be a function of the spectral reflectances of the various materials of the landmark, the atmospheric viewing conditions and the illumination level. Illumination level will be primarily a function of solar elevation, which in turn is a function of season, latitude and local time of day.

Consider first the spectral response./ The spectral response of the detector (i.e., the optical-to-optical interface device) should be such as to be responsive to the reflectance contrasts needed to identify the landmark areas without excessive interference from adverse atmospheric effects. Atmospheric effects of concern are scattering and attenuation. Scattering can be classified into three general types depending on the size of the scattering particles relative to the wavelength.*

Rayleigh scattering which results from particles much smaller than the wavelength of light is proportional to the inverse fourth power of the wavelength. Blue light at 0.45 micrometers, for example, is scattered six times as much as red light at 0.7 micrometers. The effect of Rayleigh scattering of blue light is evident to even the casual observer of the sky. Because of Rayleigh scattering an optical-to-optical interface device which is sensitive primarily to blue light could be at a severe disadvantage.**

Mie scattering results from particles closer in size to the wavelength. It is also more severe at the blue end of the spectrum but its reduction at the red end is less than that of Rayleigh scattering. Non-selective scattering results from still larger particles which may result from specific local atmospheric problems such as smoke haze and dust.

Atmospheric absorption occurs over a broad range of visible wavelengths. It becomes greater for wavelengths less than 0.5 micrometers such that the atmosphere becomes nearly opaque for wavelengths less than about 0.3 micrometers. This provides another case against use of optical-to-optical interface devices which are responsive primarily in the blue region.

Scattering in the atmosphere combines with absorption to result in reduced contrast ratios. These in turn reduce the high spatial frequency content need for recognition by the coherent optical system.

Spectral response of the optical-to-optical interface device is also of concern because of the spectral reflectivity of the various materials which consititute a landmark scene. Reference 9 provides summary reflectivity data for a variety of Earth surface materials. Most vigorous plant life has a reflectance which is influenced by its chlorophyll content. Chlorophyll has strong absorption at about 0.67 micrometers and plants generally have increased reflectance on either side of this wavelength. There is a definite tendency toward reduction of response below about 0.5 micrometers and a very strong reflectance above about 0.7 micrometers. Like many materials there is a strong reflectance in the near IR range from 0.8 to 1.3 micrometers.

---

*N. Jensen. "Optical and Photographic Reconnaissance Systems", John Wiley, New York, 1968.

**As discussed in Section 5, this appears to be the case of the PROM optical-to-optical interface device which, in many other respects, has good characteristics for optical data processing.

Brown earth and certain types of rocks typically have a peak response in the neighborhood of 0.75 micrometers with a sharp drop-off below 0.5 micrometers and above 0.8 micrometers.

A review of atmospheric effects as well as of reflectance of many common Earth surface materials leads to the conclusion that a broad response in the visible spectrum is needed of the optical-to-optical to optical interface device. Good response somewhere in the 0.5 to 0.8 micrometer band is important. If possible, some extension into the near IR regime would also be desirable.

Consider next the levels of optical power and energy. Reference 9 provides some useful data on typical input radiance levels, providing a meaningful range of input radiance levels to be anticipated. The data of this reference considers a wide range of earth surface materials and a wide range of solar illumination zenith angles ranging from the extremes of 1^{o} to 49^{o}. Thus it is a good basis for estimating viewing conditions for a wide range of landmark tracking experiments. Consider first the lowest anticipated levels of radiances. Typically the lowest reflectance is that corresponding to deep water viewed at low solar elevation angles, 1 to 2 mwatts cm^{-2} $steradian^{-1}$ per/micrometer spectral bandwidth in the visible spectral bands of interest.

The highest radiance levels to be expected will be from dry sand, snow, and clouds when illuminated at high solar elevation angles. These maximum radiances will be 40 to 50 mwatt cm^{-2} $steradian^{-1}$ per micrometer. Since some high radiance saturation as well as some low-radiance insensitivity can be allowed without degrading landmark recognition, a system design based on a total minimum to maximum range of radiance from 3 to 40 mwatts cm^{-2} $steradian^{-1}$ per micrometer of spectral bandwidth is justified. This then is selected as a design specification.

The useful spectral bandwidth is a function of the response characteristics of the optical-to-optical interface device, as well as of the spectral transmissivity of the optics. The case of the specific example of the spectral response of an optically excited liquid crystal will be considered in Section 5.3.2. However for our present illustrative purposes consider now a case of a sensor with a 0.1 micrometer useful spectral bandwidth. This would lead to a useful range of radiance levels from 0.3 to 4 mwatts cm^{-2} $steradian^{-1}$. From this we can use the well known equation (Reference 9) to determine the on axis irradiance at the focal plane (i.e., the illumination of the optical-to-optical interface device). This equation is:

$$H_f = \frac{W\eta}{4f^2} = \frac{W\eta}{4\,(F/D)^2} = \frac{\pi N\eta}{4\,(F/D)^2}$$

where:

H_f = Image (focal) plane irradiance, $\frac{w}{cm^2}$

W = Object radiant emittance, $\frac{w}{cm^2}$

f = Focal ratio of optics = $\frac{\text{focal length}}{\text{clear aperture diameter}}$

η = Optics transmittance/efficiency

N = Scene radiance, $\frac{w}{cm^2 ster}$

The off axis focal plane irradiance (or illumination) for an optical system is obtained by multiplying by the $\cos^4\theta$, (i.e., the $(\text{cosine})^4$ of the halffield of view). For the present experiment a 10^{o} field of view is planned.

However since $\cos^4 (\frac{10^o}{2}) = 0.985$ this represents a negligible correction. This is a somewhat idealized value and in practice irradiance can be somewhat different because of vignetting effects with other than perfect optics.

For this example and based on the above equation, Table 3-1 shows the anticipated range of optical power densities at the focal plane of the telescope as a function of f number, i.e., typical optical power densities to which the optical-to-optical interface device must respond. A typical optical transmittance of 0.8 is assumed.

The relative aperture specification will be determined by the maximum allowable exposure time, which in turn is determined largely by the desired system tracking performance and considerations of image motion.

Table 3-1. An Example of Minimum and Maximum Levels of Optical Power Densities Expected at Telescope Focal Plane as Function of Relative Aperture

(assumes sensitive spectral bandwidth of 0.1 micrometers)

f/Number	Minimum Optical Power Density (microwatts/cm^2)	Maximum Optical Power Density (microwatts/cm^2)
f/1.4	100	1300
f/2	50	650
f/2.8	25	325
*f/4	12	160
f/5.6	6	80
f/8	3	40
f/11	1.5	20
f/16	0.75	10
f/22	0.4	5

*Tentatively favored design.

To a first-order approximation, the primary effect of image motion is that of reducing the spatial frequency bandwidth of the optical system (i.e., reducing the modulation transfer response at high frequencies). The primary causes of image motion are: orbital motion, vehicle-attitude motion, and vehicle-induced vibrations. For the present application, the dominant image motion will be the residual motion resulting from errors in compensation for orbital and vehicle attitude motion. Orbital motion will cause a ground track velocity of approximately 8,000 m/sec. For a 370-km-altitude orbit (as favored for ATL, Reference 7) this image motion can be compensated by a continuous pitch rate of the ATL of 0.06 deg/sec. This is the nominal pitch rate required to maintain orientation of the vehicle to the vertical. We can conservatively estimate that the required nominal pitch rate can be held to within 3% of nominal. Programming the tracking mirror can further reduce this tracking error rate by an estimated factor of 3 or a total of 1% of the nominal rate. Hence, the uncompensated residual motion can correspond to a ground track of 80 m/sec. Recall that the tracking accuracy goal, in terms of ground dimensions is 100 m. Total smear due to image motion should be much less than this dimension, say 8m as a conservative estimate, in order that image motion will not be a primary limiting factor in determing tracking accuracy. Therefore, a maximum allowable exposure time should be specified as 0.1 seconds. Image formation time of the optical-to-optical interface device (i.e., to reach e of final contrast) should not exceed 50% of exposure time or 50m sec. For the example discussed with a 0.1 micrometer bandwidth sensor the typical minimum and maximum optical energy densities at the telescope image plane corresponding to this exposure time are listed in Table 3-2.

Table 3-2. An Example of Minimum and Maximum Levels of Optical Energy Densities Expected at Telescope Focal Plane as Functions of Relative Aperture for a Spectral Band pass of 0.1 micrometers and an Exposure of 0.1 Seconds

f/Number	Minimum Optical Energy Density (microjoules/cm^2)	Maximum Optical Energy Density (microjoules/cm^2)
f/1.4	10	130
f/2	5	65
f/2.8	2.5	32.5
*f/4	1.2	16
f/5.6	0.6	8
f/8	0.3	4
f/11	0.15	2
f/16	0.07	1
f/22	0.04	0.5

*Tentatively favored design.

Since we plan to perform experiments with some of the more advanced optical-to-optical interface devices as well as some with the more sensitive silver halide media we recommended that the system be designed to be responsive to energy density levels about as low as 1.2 microjoules/cm^2. As discussed above this presumes a spectral bandwidth of 0.1 micrometers. For an optical-to-optical interface device with a narrower spectral response an even higher sensitivity is needed. As discussed in Section 5.3 this is the case for an available optically excited liquid crystal device. An inspection of Table 3-2 indicates that an optical system with a minimum relative aperture of f/4 will be required for the example shown. The above analysis is applied to a specific optical-to-optical interface device in Section 5.3.

3.4 Summary of Optical Characteristics of the Input Telescope

The rationale of the foregoing discussion suggests the following characteristics of the input optical system:

Field of view	10 degrees
f/number of primary	f/4
Clear aperture of primary	11 cm
Focal length	44 cm
Image format size	50 mm x 50 mm

4.0 DEFINITION OF OPERATIONAL MODES AND PROCEDURES

4.1 Set Up

The initial procedure following orbit insertion, is the deployment of the experimental equipment by the crew. As presently conceived, this will primarily involve the removal of physical constraints to key parts of the hardware such as the 2-axis tracking mirror and the spatial frequency filter storage and retrieval device. It is anticipated that such constraints will be employed to enable these components to survive the launch environment of 3 g's. It is estimated that this set-up task will take 0.5 hr by 1 crew member.

4.2 Calibration

For on board calibration of experiment-related equipment, it is anticipated that some test input images and some test matched spatial frequency filters will be carried on board the vehicle. Five test input images and 10 test matched filters should be sufficient. These test inputs will be in the form of silver halide slides mounted in precision steel frames in much the same format as the matched spatial frequency filters which are pre-made for the operational recognition and tracking experiments. During the calibration phase these input and matched filter slides will be inserted manually into the experimental system to check out its operation and performance. Presumably, the experimental system will be checked out and calibrated on board the vehicle prior to launch. Therefore these check out and calibration functions in orbit are intended to insure that the system will not have suffered any degradation of performance or calibration during launch or experiment deployment. Parameters to be verified, and possibly readjusted, include:

- Focus of the input image
- Focus of the spatial frequency filter
- Two axis position registration of the input image
- Two axis position registration of the matched spatial frequency filter
- Two axis position calibration of the correlation "spot" electro-optical "read out" device

A keyboard-operated command/control/display console will be provided on board, and the crew will be able to insert tracking mirror position and rate commands (digital) to verify the initial calibration and alignment of the mirror. These commands can be compared with the response of the mirror as directly measured at the mirror or as displayed on the console upon request by the crew. The initial calibration procedure should take one to two hours for one crew member. The calibration should be rechecked once each day that the landmark tracking is to be performed, and should require about 0.5 hour by one crew member.

Although it is not expected to be chargeable to the landmark tracking experiment, the alignment of the inertial reference unit is of key importance to the autonomous navigation experiment. Likewise precise update of the vehicle ephemeris is also required for the experiment. These requirements are further discussed in Section 4.3.

4.3 Recognition and Tracking

Most of the experimental data will be obtained during the operational mode of recognition and tracking. Most of the recognition and tracking operations can be programmed either manually by the crew or automatically via a sequence of programmed operations stored either in the crew's written experiment procedures task list or in didital form in the command, control and display module. The crew will be able to directly perform most of the required experiment functions, including repositioning the tracking mirror with the aid of manually controlled servo drives, selection and insertion of the matched spatial frequency filter, controlling the exposure of the optical-to-optical interface device, and operating the electro-optical read-out device. These manual operations could be assisted by an automated exposure control of the input optical system as well as by a rate drive of the tracker mirror system to compensate for orbital motion. Likewise the crew will be able to delete the tracking of certain landmarks if the visibility conditions warrant. Likewise, the crew will be able to introduce new landmarks into the experimental sequence.

For the automatic sequence, the position and rate of the 2-axis tracking mirror will be programmed to track a sequence of pre-selected landmarks. One could also automate the operation of the input optical-to-optical imaging device in order to briefly record each of the candidate images. Further automation can provide enabling signals for the coherent optical processor to proceed with each of the steps of the coherent correlation operation up to and including the electro-optical two-axis readout of the correlation spot.

Automation of these operations can be based on a timed sequence of stored commands obtained from the command storage. It is evident that a time calibration relative to the vehicle ephemeris and also relative to the vehicle attitude must be very carefully initiated and controlled. Any deviations from the nominal ephemeris or attitude program must be carefully determined so that appropriate command corrections to the sequence can be made by the crew.

The commands to the tracking mirror will be made relative to an inertial reference unit, i.e., the commands which are transmitted to the tracking mirror servos will be a function of gimbal axes as transformed from direction to each landmarks; the directions to landmark in turn,are transformed from geocentric coordinates to inertial coordinates for the nominal vehicle ephemeris. The inertial reference system must be maintained in adequate alignment and the vehicle ephemeris must be near the nominal planned ephermis. Hence continual calibration of the inertial reference and updating of the current vehicle ephemeris are important. The frequency of required re-calibration will be a function of the drifts of the gyros being used.

It is anticipated that most of the data obtained during the operational phase will be recorded automatically in digital form, including the time-indexed data on orientation of tracking mirror during input-image exposure, serial identification of landmarks and matched filters, and two-axis location of the correlation "spots". The crew should maintain cryptic notes descriptive of any deviation from the norm in terms of performance or scheduling, to supplement the automated data-taking process. In addition, the crew may make photographs of some of the observed landmarks.

As discussed in Section5, it is expected that alternative input optical-to-optical interface devices will be carried on board in modular form to verify the merits of alternative approaches, e.g., rapid process silver halide, and devices using a liquid crystal, or a Pockels cell and, possibly photoplastics and ferro-electric ceramics. During the course of the experimental program it will be a crew function to select and insert one of these alternative interchangeable modules for experimentation and to change to other alternative modular devices as the program continues. The rapid process silver halide device is expected to be the standard against which the performance of the other devices is compared.

4.4 Matched Filter Making Mode

Most of the recognition and tracking experiments will be based on the utilization of pre-made matched filters. These filters will be made from existing photographs obtained from satellite altitudes. However, it is also of lower-priority interest to conduct some experiments to evaluate the feasibility for making matched spatial frequency filters on board the vehicle. These can be made with some simple modifications of the coherent optical system. The primary modification will be an insertion of a Rayleigh reference-beam lens in the system and the insertion of an image recording medium in the filter plane. The general procedure for making coherent optical matched filters is outlined in Appendix A. Most of these filter making experiments will involve manual operations; however, the acquisition and tracking of the landmark area by the two axis tracking mirror may be automated, as in the previously described recognition and tracking experiments, with optional manual override control. It is expected that most of these experiments related to filter making will use silver halide modules, and will require a 2nd silver halide module for recording the spatial frequency filter. The engineering model can be designed to incorporate this feature.

One of the required manual functions in filter making will be that of optimizing the optical energy balance between the signal beam and the reference beam and focusing the reference beam. A neutral density filter "wheel" containing an array of filters will be an effective means of adjusting the balance between the signal and reference beams. One of the most effective means of evaluating the performance of a filter is to reconstruct the original image from which the filter was made. The procedure is to remove the input image in order to illuminate the matched filter with uniform coherent light, and then observe the quality of the output image.

Relative performance of several matched filters made from the same input can be evaluated by comparing the ratio of correlation signal to noise for the various filters for the same input image.

The crew should also have the opportunity to evaluate the use of matched filters over a wide range of physical conditions, including variations of viewing angle and illumination conditions. Because the filter-making function will involve some significant time intervals, such opportunities will depend on overflight of the same landmark area on subsequent orbits.

4.5 Experiment Shut Down

After completion of the experiment, the system will be shut down by manual operation, involving cut-off of power to the laser, the electro-optical readout devices, the command, control and service console and the optical-to-optical interface device. Restraints will then be re-applied to the movable components, such as the tracking mirror and the filter selection and storage mechanism, to enable the system to survive the re-entry environment. This total shutdown operation may take about 0.2 hour by one crew member.

5.0 IDENTIFICATION OF FLIGHT EQUIPMENT

The principal flight components dedicated specifically to this experiment are: viewing window, input telescope optics and tracking mirror, optical-to-optical interface device (or devices), an exposure-control or shutter device, a laser, Fourier transform optics, a matched spatial frequency filter selection and storage device, an electro-optical correlation readout device, and a separate display and control console. Associated equipment will include angle readout encoders and control servos for the tracking mirror and electro-optical cameras to provide video signals for on-board display/monitoring purposes. The experiment package will include a rigid structural frame within which all of the key components will be mounted. The frame assembly will also include light-tight covers so that the coherent optical experiment can proceed without the necessity of darkening the interior of the ATL. Certain auxiliary equipment not totally dedicated to the experiment will be needed, such as an inertial reference subsystem and vehicle attitude control subsystem. Each key component will be described in the following sections.

5.1 Input Tracking Mechanization

The experimental program includes plans to recognize and track landmarks which are located off-nadir. Such off-nadir tracking is desirable to permit a greater selection of landmarks for any given mission. In addition, the ability to track landmarks over a wide range of aspect angles can reduce the total number of required matched filters. Laboratory experiments have shown that it may be practical to recognize landmarks in direction differing by as much as 30^{o} from the direction used in making the matched filter. In order to confirm the laboratory observation via the flight experiment, we should provide landmark viewing in a 30^{o} cone (i.e., nominally 30^{o} in all directions from the nadir).

It does not appear desirable to control the vehicle attitude in order to control the pointing direction of a vehicle-fixed telescope system, because of the possible interference with other concurrent experiments and the associated uneconomical use of attitude control system fuel. Furthermore, an instantaneous optical field of view of 60^{o} does not appear attractive from either the standpoint of potential tracking accuracy or from the standpoint of practical high-performance-telescope design. Hence, it is concluded that some type of articulation is required for the telescopic viewing subsystem. We established earlier that an instantaneous field of view of about 10^{o} is attractive from an accuracy and also from an acquisition point-of-view. Hence, there exists a problem of articulating a 10^{o} instantaneous field in a way that will provide a total conical field of view of 60^{o}. One possible alternative to such articulation would be to gimbal the entire telescope assembly. Such a gimbaling operation, however, would result in a rotation and translation of the image plane relative to the vehicle frame, which is not desirable, since this image plane is the input plane for the coherent optical data processing. In principle, the entire coherent optical processor could be attached rigidly to a gimbaled telescope, but this arrangement would be too cumbersome. A more suitable arrangement is one incorporating a 2-axis gimbaled mirror located at the input to the telescope. Control of its orientation in two axes would provide the desired off-nadir tracking. Furthermore, image motion could be compensated by proper angular-rate control of the mirror, based on transformation of inputs from the inertial reference system and vehicle ephemeris data.

The gimbaled mirror must be large enough to cover the field of view of the telescope for any permitted angular orientation of the mirror. Figure 5-1 shows a sketch of one possible arrangement of tracking mirror and telescope. Figure 5-1a shows the orientation of the tracking mirror at 45^{o} to the optical axis, required to view landmarks at the nadir (i.e., at the sub-satellite point on the earth). Figures 5-1b and 5-1c show the orientation of the tracking mirror required to view landmarks ahead and behind the nadir, respectively. These figures demonstrate only the in-track operation of the tracking mirror. However, since the mirror mount has a two-axis drive system, it is possible to orient the optical axes of the telescope anywhere in a 30^{o} cone about the nominal direction to the nadir . Note that a 15^{o} rotation of the mirror in elevation produces a 30^{o} change in tracking angle.

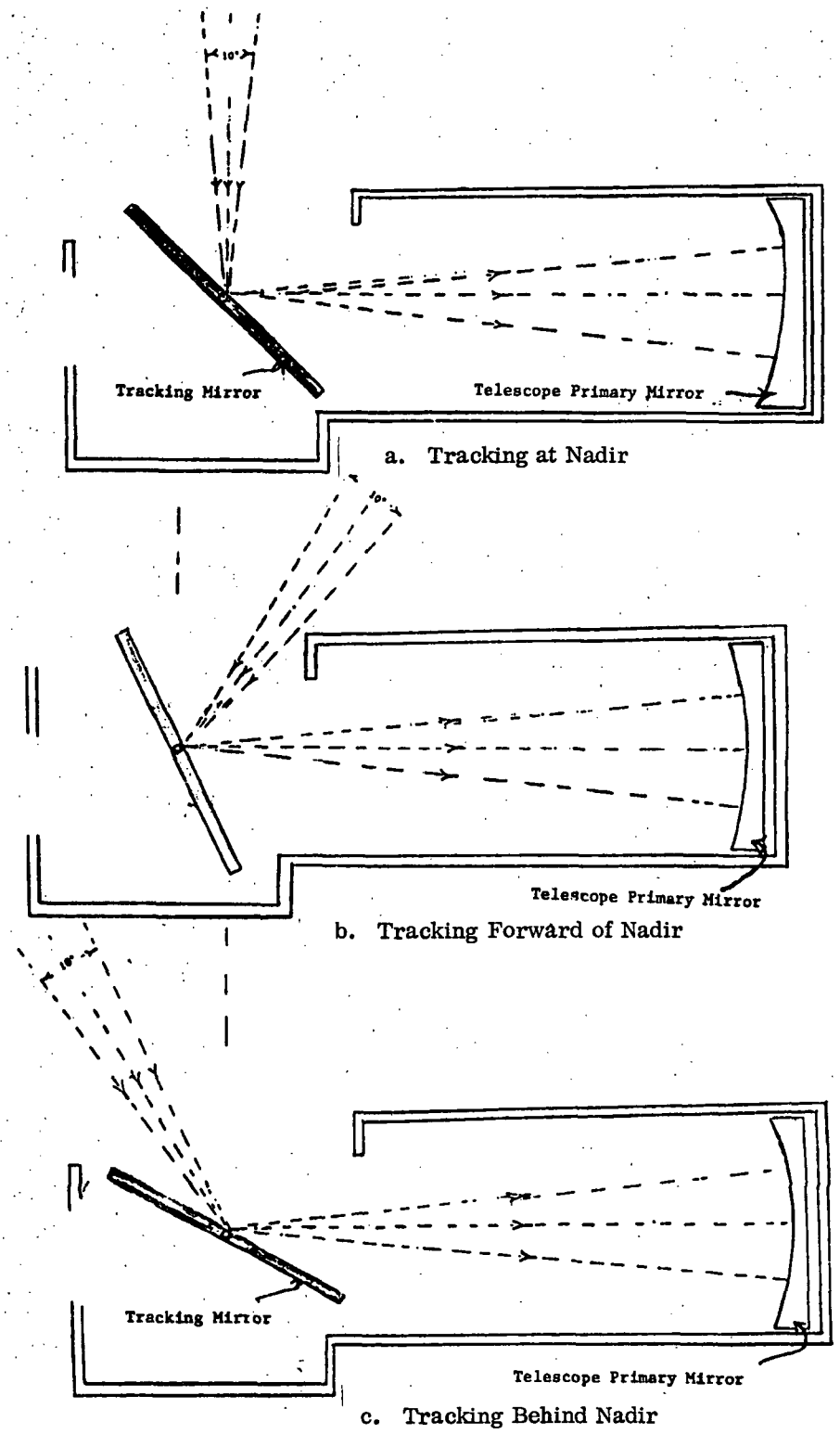

Figure 5-1. Tracking Mirror and Telescope Primary Mirror

It is anticipated that the transparent viewing window will be at the "ceiling" in place of one of the air locks. The experiment package will be oriented with the optical axes of the telescope parallel to the long axis of the ATL vehicle. The design of the articulating system for the mirror permits tracking in a 30^{o} cone about the nominal nadir-oriented direction. The maximum tracking angular rate should be at least an order of magnitude greater than the maximum rate of the angular line of sight to a landmark, i.e., 30^{o}/sec. Tentative specifications are:

Tracking Mirror Specifications

- Mirror Types: Flat front-surface mirror of circular shape.
- Mirror Diameter: $\frac{11 \text{ cm}}{\text{Sin } 30^{o}} = 22$ cm
- Mirror Flatness: 0.1 micrometer
- Reflectivity: 95% (min.)
- Protection: Sun protection cover provided when not in use for experiment.

Mirror Gimbal and Servo-Drives

A 2 axis mount with an outer azimuth gimbal and an inner elevation gimbal.

- Gimbal Freedom so as to provide full line of sight conical coverage $\pm 30^{o}$ from central axis
- Gimbal angular rates: 30^{o}/sec
- Gimbal angular acceleration (min): $100^{o}/\text{sec}^{2}$
- Gimbal braking: Positive mechanical brakes required when servos are off.
- Angular Positioning Accuracy: 0.1^{o}
- Min. resonant frequencies of servos and gimbal structure: to be determined.
- 19-bit encoders for precision readout of mirror position.

One typical 19-bit encoder is 6 inches in diameter, weighs about 6 pounds and operates on + 5 Vdc at 1.5 amperes and - 5.5 Vdc at 0.75 amperes. Another available 19 bit encoder is 5 inches in diameter, 2 inches deep, weighs 20 pounds, and operates on + 6 Vdc at 2.8 amperes, - 6 Vdc at 0.35 amperes and 12 Vdc at 0.2 amperes. Typical available encoders can provide digital angular readout over a full 360^{o} range. A further investigation is worth while to determine advantages, if any, which may result from specifying restricted angular freedom.

5.2 The Telescope

The function of the telescope is to accept the image of the earth surface scene relayed by the tracking mirror and to focus that image on the image plane where the optical-to-optical interface device is located. The telescope image will be divided by a beamsplitter to provide via an electro-optical camera a video image at the control/command console for crew monitoring. Tentative specifications are:

- Focal Length: 44 cm
- Clear Aperture: 11 cm
- Relative Aperture: f/4
- Optical field of view when operating over 50 mm. x 50 mm. image format: 10 degrees. Maximum allowable optical distortion at edge of field: 1% of F.O.V.
- Suitable corrective and relay optics

Although the telescope specified is not an "off-the-shelf-design", it is expected that there may be available telescopes which closely approximate this design.

5.3 The Optical-To-Optical Interface Device

5.3.1 Specifications

The availability of an optical-to-optical interface device which meets the performance requirements of the experiment is the single most critical factor of the present experiment. The analysis of Section 3 provides a basis for specifying the sensitivity and response time requirements.

The resolution requirements of the telescope and the optical-to-optical interface device are determined primarily by the tracking accuracy goal which, for our present experiment has been selected to be 60 arc seconds. This represents one part in 600 of the field of view.

In order to achieve this tracking accuracy it is necessary that the telescope and the optical-to-optical interface device be capable of resolving objects which are as small as one 600th of the field of view. This represents a space bandwidth product requirement of 600 line pairs or a spatial frequency requirement of 12 line pairs/mm over a 50 mm x 50 mm input image format on the optical-to-optical interface device. This, of course, presents no resolution challenges to the telescope design and represents only a modest requirement for the performance of the optical-to-optical interface device.

Since this is modest and since provision must be made for other tracking error sources a minimum resolution will be specified of 30 lp/mm (50% MTF) and a limiting resolution of 60 lp/mm.

As discussed in Section 3, spectral response should be such as to avoid the adverse scattering and attenuation which occurs in the blue end of the spectrum below about 0.48 micrometers on the one hand and to avoid the sensing problems associated with infra-red on the other. A specification is made that the primary range of sensing should be located within the range of 0.5 to 1.1 micrometers. A review of ERTS satellite imagery shows that good images of land areas showing good contrast ratios associated with many types of materials of differing reflectivity can be obtained in any of the spectral bands associated with the multispectral scanner; i.e., 0.5 to 0.6 micrometers, 0.6 to 0.7 micrometers, 0.7 to 0.8 micrometers and 0.8 to 1.1 micrometers. In all four of these bands good contrast has been obtained at land/water boundaries as well as at other boundaries associated with many types of terrain features. Although the longer wavelength of these bands may provide somewhat higher contrast images any imagery obtained in the range of 0.5 to 1.1 micrometers should provide the quality of imagery response needed for the present experiment.

Based on the above and on the analysis of Section 3 as well as overall experiment objectives, the operational specifications for the optical-to-optical interface device are outlined in Table 5-1.

5.3.2 Optically Excited Field Effect Liquid Crystal Device

5.3.2.1 Introduction

This device is the most promising candidate for the near real time optical-to-optical interface device. It has been developed for NASA under contract NAS 5-23192 (Reference 36).

This device has demonstrated (Reference 36) promising operating performance relative to the needs of the present application which are summarized in Section 5.3.1. It has a threshold sensitivity of 0.03 microjoules/cm^2 over an estimated effective bandwidth of about 0.01 to 0.02 micrometers centered at 0.527 micrometers. Although the spectral response is narrow it is within the acceptable response region as indicated in Table 5-1. Note that if we conservatively assume a 0.01 micrometer bandwidth that the above threshold sensitivity would be equivalent to a threshold energy density of 0.3 microjoules/cm^2 if the spectral band were 0.1 micrometers wide. Thus a comparison with threshold sensitivity requirements of Table 5-1 indicates an adequate threshold performance from an optical energy density point of view.

Table 5-1. Summary of Specifications for Optical-to-Optical Interface Device

Minimum Threshold Sensitivity: (1)	1.2 microjoules/cm^2
Minimum Optical Power Density to Read Full Contrast: (1)	16 microjoules/cm^2
Minimum Full Contrast Ratio:	25:1
Spectral Response must lie within 0.5 to 1.0 micrometers	
Format Size:	50 mm x 50 mm
Resolution (50% MTF):	30 line pairs/mm
Limiting Resolution:	60 line pairs/mm
Max Image Formation Time:	50 msec
Max Total Recycle Time:	50 msec
Min Number of Recycles without Degradation:	200

(1) Assumes 0.1 micrometer spectral bandwidth of optical-to-optical interface device. Required optical energy density must be proportionately higher for devices with narrower bandwidth.

It reaches full contrast when exposed to an optical power density of 400 + microwatts/cm^2. These sensitivity tests were made with an illumination which simulated the response of P-1 phosphor. It had a central wavelength of 0.53 micrometers and a 50% bandwidth of 0.023 micrometers. Because the photoconductor layer is physically distinct from the liquid crystal layer, there is a potential for selection of a photoconductor which most effectively meets the spectral response characteristics of the scene. Although the device is not inherently an image storage device, it is designed to permit simultaneous read-in and read-out without interference of the read-out and read-in illumination. This is due to the dielectric mirror and blocking layer which separates the photoconductor and the liquid crystal.

It has a estimated dynamic range of 30:1 as compared to a goal of 13:1. It has a contrast ratio of 100:1 which is adequate for the present application. It has a resolution of 60 lines/mm at 50% MTF and a limiting resolution in excess of 100 lines/mm. This exceeds the previously stated resolution goal. The device has an image formation response time of less than 10 milliseconds near saturation levels of optical excitation. At an illumination of 40 microwatts/cm^2 the excitation time is 50 milliseconds and longer for lower illumination levels. Thus a question arises as to the image formation times at low excitation levels. This should be addressed further. In the event that this is a significant problem, a wafer type of image intensifier as a front end to the liquid crystal device might offer an effective solution.

Because of these characteristics as well as the good performance demonstrated in coherent optical data processing, this device is judged to have performance which shows promise for the present application. In addition, the device is compact and is easy to excite electrically at a low voltage of 6 volts RMS at 10 kHz. Its fabrication is basically simple.

In summary, this device is a candidate for the input optical-to-optical interface which is deserving of detailed quantitative evaluation in relation to the needs of the present application.

In principle, the device can be constructed for either reflective or transmissive read-out. It is presently designed, however, for reflective read-out and has been demonstrated in coherent optical processing with this type of readout.

The present experimental apparatus can be redesigned so as to accept a reflective read-out device on the front end.

5.3.2.2 Development Summary

This most recently developed liquid crystal device is a special improved adaptation of an AC photo-activated liquid crystal device which was developed somewhat earlier. This was described in References 37 and 38.

All of these AC photoactivated devices are developments of a DC photoactivated liquid crystal cell (referred to as OTTO) (Reference 39). Even though this early device suffered from inherent noise characteristics and operational lifetime limitations, it demonstrated fairly good performance characteristics when experimentally evaluated and as reported in Reference 21 in the role of near real time optical-to-optical interface device for recognition and tracking of landmarks and star fields. In some typical experiments this device performed as follows as compared to performance with silver halide film when used in the role of an input imaging medium for the matched filter coherent optical correlator (Reference 21): In one experiment, when a Kodak 649F plate was used as the input medium a SNR response of 1000:1 was measured. Using Kodak Projection Plates (i.e. Lantern Slide Plates) a SNR of 130:1 was measured under similar conditions. Using the dynamic scattering OTTO device under similar conditions produced a SNR of 33:1. When certain local areas of high noise which existed in the liquid crystal were eliminated a SNR of 100:1 was measured. Although this response with the dynamic scattering liquid crystal was judged to be rather good it is confidentially expected that the improved AC device will produce much higher SNR results.

The original DC OTTO device had image formation times in the neighborhood of 100 to 250 milliseconds, depending on the electrical excitation. Threshold sensitivity could be observed with about one microwatt/cm^2 when the device was excited for the duration indicated above. The limiting resolution was measured in the range of 25 lines/mm. In addition the original DC OTTO device suffered from operational lifetimes. Regardless of these limitations this original device was judged to have marginally acceptable performance for near real time coherent optical processing. It is evident from the above that the new AC excited device is improved and it can be expected to exhibit better performance for the landmark tracking experiment.

5.3.2.3 Summary of Operation

The construction and theory of operation is described in some detail in Reference 36. Only a brief summary will be presented here.

The device is constructed in the form of a multi-layer thin film sandwich, the principal components of which are: a Cds photoconductor layer, a CdTe light absorbing layer, a dielectric mirror, a liquid crystal layer in which the field effect occurs and a pair of transparent electrode films for supporting the AC electric field across the device.

In addition to these thin film layers a polarizer/analyzer (i.e., cross polarizer) pair is placed on the read-out side of the device so that the incident coherent read-out light is linearly polarized and the modulated read-out light is directed onto the analyzer.

In operation an audio frequency AC voltage is placed across the entire device by applying the voltage across the two thin film indium-tin-oxide transparent electrodes.

In operation the input non-coherent image is focused onto the photoconductor. The impedance across the photoconductor is selectively reduced over the sensitive area of the device as a function of the intensity level of the input image. This in turn results in an increase in voltage across the liquid crystal as a function of intensity of the input image. The operation as described thus far is similar to that described for the earlier dynamic scattering device. Unlike that device, however, the present device makes use of two field effects rather than dynamic scattering. It makes use of the twisted nematic effect in the areas of non-illumination of the input in order to produce the dark off-state. It makes use of controlled optical birefringence to cause the bright on state.

Since the liquid crystal modulates the polarization of the coherent read-out light an analyzer is needed to produce the desired modulated output beam.

In the present construction the device is read in on one side with noncoherent illumination and read out reflectively on the other side with coherent illumination. In principle, a variant of the device could be designed so as to provide for transmissive read-out.

In order to better understand the principles of operation a brief description will be given of the off state and the on state.

In the off-state the incident read-out light is polarized by the polarizer. Passing through the liquid crystal, the direction of polarization is rotated through 45^{o}. This is a result of the twisted nematic state of the unexcited liquid crystal. In this state, the liquid crystal molecules are all oriented parallel to the plane of the cell but exhibit a 45^{o} twist across the liquid crystal about an axis perpendicular to the crystal.

This 45^{o} twist results from conditioning (e.g., by a rubbing action) of the boundaries of the liquid crystal cell. The twist of the molecular structure results in a corresponding twist of the polarization of polarized light transiting the liquid crystal.

Having passed through the liquid crystal cell, the polarized light is reflected by the dielectric mirror causing it to transit the liquid crystal again. This results in a reversal of the original 45^{o} polarization twist leaving the emitting coherent illumination to have the same polarization as the incident polarization.

It is then incident upon the polarization analyzer (i.e., cross polarizer). Since this has polarization characteristics orthogonal to the original polarizer a very high degree of extinction occurs. Thus the desired dark output results for the off-state.

The on-state read-out differs from the off state due to the changed state of the liquid crystal which in turn is due to the optically induced voltage across the liquid crystal. In this state the molecules of the liquid crystal are no longer parallel to be plane of the electrodes. Rather, they are caused by the voltage to tilt to some degree toward the normal to the electrodes. This effect destroys, to some extent, the previously described polarization capability of the liquid crystal in the twisted nematic state. If the tilt were complete (i.e., 40^{o} to the electrodes) then the desired on-state effect would not occur since the polarization of the light would then be unaffected by the liquid crystal. However, when the voltage was such as to produce only a partial tilt, then the birefringence of the molecules can effect the polarization of the light in such a way and to a degree so as to permit some light transmission through the analyzer. Thus, the desired on-state can be obtained.

This description of the operation of this AC liquid crystal device is of necessity brief. For more details the reader is referred to Reference 36.

5.3.3 An Optically-Excited Pockels Cell Device

INTRODUCTION

This device has been suggested as a possible alternative candidate for providing the optical-to-optical interface device. However, because it is primarily sensitive in the blue end of the spectrum, there is significant question as to its use for the present application unless it can be modified to have a more suitable spectral response. It is known as a Pockel's Readout Optical Modulator (PROM) and has been developed, in part, under U.S. Army Contract DAAK02-74-C-0029. It is described in some detail in Reference 40 which is the final report of that contract.

The device incorporates a single active component in the form of a grown crystal. This component, which typically is a thin slice of bismuth silicon oxide, exhibits both a high photo-conductivity which is used for image read-in and also a Pockels effect which is used for read-out. It has a threshold of sensitivity in the range of 0.1 to 0.3 microjoules/cm^2 depending on wavelength and cell thickness. The peak sensitivity is in the blue at about 0.43 micrometers.

It decreases for increased wavelength and is only about 10% of the peak value at about 0.53 micro-meters (cf. Reference 41). It has limiting resolution of over 100 lp/mm and its MTF is better than required for the present application. Contrast ratios of up to 10,000 to 1 are attained.

If this device could be modified to more closely meet the spectral response characteristics outlined in Section 3, it would become another promising candidate for the present application. In the event that the device could be made more sensitive at the longer wavelengths, then the possibility of interference with the read out illumination might, however, become significant. Unlike the liquid crystal device the optical read-in and read-out functions both take place in the same crystal material and read-in and read-out illumination must be spectrally separated. The application of a wafer type of image intensifier on the front end has been suggested as a means for correcting the present spectral mismatch on the input.

In summary, this device has many characteristics which make it very attractive for coherent optical data processing. Its present spectral response, however, precludes it being a prime candidate for the present application.

5.3.4 Other Optical-to-Optical Interface Device

Other devices have been suggested and/or evaluated for the present application. Photoplastic Recording material (PPR) has been evaluated (Reference 22). Although it has performed in laboratory experiment it is presently judged as being less promising than the liquid crystal device. Various other devices have been evaluated (Reference 6). Typical problems relate to sensitivity.

Because of the rapid advances being made in the area of optical-to-optical interface devices it is recommended that the planned experiment be designed to accept alternative devices on an alternative module basis.

5.4 The Laser

The function of the laser is to provide a coherent source of illumination for the coherent optical processor. In order to select a specific laser, we must first decide on a laser type and specify the power required. The HeNe laser is the type most widely used for coherent optical processing. It is highly stable and provides a red output which is both convenient from the standpoint of eye visibility and also from the standpoint of being outside of the region of read-in spectral sensitivity of most of the advanced optical-to-optical interface devices, i.e., coherent processing can be done without erasing the input.

The argon laser can provide greater power than that of the HeNe but is not needed for this application. The stability is inferior to that of the HeNe. Also, the green color has the disadvantage of being in the region of highest sensitivity of many of the advanced optical-to-optical interface devices, i.e., coherent processing would tend to erase the recorded image.

The pulsed ruby laser, another alternative, appears to have no advantage for the present application. Semi-conductor lasers such as Galium Arsinide may have potential at some future time for reducing the size of coherent illumination source (see later discussion). However, they presently appear to be inconvenient to work with because they produce non-visible radiation. Furthermore, they are inferior to HeNe in terms of stability and reliability. The preferred choice is that of the HeNe laser.

The power output of the coherent optical processor (correlator) will be determined by the diffraction efficiency of the typical landmark recorded image and the sensitivity of the electro optical readout device. Typically the average transmissivity of a landmark image (transparency or other imaging medium) will be about 0.02.

Experiments in which landmark images have been used as objects for optical correlation indicate that typically 0.005 to 0.05 of the light which is transmitted by the image will appear in the cross-correlation

function. Thus, the overall defraction efficiency of the input imaging medium is indicated to range from 10^{-4} to 10^{-3}. The correlation spot can be expected to have a maximum diameter of about 50 micrometers and a corresponding area of about 2.5×10^{-9} m^2. The typical noise equivalent signal for a solid state detector of the type we would expect to use (see next section) would be 10^{-6} watt-sec/m^2 (Reference 17). Hence, the noise equivalent signal over the illuminated area would be 2.5×10^{-15} watt-sec. A conservative requirement would be to achieve a minimum readout signal to noise ratio of 25. Hence, minimum required signal energy at the output plane is 10^{-14} watt-sec. If we make the realistic assumption that the detector operates in a power-integrating mode, exposure time can be traded off for laser power over rather wide limits. From the indicated diffraction efficiency, we then conclude that the laser energy required for a typical correlation operation would range from 10^{-11} to 10^{-10} watt seconds. In order to arrive at a conservative design requirement we will assume a typical energy requirement of 10^{-8} watt seconds. For a system operating with an input medium having a long-relaxation time constant, the power of the laser can be low (e.g., some small fraction of a milliwatt) because relatively long integrating time periods can be employed. For an attitude determination application utilizing a medium of fast relaxation time constant, a higher power laser would be required. For example, if the imaging medium had a relaxation time constant of 10^{-2} sec, then for an energy requirement of 10^{-8} watt-sec., a laser having a power in the range of 10^{-3} milliwatts would be required. We can conservatively conclude that, for the type of electro-optical readout described, a laser power of 0.1 mwatts would be adequate for the landmark tracking application. Therefore, we recommend that a space-qualifiable HeNe laser having an output power rating of not less than 0.1 mwatt be incorporated.

A typical such laser will fit into a cylindrical volume 5 cm in diameter and 20 cm in length, with a power supply of 10^3 cm^3. Total required power will typically be 20 watts.

For further coherent optical data processing applications, the gallium arsenide laser diode (cf. reference 18) may have strong appeal. The application of this very small low-power device to optical data processing has been described by Dr. A. Hussain-Abidi in Reference 19. The output of this device operating at room temperature is at a wavelength of 9000 Å. Some inconvenience may be expected in initial alignment of the system with non-visible radiation. Furthermore, some further investigation may be required to determine the optimum electro-optical readout with this device. At the present time all known GaAs lasers which provide coherent radiation do so in a pulsed mode (typically 100-microsec pulses at 50 pulses/sec). Some CW GaAs lasers have been operated experimentally at cryogenic temperatures. However, the cryogenic complications are clearly unattractive for the present application. If GaAs having high coherent CW outputs at room temperatures become available, they will be prime candidates for a source of illumination for the present application. The initial experiment of Dr. Hussain-Abidi (Reference 19) indicates there is reason for encouragement in the future use of this device eventually as a practical low-power compact source of laser illumination.

5.5 Spatial Frequency Filter Storage and Retrieval System

As discussed in Section 3, it is planned to take approximately 500 pre-made spatial frequency matched filters on board the vehicle during each 7-day flight when autonomous navigation experiments are to be performed. This number of filters will not only permit operation with several landmarks of various types and locations, but it will also make allowances for some landmarks being unavailable due to weather conditions. It will also allow a range of filters with different spatial frequency content for each of the selected landmarks. The storage and retrieval system will be of a random access type. Filter selection will be possible in three alternative ways:

- Programmed selection from the experiment process controller
- Selection by crew inputs at the command control and display module
- Manual selection and insertion of the filters directly at the experiment module

Since these matched spatial frequency filters will be pre-made in an earth-based facility, the use of conventional silver halide transparencies as a filter medium is appropriate.

In principle, the matched filters could be stored very compactly. Typical filters may have active diameters of as little as 3 mm. This suggests that 500 filters could be stored in matrix fashion, for example, on a single plate as small as 7 cm x 7 cm. Precision indexing could be provided in 2 dimensions to select the desired filter. Alternatively other forms of multiplexing could be incorporated. Gorstein and Hallock (Reference 20) demonstrated the use of spatial frequency carriers for multiplexing. The techniques, which were further explored by the General Electric Company (Reference 21) can lead to very compact storage of matched filters. It is expected that these compact storage techniques will have significant merit for subsequent operational autonomous navigation systems. However, they are not planned or recommended for the present experiment. Rather, a more flexible approach is recommended of storing each matched filter as a separate discrete 35 mm frame. For experiment purposes, this has the unique advantage of readily permitting additions or deletions to the filter file at any time. Although they are significantly larger than required for optical processing purposes, their size is convenient for handling purposes, and an excessively large total storage volume is not required.

Two alternate approaches based on adaptation of available devices are suggested for storage and retrieval of the matched filters: a random-access film-strip device and a random-access slide device. In the former the filters would be stored on a film loop which is controllable by selectable frames. This approach is not favored because there is some question whether such an approach can provide the precision position registration required of the matched filter in the coherent optical processor. Typically, a registration precision of 10 to 20 micrometers will be required by the system, whereas presently available film loop devices typically provide an accuracy of about 100 micrometers. Furthermore, since the film sprocket holes are subject to wear, precision of the frame registration can be expected to deteriorate with time. The alternative of using steel framed slides is favored because it provides greater potentiality for registration precision. In addition, it permits much easier revision of the file of matched filters than does the film loop approach. One typical commercial device with satisfactory registration performance employs steel framed 35 mm slides. Upon access, these slides are registered with a location accuracy of $\pm$ 12 micrometers. This device employs a rotary slide storage device which holds 256 of the steel framed slides. Random access time of any selected slide ranges from a minimum of 1 second to a maximum of 5.2 seconds. The random access and slide storage portions of this device will fit in a volume having the dimensions of approximately 30 cm x 30 cm x 30 cm. This includes the volume occupied by a holder for 256 slides. It is expected that a second such holder could be provided to permit storage of a total of 512 slides. Such a holder would fit into a volume having dimensions of approximately 25 cm x 25 cm x 5 cm. Further investigation is required to determine the relative practicality of crew changing such a slide holding device or, alternatively, using a single slideholder of larger capacity. Further investigation is also required to determine what modifications may be required to make such a device suitable for the present space application. It is presently anticipated that the matched filters will be stored in the form of steel framed slides in a selection and retrieval device similar to that described above. It is anticipated that this device, including the array of filter slides, would have the following characteristics:

- Total weight: 20 kg
- Total volume: 16,000 cm^3
- Peak power required: 20 watts

Provision will be made for a crew member to optimize the filter location via a 3-axis positioning control, if necessary. However, the total system design should provide the necessary indexing precision for most cases.

5.6 The Fourier Transform Optics

The function of the Fourier transform optics is to provide convenient display of the Fourier transformations of images, as required by the coherent optical data processor. In particular, we require a spatial frequency transformation of the candidate input image which is momentarily recorded on the input optical-to-optical interface device, and a transformation of the spatial frequency filtered image back to the spatial domain. In principle, these coherent optical transformations can be performed with simple optical components in the form of either transform lenses or transform mirrors.

Most coherent data processing has been performed on optical benches via lenses as the primary Fourier transform optical elements. However, for a compact flight-qualifiable device, optical folding of the system with reflective elements is attractive. Hence, it is opportune to ask whether, in such an application, it is appropriate to design the entire system with reflective Fourier transform components. Such a design would use parabaloidal mirror segments to provide both the Fourier transformation and the optical folding. This could typically eliminate four optical surfaces and the scattering associated with them. A recent report (Reference 19) has described the application of paraboloidal mirror segments to obtain the Fourier transform and at the same time provide folding of the system. The author of the referenced report has also demonstrated good performance of such a system in the laboratory.

Since there is apparently no experimental evaluation of a mirror system versus a lens system evaluated under the same conditions, it is difficult to make a performance comparison. However, recent advances in "laser quality" optics indicate that the elimination of four optical surfaces (i.e., the flat folding mirrors not needed with the system using paraboloidal mirror segments) may not be a significant advantage. Mirrors with hard dielectric coatings have reflectivity in excess of 99.7% and with absorption and scattering of about 0.2% are commercially available. Thus, the inclusion of four flat folding mirrors would reduce the intensity of the output signal by only about 1% and would increase the scattering by less than 1%. Experience in coherent optical processing indicates that this represents an insignificant performance degradation. Because of this and because of the much greater experience with, and availability of, Fourier transform lenses as compared to paraboloidal mirror segments, a recommendation is made to design the experiments based on the use of lenses.

Just as the folding plane mirrors need multi-layer dielectric coatings to achieve high reflectivity so also do the lenses need multi-layer dielectric coatings to achieve low scattering and high transmissivity. Such coatings are available which give less than 0.25% reflectivity at their surface. Multi-layer dielectric coatings achieve their performance by means of a composite of thin films of highly transmissive materials of different indices of refraction. Layer thicknesses and indices are selected so as to provide the constructive or destructive interference as needed to achieve the desired reflectivity or transmissivity. Because these coatings can be optimized to operate at the wavelength of the HeNe laser (i.e., 0.6328 micrometers) very high performance can be achieved.

As described in Section 8, the coherent optical path will include two lenses and five mirrors. Based on the above, the surface of each mirror will scatter not more than 0.2% of the incident illumination and the surface of each lenses will scatter not more than 0.25% of the illumination. Thus, total scattering due to these passive optical elements at the surfaces can be expected to be less than 1.5%. Based on previous optical data processing experiments this is an acceptably low level. Additional scattering will take place within the lenses due to imperfections in the material. However, by selecting high quality lens material, such as Schlieren grade fused silica, total scattering within the lenses can be acceptably low.

We consider now the sizing and scale factor of the Fourier transform optics, which will largely determine the size and performance of the total experimental equipment package. The scale factor relates the displacement on the spatial frequency (or matched filter) plane to spatial frequencies existing in the spatial (or "input") plane. The scale factor is proportional to λF where F is the focal length of the transform optics. In order to achieve a convenient scale factor (i.e., one providing adequate diffraction displacement in the filter plane), a relatively slow transform lens is needed. In addition, such lenses with long focal lengths will reduce off axis light incidence at the optical surfaces as needed for maximum effectiveness of the thin film coatings. Typically coherent optical processors operate best with relative apertures of f/16 or slower. In the case of the HeNe laser, the wavelength will be 0.6328 micrometers. As we discussed previously, the dimensions of the matched filter and the output plane will be 35 mm x 35 mm. In order to provide a convenient scale factor with these dimensions, we recommend f/20 lenses having a 40 mm diameter and 800 mm focal length. These lenses will each have a thickness of about 5 mm, resulting in a transmissivity in the range of 94% to 97% per lens for typical high quality lens materials. Since optical power from the laser is a non-critical item, this total absorption of about 10% by the lenses is very acceptable.

Although careful selection of optical components can lead to high performance, this performance can be maintained during both the pre-flight evaluation and flight experiments only if all optical surfaces are maintained in a very clean condition. Standards and procedures for achieving the needed high cleanliness need to be developed.

5.7 ELECTRO-OPTICAL READOUT DEVICES

There are two distinct needs for electro-optical readout for the planned experiment:

- Precision digital readout of the "correlation spot"
- Video display of telescope views for crew monitor

The first of these is of sine qua non importance to the experiment, whereas the second (discussed in Section 5.8) is of ancillary significance.

Consider the problem of "correlation spot" readout. The problem is to precisely determine the location of the correlation function (i.e., "correlation spot") in the "output" plane. The size, shape and the intensity of the correlation function as a function of image type and degradation of the image has been investigated by experiment and analysis (Reference 22), which have indicated that the typical correlation function will have a diameter ranging from 10 to 40 micrometers, as measured to the half-power points.

For the system scale factor favored, the correlation function will be located somewhere in an output plane having dimensions of 50 mm x 50 mm. The problem of locating the correlation function in the output plane is very similar to that of locating a star image with an off-axis star tracker, except for one important difference: the accuracy of the off-axis star tracker is usually limited by the dynamics of the vehicle and tracking system. In the case of the coherent optical correlation tracker, the detection of the correlation spot will have the dynamics of the optical-to-optical input device. In the case of a navigator using an optical-to-optical interface device with a memory the correlation spot then is stationary and its readout could be smoothed over a relatively long period of time (e.g., many milliseconds). In the case of a non-storage optical-to-optical interface device (e.g. an optically excited liquid crystal device), a somewhat lower-accuracy readout might be expected for those cases where the vehicle attitude is experiencing rapid changes.

Alternative Electro-Optical Readout Devices - Several investigators have automated the operation of reading out the correlation function, using image orthicons, vidicons and image dissectors. In some cases the sensor was used only for TV display of the output signal, whereas in other cases a digital position readout has been incorporated. Using similar technology off-axis star trackers have been developed, which in static tests, have demonstrated high position-determination accuracy throughout a field of view comparable with that associated with the present application. One such off-axis tracker used a one-inch vidicon which incorporated a special reticle on the face of the tube to establish linearity references for the tube (Reference 23). The tracker also incorporated interpolation and pulse-center detection techniques of an advanced design to detect the center of a small star image. In tests, the optics imaged simulated static star images in the 20 to 50 micrometer diameter range on the face of the tube. These tests demonstrated tracking accuracy in the x-axis with uncertainties of 10^{-3} (1σ) of the field of view and in the y-axis with uncertainties of 1.6×10^{-3} (1σ).

Another approach to electro-optical readout involves application of an image dissector tube. Preliminary investigations indicate that this device can result in position determination uncertainties that are less than 10^{-3} of the field of view. Space-qualified trackers of this type have been developed and produced. Thus, there is considerable background in point readout with various image tubes with accuracies in the neighborhood of 10^{-3} of the field of view.

The Preferred Approach - Parallel Electro-Optical Readout - the favored alternative to the scanning devices discussed above, however, is the use of solid state electro-optical detector arrays. In principle, either linear or area arrays can be used. Until recently, the use of the linear array was favored for the present application. However, in order to use a linear array, one must either sweep the image plane past the array or convert the correlation function to a linear function which intersects the array. Mechanical sweeping is clearly unattractive for a space application (Reference 17).

If the correlation function could be transformed into a cruciform image (i.e., a cross which spans all or part of the output plane in two axes), then two linear arrays mounted orthogonal to each other could read out the correlation function. There are at least two ways in which the correlation function can be transformed into such a cruciform image: by the application of a beam splitter and two orthogonally mounted cylindrical lenses (one for each split-beam segment), or by use of a cruciform-encoding spatial frequency filter. By an encoding filter we refer to a spatial frequency filter which would be designed to directly produce the desired cruciform image instead of the more usual correlation spot. Such a filter would be made by using a reference beam imaged in the form of the desired cruciform before interfering it with the candidate image, in contrast to the usual approach of bringing the reference beam to a point-focus before interfering it with the reference signal (see Appendix A). Although the cruciform approach to readout is conceptually feasible, some limitation will exist due to the reduction of signal-to-noise ratio which will result from spreading the energy over a line. Presently available linear detection arrays are available with typical spacing density of more than 30 elements per mm. However, since the use of the cruciform reference technique has not yet been verified in the laboratory, and since recent advances have been made in solid state detector area type of arrays, we favor use of the area array rather than the linear array for readout of the correlation spot.

Several types of area arrays are available and others are expected to soon be available. Among the first of the area arrays available was the self-scanned photodiode type. A typical area array of this type, example, has 1024 active elements in a 32 x 32 matrix format, and will probably be limited to sizes not larger than 64 x 64; hence, it will have limited applicability for the present experiment.

The solid state detector arrays which have received the most attention are of the CCD (charge coupled diode) type (Reference 24). There are in various stages of availability and development. Other developments are based on the "bucket brigade" process.

A brief survey, however, indicates that the Charge Injection Device (CID) may be the most attractive correlation spot readout technique. Unlike the CCD which is read out on a line-by-line basis, the CID is read out on a point-by-point basis. Hence, the CID can be read out either sequentially at conventional TV rates or by random access. This means that the readout can be "electronically zoomed" to concentrate the readout in the immediate area of the correlation spot. This is a mode of operation of the type which is possible with an image dissector and which can be used to improve readout accuracy and/or to reduce bandwidth. CCD types of arrays do not have this capability. A further advantage of the CID is the large ratio of sensitive area to "dead area" (between sensitive elements) of the CID arrays relative to that for most CCD arrays. This feature is important because it reduces the likelihood of the correlation spot being "lost" between sensitive elements. The only non-sensitive areas of the CID's are the vertical electrodes which are presently about 4 to 5 micrometers wide, as compared to the active areas which are presently about 50 to 60 micrometers wide. In the present designs, about 88% of the CID area is active, in contrast to a value of 40 to 50% typical of CCD's. Because non-active areas between the elements of CCD's may be as wide as the active areas (e.g., 30 to 50 micrometers), there is a significant likelihood that the correlation spot may not be detected with this device. The CID's have a nearly uniform spectral response (about 0.2 micro amp/microwatt) in the spectral band from 0.4 to 1.0 micrometers. Sensitivity is nearly linear with irradiance for excitations up to about 140 μ W/m^2. Availability of the CID is indicated in the following:

Elements in Array (V x H)	Overall Dimensions	Availability Date
100 x 100	6 mm x 8 mm	Available now
200 x 188	20 mm x 15 mm	Available 1975
500+ x 500+	18 mm x 24 mm (est.)	1975 or 1976 (est.)
1000+ x 1000+*	36 mm x 48 mm (est.)	1976 (est.)

Because of probable lack of need, imaging arrays may not become available except for special designs in sizes much greater than 500 x 500 elements. However, there is potential for, increasing the number of available elements by juxtaposition of 4 of the CID standard arrays, made possible because the readout connections are confined to top (or bottom) and one side of each array. Such juxtaposition may result in some loss of active elements at the joint (2 to 4), but this loss may be avoided by precision laser trimming before jointing. Recommendations for the ATL experiment are as follows: Use a 244 x 188 CID array for the engineering test model and initial tests. Plan on use of 4 juxtaposed 500 x 500 element arrays for flight test on ATL. Detector arrays technology is in a rapid state of development, however, and it is important to continue to evaluate newly developed devices for potential use in this experiment.

5.8 Video Cameras for TV Monitor

One (or more) video camera is needed to provide the crew with a continuous view of the scene imaged by the tracking mirror and input optical system, to allow them to better follow the experimental program and to make appropriate changes if necessary. A single video signal can be used to drive more than one TV monitor within the ATL, if such an arrangement increases the crew's efficiency in their total work schedule. Currently, it appears practical to use the CID type of area array for transmitting video information, as well as for the correlation function detection. It has advantages of being smaller, more reliable and more spatially linear than the vidicon. We recommend using the 244 x 188 element model for the engineering model and, as it becomes available, the 500+ x 500+ element model for the ATL flight-test equipment. We suggest that two such electro-optical cameras be incorporated to provide a video signal for TV monitoring by the crew. One camera would be an integral part of the experiment package and would operate with the same input image as that input to the optical-to-optical interface device of the coherent optical processor. It would share the image provided by the tracking mirror and telescope. The second camera, based on a solid state array would be fixed relative to the ATL vehicle near the tracking mirror, and would operate independently of the tracking mirror. It would provide a wider field of view than that provided by "tracking view" camera just described and will be referred to as the "acquisition view" camera. This camera should provide a total field of view of 35^{o}. The crew would be able to select either the tracking view or the acquisition view via a selector switch for display on their monitor screen.

5.9 Command, Control and Display (CC and D) Console

This console as shown in the sketch of Figure 5-2 will provide these functions:

- One of the means for achieving a crew interface with experiment.
- Storage and execution of certain programmed commands for the experiment.
- Storage of data obtained in experiment.
- Certain data processing functions.

Man-Experiment Interface

This CC and D console provides a man-experiment interface. However, it will not be the only such interface. The experiment module itself will be available to the crew for interactions, such as adjustments of optics and manual filter selection. Crew-experiment interfaces through the CC and D module will include:

- Display of scenes obtained by TV cameras described in Section 5.8. TV camera to be selected by crew.
- Optional two-axis manual override control for tracking mirror, via a control stick (Figure 5-2).
- Display of stored landmark slides on back-projected screen for cue purposes. Specific slide for viewing selected by command of crew.

- Digital display of experiment parameters upon command of crew. Typical displays include serial number of matched filter being used, azimuth and elevation of tracking mirror and x, y readout of correlation spot.
- Program and data inputs by crew via the keyboard. Typical inputs include coordinates of landmarks to be added to file of landmarks.

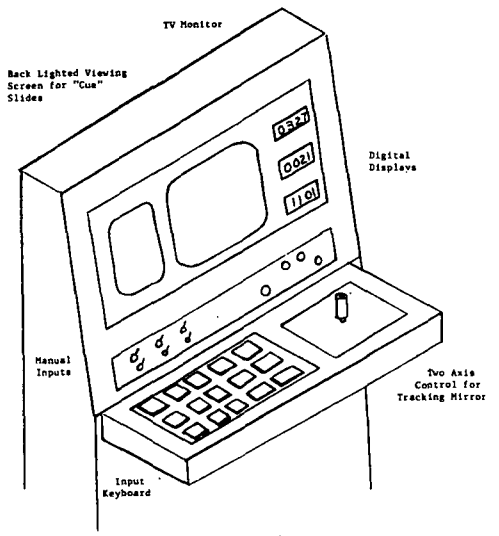

Figure 5-2. Conceptual Design of Command Control and Display Module

Storage and Execution of Commands

Data obtained in pre-flight operations and to be stored include:

- Latitude and longitude of all landmarks, together with serial numbers of matched filters of those landmarks.
- Nominal vehicle ephemeris data - specifically, vehicle position data as function of time (subject to update based on navigation data).
- Expected illumination and viewing conditions over each landmark for each pass of nominal orbit (subject to update based on navigation data).
- Nominal sequence of experiment operations. This includes tracking angles, rates of tracking mirror and acquisition numbers of stored matched filters. The sequence is subject to manual change and/or override by crew.)
- Sequenced executive commands for experiment functions. (Subject to manual change and/or override by crew via keyboard.)

Storage of Data Obtained in Experiment

Data to be stored includes:

- The two-axis digital data describing the location of the correlation spot as indicated by the solid state detector array.
- Serial numbers and time sequence of all matched filters used, as well as the time of their use.
- Manually inserted data for inspection by crew. This may include notation of viewing conditions, etc.

Data Processing Functions

Data processing to be performed in the CC and D Console includes:

- Conversion of spatial coordinates (for example, those of the tracking mirror relative to those of the vehicle).
- Landmark tracking angles and illumination angles versus time, based on updated navigational data. (An optional function for initial flight experiments.)

It is anticipated that the command, control and display console will have dimensions typically at 30 cm x 30 cm x 20 cm and that it will weigh about 8 kg. Its peak power requirement is expected to be about 50 watts. This console may be remotely located from the experiment itself. Ideally the console should be attached to the experiment module by a cable of sufficient length to permit its location either near the experiment module, or, alternatively, for certain phases of the mission, at a location in the ATL which is more central to the other areas of activity of the crew.

5.10 Magnification and Rotation Compensation

Consideration should be given in the experiment design to the incorporation of techniques to compensate for changes or uncertainties in image magnification and also for image rotation about the optical axis. The former effect can result from changes or errors in determination or range to the landmark and the latter can result from changes or uncertainties in yaw angle. We might regard the inclusion of compensation effects as optional, since magnification discrepancies typically as great as 20% and rotation discrepancies typically as great as 20^{o} can be tolerated. For the shuttle flight, we expect that range and yaw angle discrepancies will be well below these values; therefore, we are not including rotation or magnification compensation.

For the initial flight tests on ATL, the discussion here of approaches to such compensation is worthwhile in view of the likelihood of needing such compensation on later operational satellite vehicles. The cost of providing such compensation effects must be weighed against the benefit derived. Possible benefits of providing these compensations are:

- Reduction in the number of matched filters which are needed.
- Greater freedom in the selection of, or changes in, orbit or flight profile.
- Improved correlation response under marginal conditions.

We consider next some possible methods of providing compensation for rotation and magnification.

Rotation Compensation

An axial rotation of the candidate image relative to the matched filter will provide the proper rotation compensation, and it can be done in several ways (Reference 2), e.g.,

- Rotation of optical-to-optical input device.
- Rotation of the matched spatial frequency filter.
- Rotation of a "de-rotation" prism located between the optical-to-optical input device and the matched spatial frequency filter.

Rotation of the matched filter is not an attractive approach, because it would be necessary to provide rotation with an axial displacement less than an interference fringe recorded on the filter. Although rotation of the input image may be more acceptable than rotation of the matched filter, it is not consistent with the concept of using a replaceable optical-to-optical interface module. On balance, the use of a de-rotation prism appears to be the most practical approach. Both refractive and reflective prisms (i.e., assemblies of optical flats) are available for de-rotation purposes (Reference 25), such as the Dove, Double Dove, Pechan and "K" prisms. Although the Dove prism is the most common, the Pechan and K prisms are preferred because of their greater off-axis capability and shorter lengths. De-rotation prisms mounted in high precision bearings are used in certain types of military periscopes. For the ATL application we would prefer a continuously driven prism, with provision for alternate manual positioning. Rotation rates would be selected which are compatible with the time constants of the input imaging device and the electro-optical read-out. An angular pick-off could be provided to obtain prism rotation attitude as a function of time.

The reflective prisms are generally lighter and less expensive than the refractive prisms and have performance which is generally independent of wavelength. With respect to stability and accuracy of performance, some conflicting claims are made by various designers and manufacturers of prisms. The reflective prisms are appealing, but the lack of extensive performance data suggests that further evaluation of their performance is needed. A review of available data supplied by several manufacturers and a survey of the technical literature lead us to favor a refractive Pechan prism. There are indications that these are operable over angular fields of view ranges of 10^{o} or more with lateral and angular deviations which would be equivalent to 2×10^{-5} radians or less, an error which would not be observable within the expected resolution limits of the input image system.

Magnification Compensation

Magnification compensation (References 26 and 27) can be accomplished by placing the input image in a converging coherent optical beam rather than in a collimated one. The general approach to magnification compensation is illustrated in Figure 5-3. Scale changing can be accomplished by moving, as a unit, the input image, the final transform lens and the read-out (output) plane relative to the rest of the system. That is, we vary Z_1 from a reference value Z_0 to effect a scale change Z_1/Z_0, while at the same time maintaining $(Z_1 + Z_2)$ equal to a constant and Z_3 equal to another constant. Scale changing by this method depends upon the validity of the usual small-angle approximations. The approach is typically valid for magnification changes up to 25%.

Evidently, scale changes can be made by the technique just described in either of two ways:

- Moving the input optical-to-optical interface device, the second transform lens and the output plane (i.e., solid state detector) as a unit in the axial direction, while leaving the matched filter plane and the converging lens fixed.
- Moving the matched filter and the converging lens, while leaving the optical-to-optical interface device, the second transform lens and the output plane fixed.

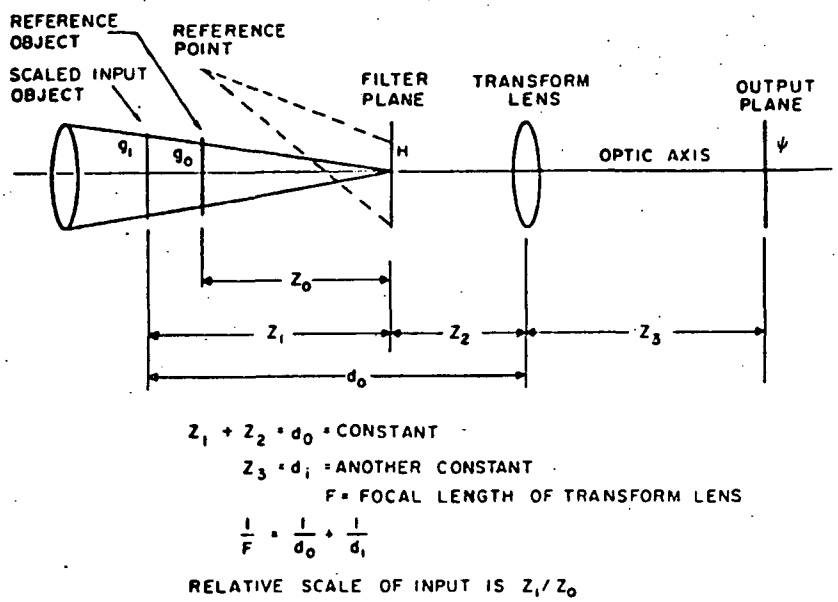

Figure 5-3. Optical Matched Filtering with Scale-Change Capability

The first approach is the more usual one. However, for the present application, it has the disadvantage of moving the input image from the focal plane of the telescope. In the event that the system were to be mechanized to accept an optical-to-optical interface device which could be read out either transmissively or reflectively, then providing capability to move that device could significantly increase the design complexity. The alternative of providing for motion of the matched filter and the converging lens is simpler. However, it does require that the filter registration be maintained to within one fringe of displacement during the translation. That is, registration must be maintained typically to within about 5×10^{-3} mm during translation.

It is recommended that the initial flight experiments not incorporate magnification compensation. However, further experimentation is recommended to evaluate the two techniques described above for subsequent operational vehicles.

5.11 Optical Bench

The function of the optical bench is to provide a base on which to position all the optical components used in the coherent optical data processing. In addition, it provides a frame on which the light tight covers are mounted. The optical bench is designed to provide a folded optical path as shown in Figure 1-1. It must have a high degree of rigidity and yet be as lightweight as is consistent with that rigidity and its functional requirements. It must be designed to be adaptable to alternative modes of operation including that of making of matched spatial frequency filters. Furthermore, the optical bench design must be such that it holds all of the various optical components in place without backlash or creep without dependence on a gravity field. This last requirement eliminates certain types of commercially available rails which depend on gravity for holding of certain components.

In order to avoid excessive costs, the optical bench should, if possible, be based on commercially available hardware. A review of such hardware has resulted in preference of a design based on the concept of an optical "erector set". This commercially available design is based on the application of tubular stainless steel rails. Support frames are provided to assemble four tubular rails in a framework which then provides a base on which the various optical mounts are positioned. The assembly of tubular rails can be designed not only in a straight line but can also be designed to provide right angles as needed for optical folding. This arrangement provides positive positioning of components to eliminate unwanted displacements in any direction. The tubular stainless steel rods provide the needed rigidity while at the same time being relatively lightweight.

6.0 IDENTIFICATION OF MAN'S ROLE

Most of the experimental equipment will be available to the crew in the ATL laboratory, to permit the crew to perform manual functions in the experimental procedures as well as to permit the crew to modify the experimental procedures and equipment appropriately during the experimental program. Specific functions of the crew will be:

a. Deployment of the Experimental Equipment

After insertion of the Shuttle ATL laboratory in orbit, the crew will need to make certain preparations for using the landmark tracking experimental equipment in the experimental program. It is presently anticipated that all of the experimental equipment will be in its proper location for the experimental program. However, it is also expected that certain mechanical constraints will be employed on certain parts of the equipment to permit it to survive the launch environment. For example, the gimballed tracking mirror located at the telescope aperture (Section 5) can be expected to require such constraints, which must be removed by the crew. There may also be constraints on the spatial-frequency filter storage and retrieval device (Section 5.5) or on the optical-to-optical interface device. It is anticipated that these preparation operations can be accomplished by one crew member in approximately 0.3 hour.

b. Experimental System Checkout

After the system preparation, the crew will perform a checkout of the entire system. Emphasis will be on verifying the operation of all mechanical moving parts, including the 2-axis tracking mirror and the spatial frequency filter storage and retrieval system. Electrical test signals will be applied to these moving parts to verify their proper operating condition. In addition the operation of the critical electronic equipment, such as the electro-optical readout device, will also be verified by the introduction of electrical test signals. In the event that proper operation of any experimental equipment cannot be verified, then appropriate remedial action will be initiated by the crew, with guidance, if necessary, from earth-based personnel. It is anticipated that system checkout will be a one-time event on a given flight which can be accomplished by one crew member in approximately 0.4 hour.

c. Viewing Conditions Evaluation

Evaluation of the viewing conditions will provide a basis for a "go/no-go" decision relative to the experimental operation with each of the landmark tracking experiments on the flight plan. This decision will be based on a direct observation of a large area of the Earth's surface through the 0.305-meter observation window, as well as by way of the TV monitor. It is anticipated that the "go/no-go" decision may also be assisted by a cloud-cover monitor[1] if available, which might provide another indication of the viewing conditions. There may also be some input from ground stations on viewing condition. In the event that one or more of the landmark areas of the baseline plan are judged to be unavailable, the crew will evaluate the viewing conditions of the alternative landmark areas and will make an appropriately revised experimental plan of the tracking procedures.

d. Initiation of Tracking and Recognition Experiments

We anticipate having a planned sequence of landmarks for which the acquisition and tracking will be enabled automatically by the application of data from the inertial reference subsystem. The crew will initiate the experimental operation, and will re-initiate it, if necessary. The planned

[1] No cloud cover monitor is presently being assigned to this experiment. The reference here is to its possible use if it were already available on ATL for other reasons.

agenda of the experiment will include a listing of landmarks to be identified and tracked, together with the nominal times when they should be available for viewing and the nominal directions for that viewing.

e. Crew-Monitoring Functions

The crew will be provided with facilities to monitor key functions of the system. The same candidate "live" image which is being introduced to the coherent optical data processing system will be made available for observation by the crew, via a shared image of the scene observed by the telescope (Section 5). In addition, a wider-angle view of the earth's surface, including the landmark area, will be available through the ATL viewing port which is located between the two air locks.

During the coherent correlation procedure, a scope will permit a viewing of the "correlation spot" which is produced on the electro-optical read-out device, made possible by way of a split-screen technique. Such an observation will permit estimates of correlation signal-to-noise ratio during the performance of the experiments.

During the experiment certain numeric displays will be provided which will permit monitoring of the progress of the experiment. These numeric displays will be provided on the control and display monitor console which will be part of the experiment equipment package. Available for digital display, upon command, will be the following:

- Two-axis orientation of the tracking mirror
- Two-axis commanded orientation of the tracking mirror
- Two-axis electro-optical readout of the location of the "correlation spot"
- Serial code number of the candidate landmark being recognized and tracked
- Serial code number of the matched spatial-frequency filter being used
- Percent cloud cover of scene observed through telescope and obtained through the cloud cover monitoring sensor if available (optional)
- Electrical parameters (e.g., sensitizing AC and DC voltages) of the optical-to-optical interface device. Typically these devices will require some electrical pre-sensitization which would be desirable to monitor.

f. Data-Taking Functions

There will be some requirements for manual data recording, primarily notations of progress of the experimental program and of performance deviations from the planned baseline experiment program. Such data will supplement the primary data which will be recorded automatically via the experiment monitor and data-recording subsystem.

g. Experimental Equipment Adjustments

The experimental package is designed to incorporate optical and other components which are either fixed or precision indexed to a particular location or orientation. However it is recognized that it will also be desirable to provide some precision adjustments for the alignment and focusing of such elements to permit optimization of system performance and compensation for any disturbance to which the equipment may be subjected. It will be a crew function to monitor disturbances and to make appropriate adjustments. The need for such adjustments should be infrequent (e.g., once or twice

a week) because of inherent high stability and will take relatively little time (e.g., 0.1 hr.) by one crew member.

h. Making of Matched Spatial-Frequency Filters

As we discussed previously, we plan to operate the experimental program primarily with matched spatial-frequency filters pre-made in an earth-based support laboratory facility and stored on-board the ATL for use in the matched filter storage and retrieval subsystem. However we recommend that some limited experiments be performed to evaluate the feasibility of making such matched filters on-board the ATL. On-board production of filters would involve only minor changes in the coherent optical system but would require some film processing to provide filters that can be stored and subsequently made available. Semi-dry processing of a silver halide medium might be a suitable approach, but the subject needs further investigation.

i. Constraining of Experimental Equipment

At the completion of the experimental program in any one flight, the crew must stow the equipment and/or re-fasten constraints, as required in preparation for the de-orbit, re-entry and recovery operations. It is anticipated that it will take one crew member 0.5 hour to make the necessary preparations.

7.0 DEFINITION OF LANDMARK TARGETS

It is planned that sufficient landmarks be defined as either primary or backup candidate targets for the coherent optical recognition and tracking experiments. These landmarks will be cataloged by serial number and location in terms of latitude and longitude. The landmarks will be selected on the basis of:

a. Observable location relative to the anticipated ground track of the ATL vehicle.

b. Spatial and spectral characteristics and location compatible with the objective of experimenting with a broad range of landmark types and characteristics.

c. Availability of previously recorded imagery (e.g., from previous space missions) which is suitable for making matched filters prior to the flight experiment program.

Technically, the landmarks will actually be landmark areas. Typically they will be circular in area and will have diameters ranging from as little as 5 km or less to as much as 100 km or more.

It will be desirable to select many landmarks that will be observable from the ATL on different orbits under different illumination and viewing angle conditions in order that we may evaluate the effect of illumination and viewing angle on the correlation response. Desired illumination conditions range from early morning to late evening.

The crew should have available for cue purposes a file of slides (conventional image domain) of landmarks, to be automatically displayed by the viewing mechanism provided for that purpose and described in Section 5.9 (Figure 5-2).

Number and Selection of Landmarks and Spatial Filters

In order to provide a basis for evaluation of the landmark tracking concept, the experimental program should be designed to permit recognition and tracking of a large number of landmarks. In order to provide a wide range of landmark types, sizes and illumination and viewing conditions, an estimated 30 primary landmark areas and another 20 backup landmark areas should be identified. For each of these primary and backup landmarks, sufficient number of matched filters should be prepared in the earth-based facility prior to the flight in order to compensate for small magnification changes, illumination and seeing condition variations, and some variations of viewing angle. In addition, enough spatial frequency filters should be made to provide a range of spatial-frequency bandwidth. Presently we estimate that an average of 10 filters for each of the 50 landmarks should be prepared before the flight. Consequently, there would be a total of about 500 filters to be taken on board the spacecraft. During the experiment, the matched filters will be selected at given times based on the expected visibility of landmarks. Since any given candidate image will be formed on the optical-to-optical interface device, there may be opportunity to perform a sequence of tests to compare the relative performance of several matched filters made for a given landmark. The number of such tests which can be made will be limited only by the dynamics of the scene and/or storage life, if any, of the optical-to-optical interface device.

It is not anticipated that multi-plexed matched filters will be used on the early flight experiments. However, the use of such filters represents a possible future step.

Previous manned flight plans and operational results provide a basis for selection of landmarks for the ATL experiments. Reference 28, for example, lists several hundred landmarks planned for use with the Apollo program. This reference places each of these landmarks in one of 5 categories on the basis of suitability for recognition and tracking. Other programs such as Gemini, ERTS and Skylab have also provided suitable imagery. The Army Map Service has provided 3-dimensional information on some 537 earth landmarks for use with the Apollo program. Latitude and longitude are provided to the nearest 0.001^{o}. Elevation from reference ellipsoid is provided to the nearest 10^{-4} nautical miles (0.18 m).

In one example, selection (partial) of earth landmarks could be based on a set of 14 earth targets selected as a basis for assessing communications and navigation experiment requirements (from Reference 7). These landmarks are all located in the U.S. A listing of these landmarks as taken from Reference 7 is presented in the table below:

Location of 14 Ground Target Sites

Taken from LaRC Report

Sites	Latitude	Longitude	Altitude m	Altitude ft
Juneau	58.5 N	134.5 W	0	0
Mt. McKinley	63.2 N	151.4 W	6194	20320
Kilauea Crater	19.4 N	155.3 W	1111	3646
Ches. Bay Bridge	37.05 N	76.1 W	0	0
Mobjack Bay	37.3 N	76.4 W	0	0
Havre de Grace	39.55 N	76.1 W	0	0
Wallops Island	37.9 N	75.5 W	0	0
S. W. Everglades	25.1 N	81.1 W	0	0
N. W. Everglades	25.8 N	81.4 W	0	0
N. W. Everglades	25.8 N	80.7 W	0	0
S. E. Everglades	25.2 N	80.5 W	0	0
Shenandoah Park	38.5 N	78.5 W	457	1500
Mojave Desert	35.0 N	116.0 W	610	2000
Royal Gorge	38.4 N	105.2 W	1524	5000

Reference 7 also indicates that a computer program has been developed at the NASA Langley Research Center to assess and evaluate the viewability of specific landmarks from a given orbit. For a favored 370 km 57.5° inclination orbit, the above-tabulated landmarks were determined to be typically 'viewable" (i.e., 20° minimum viewing angle cut-off) about 2 to 3 times per day for durations varying from 3 to 4 minutes. It is recommended that this LaRC program be used to evaluate viewability of other landmarks from other orbits which may be considered.

8.0 EXPERIMENT PACKAGE DESIGN AND LOCATION

8.1 Location

It is planned to incorporate all the experimental hardware, including the telescope scanning and tracking mirrors, the coherent optical data processor and all the crew interfaces, into a single package. In addition, there will be a separate control, command and display module. This plan represents somewhat of a departure from the more usual laboratory arrangement of separate components of the coherent optical processor on an optical bench or table. Our approach will facilitate operational check-outs, prior to installation in the ATL as well as after installation. Furthermore, the integrated-package design will insure a very high degree of mechanical stability and rigidity in the positioning of all of the optical components, as desired for operation of any coherent optical processor. The entire experiment package should be accessible to the crew to permit full participation of the crew in running the experiments and in taking any corrective action that may be required. The guidelines clearly preclude locating the experimental package on the pallet or at a location in the ATL which is not close to the shell of the vehicle. Accordingly, it is recommended that the experiment package should be located on the "ceiling" of the ATL, a logical location, since in normal operation the ceiling will be oriented toward the earth during most of the experiment mission. A location previously planned for one of two airlocks could be covered with a window to provide a suitable optical port, needed for telescopic observations of the earth. For the tentative design proposed, the volume of space near the port required for the experimental package would be 1.4 m x 0.55 m x 0.5 m (length x height x width), or a total volume of about 0.4 m^3, and it would be necessary to introduce a package of this size into the ATL.

Because crew participation in the experiment is of key importance, it will be necessary to have free access volume on all sides of the experiment package. Assuming that the free space about the experiment package should average about 0.3 meters, we require a total volume dedicated to the experiment package and the associated unobstructed-access space of 2 m x 1.1 m x 1.1 m or a total volume of 2.4 m^3. Figures 8-1, 8-2, and 8-3 present sketches of the suggested arrangement of equipment within the ATL. The bottom of the experiment package would be about 2.5 m above the ATL floor and therefore some handholds and footholds above the floor would be needed. Four holds of each type would probably be adequate.

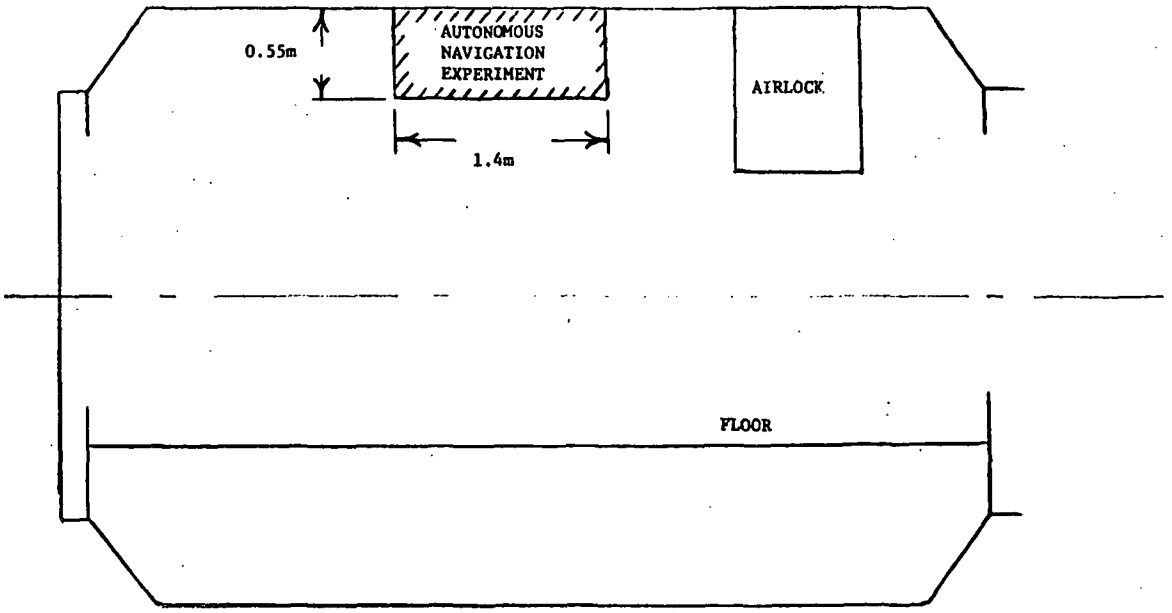

Figure 8-1. Side View of ATL Showing Volume Reserved for Autonomous Navigation Experiment Package

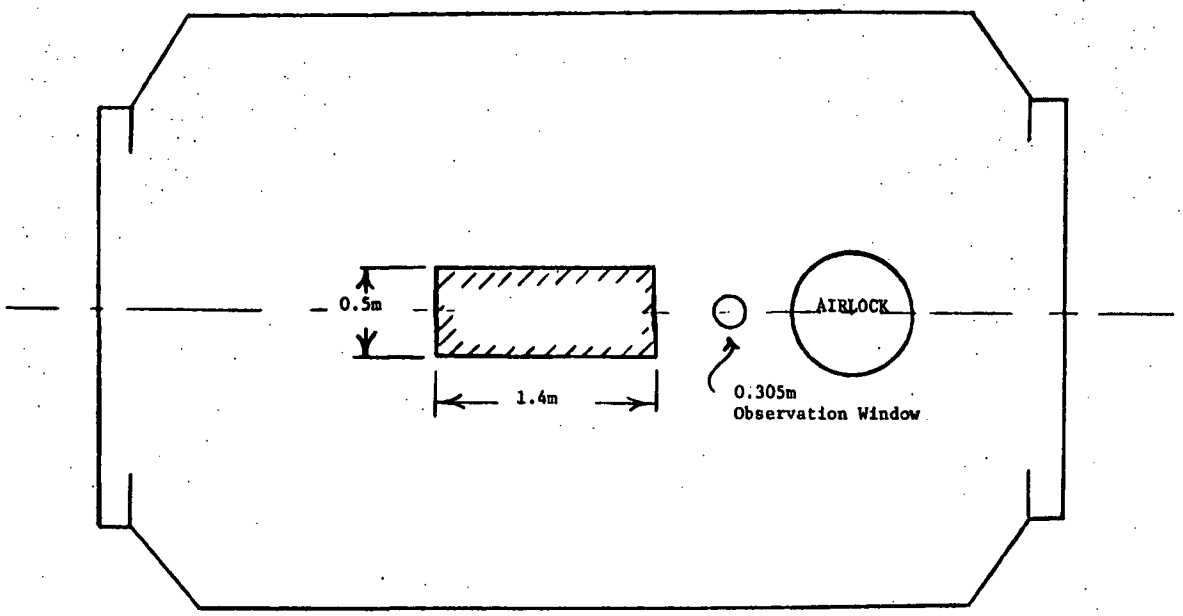

Figure 8-2. Top View of ATL Showing Volume Reserved for Autonomous Navigation Experiment Package

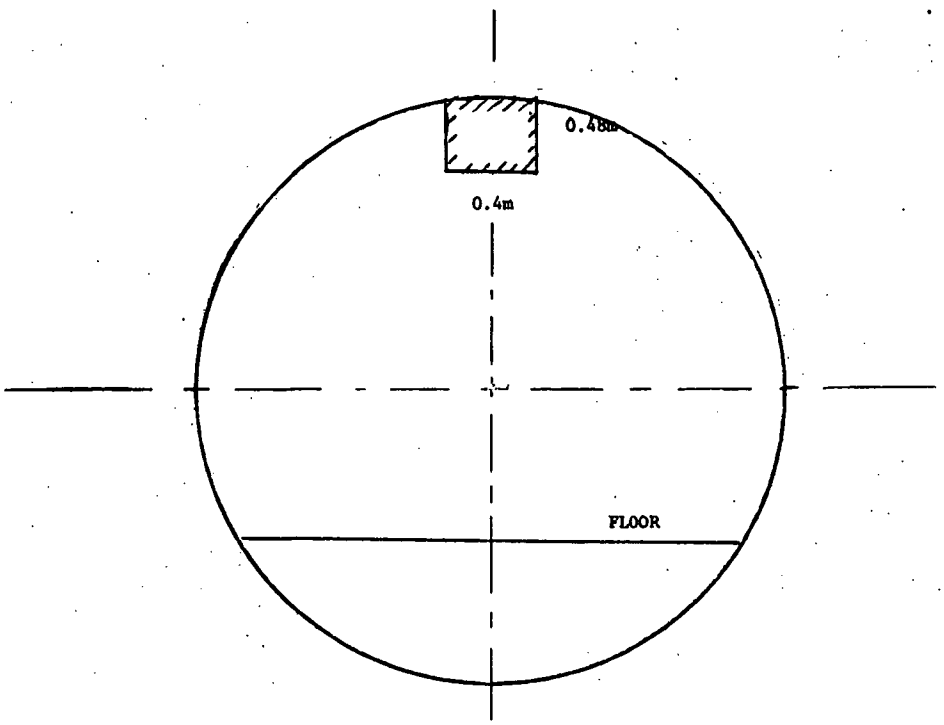

Figure 8-3. End View of ATL Showing Volume Reserved for Autonomous Navigation Experiment Package

The control, command and display module, as presently conceived, would occupy a volume with dimensions 0.3 m x 0.3 m x 0.3 m, or a total volume of 0.03 m^3. The location of this module is not critical from the standpoint of operation of the experiment. Since all of the interfaces between the experiment module and the display console will be by electrical cable, the console can be located remotely from the experiment module. Probably, it will be desirable to incorporate it into the ATL's crew-station console. The volume and the recommended location in the ATL for the experimental package are shown in three views in Figures 8-1, 8-2, and 8-3. The location of the control, command and display module is not shown since its location is very flexible and can be arranged to conform to the requirements of the crew and other ATL functions and equipment.

8.2 Design of the Experimental Package

Figure 8-4 shows a proposed layout of the experimental package. It is assumed that a protective "blow off" cover plate fastened to the vehicle skin to protect the viewing port has been removed. The proposed arrangement features folded optics to provide a compact design.

Figure 8-5 shows a shaded sketch of the proposed design ephasizing the TV-monitor camera and its integration into the input end of the system. A beam splitter is used to share the input image between the TV camera and the optical processing system. It is anticipated that a 90/10 beam splitter will be suitable, allowing 10% of the input energy to be transmitted to a relatively sensitive TV camera and 90% of the input energy to be transmitted to the relatively less sensitive optical-to-optical interface device. Not shown in the sketch is a viewing eyepiece also operating from the image provided by the telescope.

Figure 8-6 shows the proposed configuration with emphasis on the optical path required to produce an image on the optical-to-optical interface device. Figure 8-7 shows the same view but with emphasis on the folded optical path of the coherent optical data processing system. It includes the optical-to-optical interface device, as well as the Fourier transform lenses, the spatial frequency filters, the electro-optical readout device, and the path-folding mirrors.

Figure 8-8 shows an alternative configuration not employing folded optics in the coherent optical data processing system. It may have certain advantages relative to optical alignment and component accessibility. However, because it represents a less compact system, it is not a favorable design.

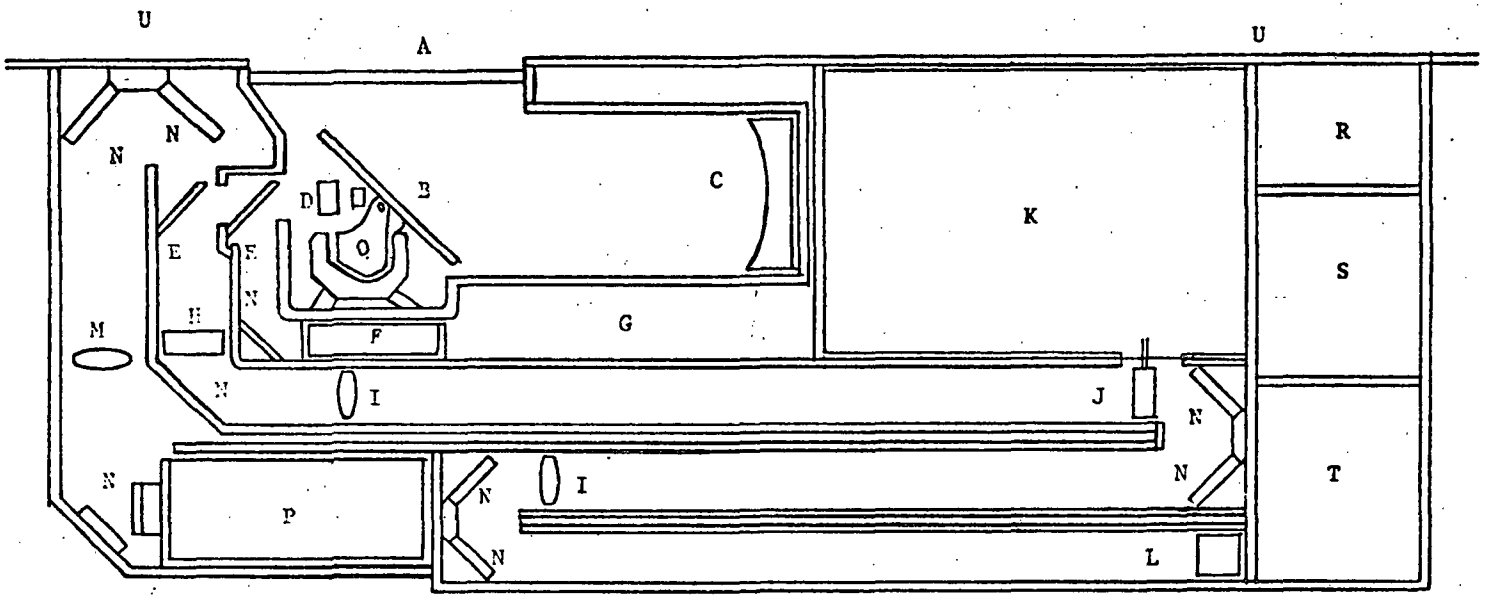

A - Window
B - Two Axis Tracking Mirror
C - Telescope Primary Mirror
D - Correction and Relay Optics
E - Beam Splitter
F - TV Monitoring Camera and Optics
G - TV Electronics
H - Optical-to-Optical Interface Device
I - Fourier Transform Lenses
J - Spatial Frequency Matched Filter
K - Matched Filter Storage and Retrieval Device
L - Electro-Optical Readout Device
M - Colimating Lens
N - Plane Mirrors
P - Laser and Expansion Optics
Q - Two Axis Drive for Tracking Mirror
R - Laser Power Supply
S - Two Axis Mirror Drive Electronics
T - Electro-Optical Readout Electronics
U - Vehicle Outer SKIN

Figure 8-4. A Proposed Configuration for a Coherent Optical Autonomous Navigation Experiment

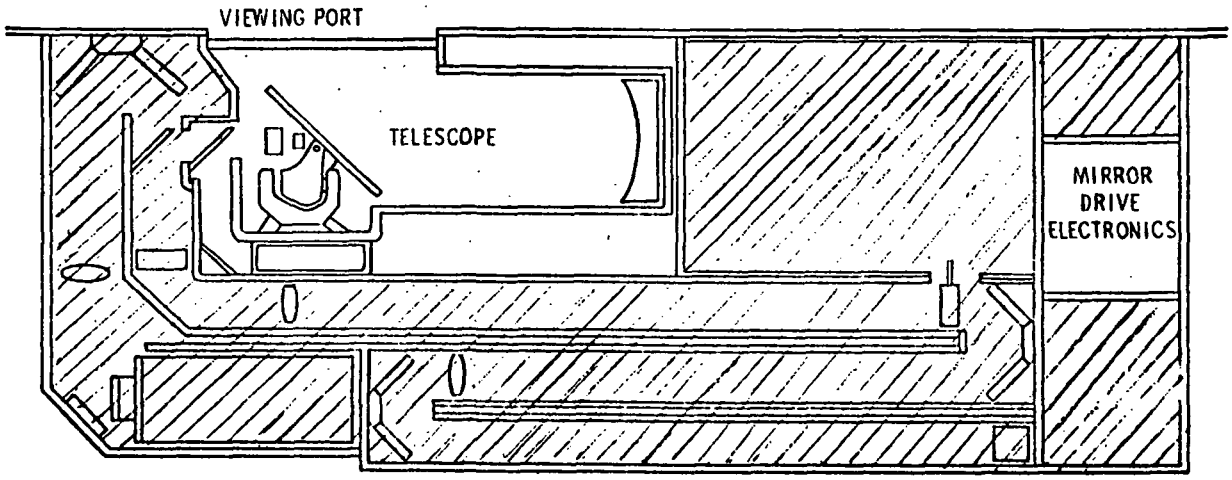

Figure 8-5. A Proposed Configuration Emphasizing Components Used for Video Camera Monitor

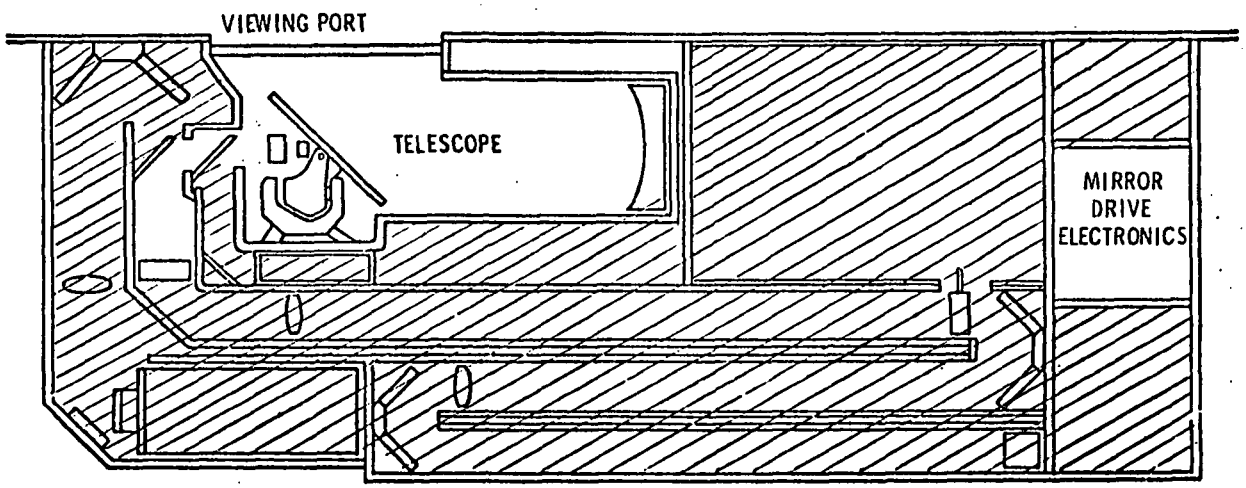

Figure 8-6. A Proposed Configuration Emphasizing Components Used in Recording Input Image

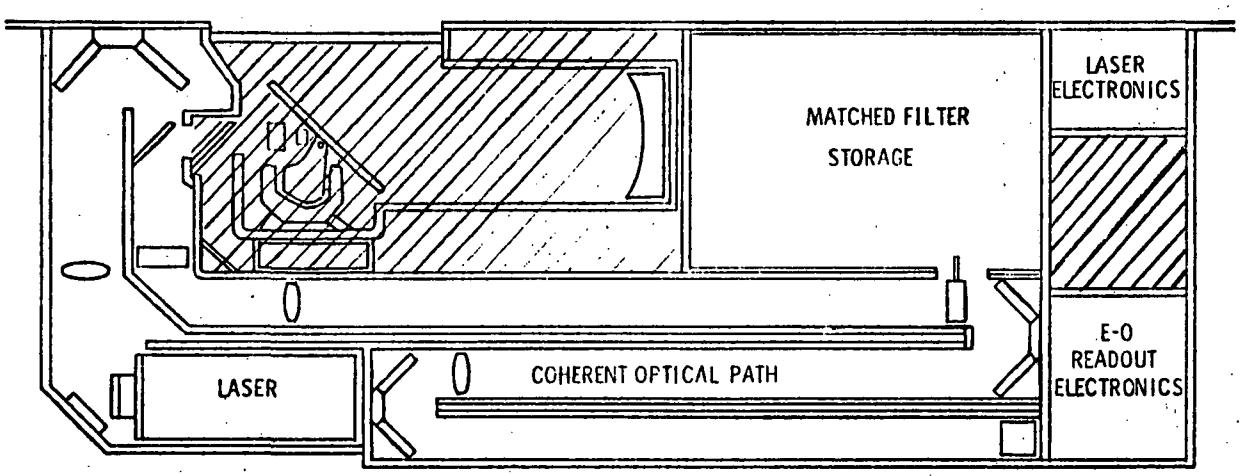

Figure 8-7. A Proposed Configuration Emphasizing Elements of the Coherent Optical Processor

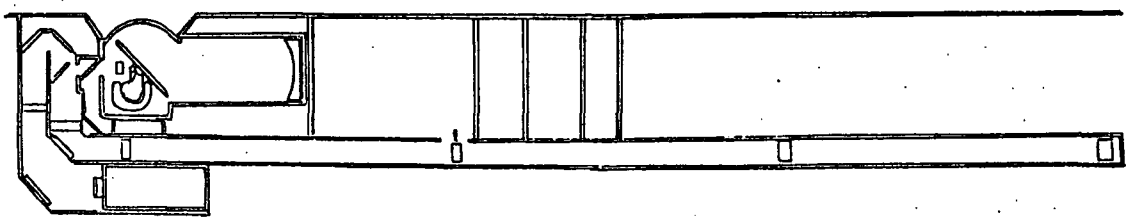

Figure 8-8. An Alternative Configuration for the Autonomous Navigation Experiment

9.0 VEHICLE-ATTITUDE CONTROL AND STABILITY REQUIREMENTS

For purposes of experiment design, we assume that the vehicle will be nominally oriented to the local vertical. As we indicated in Section 5-1, a two-axes plane tracking mirror will provide acquisition and tracking of landmarks located off the local vertical, obviating the need for specific vehicle attitude maneuvers. Rotation of the tracking mirror will provide a capability for directing the effective telescope optical axis up to about 30^{o} in any direction from the nominal vehicle attitude. In addition to permitting off-nadir tracking of landmarks, the mirror can provide some compensation for the vehicle attitude should it be directed off the direction to the nadir. We estimate that the vehicle could be oriented as much as 10^{o} off the direction of the nadir for large portions of the experimental flight program without significantly degrading the experiment.

With regard to instabilities of vehicle attitude rates, there are no critical requirements so long as these disturbances have frequencies well below those in the range of capability of the tracking mirror servos and also below any critical response resonant frequencies of the mirror or of any other mechanical components. Since the servo response can be designed with response as high as 50 radians/sec and since the mirror and other mechanical components can be made sufficiently stiff to have characteristic response frequencies even higher, there does not appear to be a severe mechanical stability requirement imposed on the vehicle by the experiment. Possibly the most serious problem of this type will be the effect of the crew's motion on the experiment. In the worst case, however, it may result only in the imposition of some restrictions on movement of the crew during certain critical stages of the experiment. The time intervals during which their motion might have to be restricted should not exceed 5 minutes.

10.0 PERFORMANCE ERROR ANALYSIS

10.1 Error Sources

This section will be concerned with the primary sources of error in the experiment. The purpose of this discussion is to pinpoint error sources and to arrive at a budget of error sources to be used as a guide in experiment design and evaluation. These error sources, not necessarily all distinct, can be listed and categorized as follows:

Instrumentation Error Sources

- Refraction of viewing port
- Angular position uncertainty of tracking mirror.
- Misalignment of telescope optical path from tracking mirror to optical-to-optical interface device
- Image position uncertainty on optical-to-optical interface device
- Laser beam alignment uncertainty
- Alignment Uncertainty of the Fourier transform optical path
- Position uncertainty of the matched spatial-frequency filter
- Landmark position definition uncertainty encoded in matched filter
- Resolution and linearity limitations of electro-optical readout
- Errors due to rotation and/or magnification compensation technique (not included in preliminary design)

Observation Error Sources

- Mapping uncertainties of landmark.
- Refraction effects of atmosphere.
- Errors due to image motion.
- Measured position uncertainty due to viewing degradation (e.g., viewing angle effect).

Each of these error sources will be discussed in the following sections.

Computational and System Error Sources

Certain of these latter error sources are uniquely related to the autonomous navigation algorithms and other design features of a navigation system. Since performance of a total autonomous navigation system goes beyond the scope of the present experiment, these computational error sources will not be considered further here, except for a listing of the primary ones:

- Errors in time reference.
- Errors in gravity model.

- Errors in drage estimation.
- Attitude reference errors.
- Other computational errors.

10.2 Refraction by Viewing Port

The primary source of tracking error associated with the viewing port is expected to be residual distortion of this optically flat surface due to the pressure differential between the spacecraft and outer space. The distortion can be minimized by intentional introduction, during manufacturing, of compensating curvature, so that the port will have a nominal flatness when subjected to the differential-pressure stress. As a tentative specification, we required that the viewing port contribute no more than 4 arc seconds of error (1 sigma) while the telescope is operating anywhere within its intended field of view.

10.3 Angular Position Uncertainty of Tracking Mirror

In general, a given uncertainty in the position of the two-axis tracking mirror will result in a viewing-angle error which is twice that of the position error of the mirror. Proper design considerations should hold the errors in tracking-mirror angle to acceptably small values, e.g.,

- Use of precision shaft encoders for both axes of the tracking mirror drive
- Use of high-stability lightweight mirror mounts and gimbals
- Use of the laser in the mirror alignment

Most of the available encoders make use of optical encoding techniques. Shaft encoders exist that have resolutions up to 23 bits (readout resolution of $2^{-23} \times 2\pi$ rad). However, for the present application encoders with somewhat more modest performance are recommended. Either a 19-bit or 20-bit encoder should be appropriate. These can provide mirror position readout resolutions of 2.48 and 1.24 arc seconds, respectively, or tracking resolutions of 4.96 and 2.48 arc seconds, respectively. Maximum tracking error is one-half the tracking resolution. (For example, a 19-bit encoder is expected to provide a maximum tracking error of 2.48 seconds.) For present planning purposes a one-sigma tracking error of 2.48 arc seconds is assumed in each of the two orthogonal tracking axes, or a 2-axis uncertainty of 3.4 arc seconds (one sigma). These errors correspond to the incorporation of 19 bit encoders in each axis. A brief summary of available angle encoders has been presented in Section 5.

The use of high-stability light-weight mirror mounts and gimbals would reduce uncertainty in mirror orientation. These components made, for example, of berylium, could be expected to have high mechanical stability, due to the inherent high strength-to-weight ratio of berylium.

By use of the laser in a mirror-alignment calibration mode, it is expected that error in the tracking mirror alignment can be kept small. Such an active calibration may be either an initialization type of calibration or it may be a continuing calibration which takes place as part of each tracking operation.

Two other approaches have been considered for determining mirror orientation but are not recommended for the initial flight experiment. One approach would be to use discrete indexing of the mirror angle orientation in two axes via precision mechanical detents, as an alternative to use of precision shaft encoders. Such an approach is possible, since the tracking mirror is not to be used as a nulling device. A sufficient number of mechanical detents would be required to permit the total field of view to be covered by repositioning of the instantaneous field of view at discrete intervals. Although this approach has the advantage of simplicity, it is not recommended because it has less operational flexibility than that afforded by precision optical encoders and because it does not permit any image motion compensation by means of the tracking mirror.

The other approach to mirror-position determination that we have considered involves relating the vehicle attitude measuring system (or the inertial reference system) directly to the tracking mirror, thereby eliminating first order effects of tracking mirror misalignment. This approach could be implemented by using optical techniques for referencing the inertial reference unit to the tracking mirror, possibly making use of the laser of the landmark tracker as the source of illumination for the alignment reference optical path. Although this type of optical alignment has merit, is is not presently judged as essential to the operation of the experiment and hence is not recommended for incorporation in the initial experiment mechanization package.

10.4 Misalignment of Telescope Optical Path from Tracking Mirror to Optical-to-Optical Interface

The telescope optical elements are the primary telescope mirror, the refractive correction elements and the beam-splitting optics used to form the input image as shown in Figure 1-1 or Figure 8-4. Unlike the tracking mirror, the reflective or refractive elements of this optical link are not intended to move. Our concern then is to maintain and confirm the mechanical rigidity of these elements when they are subjected to the mechanical and thermal stresses during and following the launch operation. It is expected, therefore, that it will suffice to provide only a one-time alignment check of this optical path. Any misalignment of the tracking mirror and of the telescope would be measured as a single entity. However, in evaluation of this experiment or subsequently in an autonomous navigation system, compensation for mechanical misalignnment need not be performed mechanically; it can be performed analytically in the data processor. A preliminary analysis indicates that the total uncompensated misalignment of the telescope optics can be maintained to 2 arc seconds (one sigma). If we use this approach of misalignment compensation, the misalignment of the telescope optics does not appear as a first-order effect.

10.5 Image Position Uncertainty on Optical-to-Optical Interface Device

As we discussed in Section 5, we plan to design the experiment hardware to accept any one of several alternative modular optical-to-optical interface devices. Hence, all possible image-position error sources should be considered for each of the candidate devices. In most cases the candidate interface media are expected to be operated entirely in situ in the coherent optical chain. Therefore, the primary source of position uncertainty is the possible shift in the mechanical indexing of the optical-to-optical interface during the in situ operation. Mechanical detent indexing of modules of this type can commonly be accomplished with 1 sigma uncertainties of 5 to 10 micrometers, corresponding to 10^{-4} to 2×10^{-4} of the 50-mm image format size, or to 3.6 to 7.2 seconds of the selected 10^{o} field of view. Recognize, however, that this represents uncertainty between successive re-indexing operations. For in situ operations, the uncertainty in continued indexing will be much less. An allowance of 0.5 are seconds (1 sigma) for this uncertainty should be reasonable, for modules with in situ operation. The only exception to in situ operation presently being considered is that of conventionally processed silver halide media, which would require that the photoplate of film be removed from the optical path for development. Errors may result from re-indexing the film module after development and also from migration of the image on the film due to film warping and shrinkage. Since both of these sources of error are expected to be in the neighborhood of 10^{-4} of the image size, a resultant error of 5 arc seconds (1 sigma) would be expected for image-position uncertainty in using silver halide media.

For most of the other devices there is not expected to be any observable shift in the location of the image relative to the module frame. Some additional small shift may occur in the case of the in situ liquid development device. However, this is expected to be much less than conventional development since the liquid development does not involve drying of the film and since the liquids used can have "matched" swelling properties of the gelatine and hence can reduce "grain migration" in the image. However, since this is expected to be less than the registration uncertainty of the module itself it will be neglected.

In summary, this source of error (1 sigma) is budgeted at 0.5 arc seconds for all alternative devices except conventionally developed silver halide, which is budgeted at 5 arc seconds.

10.6 Laser Beam Alignment

In the ideal case the input image recorded on the optical-to-optical interface device will be illuminated by a uniform collimated laser beam which is incident normal to that device. Obliquity of incidence can cause two effects: displacement of the spatial frequencies of the input image relative to the recorded spatial frequencies of the matched filter and displacement of the recognition (correlation) spot on the output plane. The first effect will reduce the level of the correlation signal, whereas the second effect will introduce error into location of the landmark. We will at first assume that, for the spatial frequencies of interest, the first effect will be negligible. The second effect will provide a position uncertainty which is equal to $2F\ (\delta x)$, where F is the focal length of the Fourier lenses and (δx) is the laser illumination misalignment angle. Misalignment can be reduced by an initial manual alignment calibration and correction, consisting, e.g., of inserting a recorded test pattern at the input plane and reading out its location at the output plane. In the simplest case, the test pattern can be a pinhole. If a single-unit calibration procedure is followed we expect that laser alignment (δx) can be maintained to 1 arc second or 0.5×10^{-5} radians (1 sigma), corresponding to a displacement error of 4.4 micrometers for lenses of 44 cm focal length. These tolerances correspond, for the 10° field of view and 50 mm frame size, to a landmark pointing error of 1 arc second (1 sigma).

10.7 Alignment of the Fourier Transform Optical Path

The effect of misalignment of the transform optics is similar to that of misalignment of the laser. One can minimize this effect by rigidly mounting the components. The design of optical components and equipment having both good position stability and positioning ability, while operating in a zero-g environment, represents a major task in the ATL experiment design. From an evaluation of existing equipment and an evaluation of the expected effects of a zero-g environment, we expect that alignment of the Fourier optical path can be maintained well enough to prevent more than a 3-sigma position error at the output plane, i.e., an error equivalent to that associated with the expected laser-beam misalignment.

10.8 Position Errors of Matched Filter

In order for the desired correlation to be obtained, it is necessary that the matched spatial frequency filter be properly located in the coherent optical readout system. Errors in filter location will generally reduce correlation performance in terms of signal-to-noise ratio, but generally will not cause significant error in position readout. Both lateral and longitudinal errors need to be considered (Reference 29). For an assumption of uniform white noise, the performance, P, is defined as:

$$P = \mathrm{Sin}^2 \left(\frac{2\pi}{\lambda} \frac{L}{F}\right)$$

Where:

λ = laser wavelength

L = a characteristic "length" of the signal

F = the Fourier lens focal length.

Reference 29 indicates that, to avoid measurable pointing error, one should insert the matched filter with typical maximum uncertainties of 5 to 20 micrometers, values well within the capability of manual or mechanical positioning devices.

10.9 Landmark Position Uncertainty Encoded on Matched Filter

The matched filter, together with the geometry of the correlation recognition system, provides encoded information relative to the location of the landmark. Of key importance is the lateral position of the reference beam relative to the recorded landmark image on the optical bench when the matched filter is

synthesized. The location of the reference beam determines the spatial-frequency carrier pattern with which the landmark image is encoded.

After the filter is synthesized, a calibration should be made to determine the precise position of the correlation spot associated with the filter's use in the operational correlation, for an on-axis location of the input. This calibration would be performed as a pre-flight operation on all of the matched filters. Errors associated with the calibration process must be much less than those errors associated with the operational recognition and tracking procedures. To assure small calibration errors, we suggest that, for the calibration, the correlation spot be photographed on a high-resolution photographic plate and the location of the test correlation spot can be read out with a high-accuracy "monocomparator." Many companies make such measuring instruments that have readout positional accuracies typically in the range of 1 to 5 micrometers. One model, for example, can read out the position of a small spot with accuracies of one micrometer over a 100 mm. field. Therefore, it seems reasonable to budget an error of one micrometer for this error source (1 sigma). This corresponds to a landmark pointing error of 0.7 arc seconds (1 sigma).

10.10 Errors in Readout of the "Correlation Spot"

For most landmark tracking operations, errors in correlation-spot readout are expected to be the dominant instrumentation source of error. There are several components of this error, related principally to: finite dimensions, and non-symmetry of, the correlation spot; resolution and pulse center detection limits of the electro-optical sensor; and nonlinearities and other geometric uncertainties of the electro-optical readout device. One of the major advantages for using a solid state detector array for readout, in addition to the small size and weight, modest required power, and low voltage, is that it avoids the last of the above-mentioned sources of error. Scanning devices, by contrast, experience non-linearities and geometric-uncertainty errors which may vary with such factors as aging and levels of voltages and temperature. It has been shown (Reference 8) that these sources of errors may be reduced for these conventional electro-optical readout devices only by introducing complexity (e.g., use of reticles and/or design of ultra-linear sweep electronics).

In principle, either linear or area solid state detector arrays can be used for correlation spot readout. The linear arrays have advantages relative to cost and availability at the present time. However, they do require use of specialized type of encoding beam for making the matched filters, e.g., the use of a cruciform reference source rather than a point source (see Figure A-2, Appendix A). Hence an area array is preferred over a linear array.

Laboratory experiments indicate that typical dimensions of the correlation spot range from 1 to 10 micrometers, depending on the degree of degradation of viewing conditions. Typical solid state detector arrays will have center-to-center spacing of the sensitive elements of 10 to 21 micrometers with, interelement spacing of about 2 micrometers (Reference 30). Hence, it is realistic to assume that the correlation spot will not be larger than a single detector element. Therefore, the error in readout can be expected to be FOV/2n, where n is the number of elements in the array. It is tentatively planned that n will be 1,000 (Section 5.7). Hence, tracking error due to finite resolution of electro-optical readout can be budgeted to be 18 arc seconds (1 sigma) for the 10^{o} field of view selected.

10.11 Observation Error Sources

Mapping Uncertanties

Uncertainties of some U.S. landmark locations are measured in the tens of meters, whereas some landmark errors in the more remote areas of the world are measured in the thousands of meters. Several investigations have explored the effects of such errors on navigation performance. Reference 30, for example, shows the performance advantages that can result from including estimates of such errors in the navigation algorithms when the errors are more than 30 meters. However, since mapping errors are of primary concern for the autonomous navigation application, we will not consider them further for the landmark tracking experiment. Position errors do relate to the performance evaluation of the present experiment, but the effects of such errors can be neglected for landmarks chosen on the basis of low uncertainty of location.

Atmospheric Refraction

Atmospheric refraction causes an angular deviation between a straight line direction to a landmark and the actual observation direction (optical path), due to the decrease in air density with altitude. Reference 31 refers to this as "photogrammetric refraction". That reference shows that at the orbital altitudes of interest to the present experiment the photogrammetric refraction, $\delta\theta$, for viewing a landmark at sea level at 45^{o} from the vertical is given by (on basis of certain assumptions):

$$\delta\theta = \frac{2.34}{z} \times 10^{-3} \text{ radians}$$

where z is the altitude in km. Thus, at an altitude of 200 km this refraction angle will be 2.4 arc seconds, a value representing extreme conditions. At more realistic viewing angles (i.e., less than 45^{o}) and at higher satellite altitudes, the photogrammetric refraction will be less than 1 arc second. Reference 32 provides tabulations and algorithms to determine refraction angles for various viewing conditions, data which should be useful for a precision performance analysis of the present experiment.

Note that the above discussion relates to predicted refraction. However, for the present error analysis, the main interest is uncertainty in that prediction. The uncertainty will generally be an order of magnitude less than the predicted value, i.e., less than 0.1 arc second, and practically negligible.

Image-Motion Error

Image-motion error was discussed in Section 3. The maximum allowable exposure time was selected to typically result in a maximum image smear of 8 meters, corresponding to a pointing error of 5 arc seconds for landmarks near the nadir. Hence a 5 arc-second (1 sigma) error will be budgeted for this source of error.

Additional Errors Associated with Off-Nadir Viewing

For off-nadir viewing angles, there are possible additional errors in landmark position determination that we have not yet discussed. Some effects, such as earth curvature, are predictable and can be corrected from purely geometric considerations. It can be shown that a combination of off-nadir tracking and partial obscuration of the landmark can cause tracking errors which are not completely predictable and hence cannot be completely compensated for. In an earlier investigation (Reference 32) a computer program was developed to evaluate this effect. An example of the results is shown in Figure 10-1. These results are for a 185 km orbit altitude. For a 370 km orbit, the effect will be less severe. The figure shows the error in tracking which can occur due to obscuration of exactly one half of a landmark when it is viewed at various angles from the nadir. It shows both the total expected error and that part of the error which can be anticipated on the basis of pure geometry. Results shown are for a circular landmark having a diameter of 31.5 km and also for a landmark of 7.7 km diameter. In both cases the 50% obscuration is assumed to be that of the "nearest half" of the landmark. The figure shows that the tracking error, particularly the non-predictable part, increases rapidly as viewing angle from nadir increases, especially for the large landmarks. This type of error can be minimized by using smaller landmarks, by avoiding tracking under adverse conditions and by viewing landmarks from directions as close to the nadir as possible. When tracking at 10^{o} from the nadir the curve shows that unpredictable tracking errors due to partial obscuration can range from 25 to 50 arc seconds, whereas similar conditions at 5^{o} from nadir will cause unpredictable errors ranging from 6 to 15 arc seconds. We should recognize that 50% obscuration and a 185 km orbit represent an extreme condition, worse than that anticipated for the experiment. We are ignoring obscuration effects in our error budget, limiting our considerations to near-nadir viewing and/or low-obscuration conditions.

Because of the rather complex nature of this adverse effect and because, by the means discussed above, it can be to a large extent avoided, these effects are not included in the experiment error budgets. From this point of view the error budget can be considered to be established for conditions of low obscuration or near nadir.

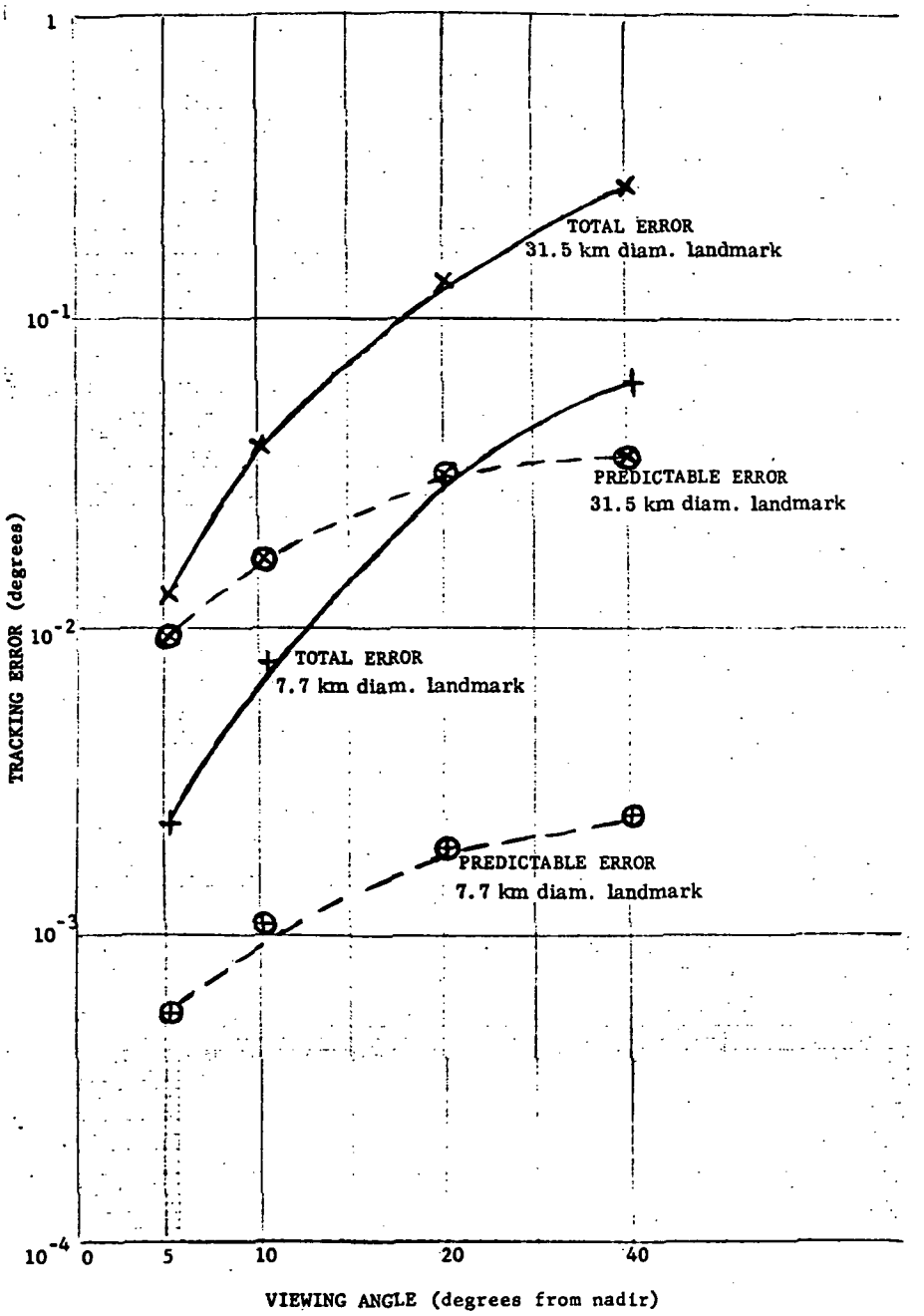

Figure 10-1. Tracking Error Due to 50% Landmark Obscuration vs. Viewing Angle, for Two Sizes of Landmarks (for 185 km orbit)

10.12 Error Summary

The foregoing discussion has provided a rationale for arriving at a 3-sigma error source budget which is presented in Table 10-1. It should be recognized that these values are nominal budgeted values for somewhat stylized conditions. The RMS coverage of the error values is 60 arc seconds, which was previously indicated as the performance goal.

Table 10-1. A Tracking Error Budget

Error Source	Magnitude of Angular Tracking Error (3 sigma) (arc seconds)	Equivalent Unsmoothed Satellite Position at 370 km Altitude (meters)	Comments
⊙ Viewing port refraction	12	20	
⊙ Tracking mirror angular position	10	16	Limited primarily by optical encoder
⊙ Telescope alignment	6	10	
⊙ Optical-to-Optical Interface Position Uncertainty	1.5	2.5	For conventionally processed silver halide material, the error and position values would be 15 arc sec and 25 m, respectively
○ Laser Misalignment	3	5	
● Fourier Optics Misalignment	3	5	
⊙ Matched Filter Position Uncertainty	< 1	< 2	Negligible error source
⊙ Position encoding Uncertainty in Making Matched Filter	2.1	4	
⊙ Resolution and linearity limitation of electro-optical readout	54	90	Position readout of "correlation spot" is dominant error source
⊙ Landmark Mapping Errors	Not included		Not included since they relate to system application not necessary to experiment
⊙ Atmospheric Refraction Uncertainties	< 1	< 1	Not a significant error
⊙ Errors due to Image Motion	15	24	Brighter scene and/or more sensitive optical-to-optical interface devices can reduce these errors
⊙ RMS Error	60	100	60 arc seconds (3 sigma) - corresponds to performance goal established for experiment

11.0 THERMAL CONSIDERATIONS

It is planned that all of the experimental equipment be located in the pressurized laboratory of ATL. Since the laboratory is designed to have an environment benign to human habitation, no extremes of thermal conditions are anticipated which might adversely affect the performance of the experimental hardware. During the course of the experimental program, the experimental equipment including the Control, Command and Display Module will release an average of about 100 watts of heat to the ATL vehicle.

12.0 DATA SYSTEM

On-Board Data Processing

There are two primary requirements for serial data processing to support the experimental program: (1) the coordinate transformations between the inertial frame and the tracking mirror pointing axis, and (2) the coordinate transformations between the tracking mirror pointing direction and the vehicle body axes. These transformations must be computed to provide the desired pointing of the tracking mirror and the digital-readout indication of the pointing. These computations should be made with sufficient accuracy so that the 3 sigma computation error is no greater than 0.005 degrees. It is anticipated that the required data computation capability may be incorporated into a central data processor in the ATL or, alternatively, in special-purpose logic modules which may be incorporated as part of the experiment command, control and display module.

13.0 INTERFACE REQUIREMENTS

13.1 Attitude Reference

The planned program requires an interface between the primary experimental apparatus and a vehicle attitude reference system to provide these two functions:

- A non-precision attitude reference for use in obtaining the desired landmark in the field of view of the landmark-tracker telescope.
- A high-precision attitude reference to provide attitude data for experiment validation (i.e., to determine the accuracy of the landmark tracking).

It is expected that the same inertial reference system will serve for both of these functions. As far as accuracy is concerned, it is the last of these two functions which is most significant. For this function, attitude accuracy should be significantly better than the accuracy goals of the landmark tracker itself (i.e., significantly better than 60 arc sec $\approx 1/3$ mrad, as we discussed in Section 3). The specific validation requirement relates to attitude determination of the base of the two axis tracking mirror. It presently appears that the inertial reference unit should provide 3-axes readout information of the tracking mirror base that has cumulative biases no greater than 0.01 mrad (3σ) and that total random errors should be no greater than 0.02 mrad (3σ). These errors include any uncertainty in the vehicle mechanical stability due to flexure or warping of structure between the inertial reference unit and the mirror base. Readout rates of the inertial reference unit of not less than 1 KHz must be available during the experiment.

The format of the reference readout, not yet specified, must provide 3-axis attitude data needed for the experiment and experiment-validation functions.

13.2 ATL Navigation

It will be necessary to provide the experiment with vehicle ephemeris for these functions:

- An approximate ephemeris, to relate the known landmarks to the landmark tracking telescope (and also to the vehicle attitude determination systems).
- A precision ephemeris, to provide the true vector direction from the ATL to the landmark during the landmark tracking. Since this function is required for experiment validation, this navigation data must be considerably more accurate than the constraint data obtained from the landmark tracking.

From the considerations in Section 3, it appears that the ATL navigation system should provide location data in 3 dimensions at the time of the tracking experiments with uncertainties of no greater than 200 meters (3σ).

The experiment validation will not be performed on the vehicle. Hence the required navigation data would not need to be in real time and would not need to be available on board the ATL. It is tentatively recommended that such data be available at the earth-based experiment-validation facility within 8 hours after the landmark tracking experiment.

14.0 EXPERIMENT VALIDATION

14.1 Objectives and Procedure

One of the principal validation tests is to determine how accurately the experiment determines the vector-direction from the spacecraft to the landmark. For each landmark recognition and tracking experiment, the location of the correlation spot on the output plane of the coherent correlator will be precisely obtained by the readout detector. The validation test requires knowledge of both the vehicle attitude and the vehicle location at the time of each tracking experiment, and will consist primarily in measuring the errors in the actual location of the correlation spots relative to the predicted location obtained from an interpretation of the ephemeris data from the Shuttle navigation system and the Shuttle attitude data from the inertial reference unit. Hence, both accurate attitude and navigation data is required for complete validation of each experiment. Experiment validation will also include some evaluation of recognition performance in terms of signal-to-noise ratio. These evaluations will be made for the various determinations on landmarks representing different spatial characteristics, contrast ratios, size, obscuration characteristics, viewing angles, etc.

Records of the landmarks images on which correlation data is obtained will be kept to aid in the experiment validation. These records will be tape recordings of the signal from the TV camera incorporated in the experiment package and/or photographs taken directly through the viewing optics. The video-tape data could be available on the ground through telemetry, whereas the photos would be available on the ground only after the completion of the flight. Data required for experiment validation will include the date and exact time of a correlation readout as well as a record of the matched filter being used.

In summary, the experiment validation would be a cooperative function between the ATL crew and the ground station, based on shuttle navigation and attitude data, the readout data of the correlation experiments, and image records of the landmarks taken at the time of the recognition and tracking experiments. Because the availability of independently obtained ephemeris and attitude data is essential to the validation we will discuss these data next.

14.2 Problems of Independent Attitude and Orbit Determination

Consideration here is given to the applicability of the baseline attitude determination and navigation system of the Shuttle to the experiment. Reference 33 provides information on the anticipated performance of the baseline Shuttle payload pointing system. Table 3-4 of that reference (reproduced here as Table 14-1) provides an indication of how well the baseline payload pointing system can determine the direction to the local vertical and also the direction to a given point on the earth (for looking at vertical or 30^{o} off vertical). In the table, the "Local Vertical" data includes attitude reference errors but not navigation errors, whereas the "earth Target" data includes both attitude references and navigation errors. It appears that landmark mapping errors are not included in any of the tabulated data.

For evaluation of the present ATL experiment, the "Earth Target" predicted errors of the baseline Shuttle system are of interest. Errors of the baseline system ranging from 0.16^{o} to 0.29^{o}, are indicated depending on altitude, viewing, aspect angle and whether the STDN[1] or the TDRS[2] navigation technique is being used as the baseline system. Note that for the STDS technique, the navigation system error contribution is nearly negligible, whereas for the TDRS technique the navigation error causes significant increase in total error, especially at low altitude, where it nearly doubles the error. Note that this attitude determination capability is about 10 to 20 times worse than the tracking performance goal of 60 arc seconds (i.e., 0.017 degree) for the presently planned ATL experiment.

(1) Space Track Data Net.

(2) Tracking and Data Relay Satellite.

Table 14-1. Payload Pointing Errors for Earth Targets (reproduced from Reference 33)

	Orbital Altitude		
	185km	370km	556km
		-DEG-	
• Local Vertical			
- STDN	0.16	0.16	0.16
- TDRS	0.16	0.16	0.16
• Earth Target			
- Looking vertical			
• STDN	0.18	0.16	0.16
• TDRS	0.28	0.2	0.18
- Looking 30° Off Vertical			
• STDN	0.20	0.17	0.16
• TDRS	0.29	0.20	0.18

The above discussion indicates a potential problem in validation of the present ATL experiment. Certain validations can be made statistically by evaluating the variance of the sequence of measurements, but presently the planned Shuttle base-line pointing determination capability appears to be about too inaccurate, by a factor of about 10 to 20, to evaluate the tracking performance goal of the coherent optical landmark tracker. Of course, the presently planned baseline system can be used to validate the principle of the landmark tracking experment, even if it is inadequate to evaluate the present goal performance.

We consider now in more detail the baseline Shuttle navigation performance. Table 14-2 (Table 3-1, Ref. 33) provides an indication of the expected navigation system performance. Position uncertainties are indicated to range between 90 and 740 meters, depending on the various factors cited, as compared with a tracking performance goal of the present experiment of 100 meters, in terms of earth-surface position. However, by making use of the STDN operation during the experiment, we could limit position uncertainties to a maximum value of 222 meters (3 sigma) for the present experiment. Thus a potential problem also exists in ephemeris determination for experiment validation purposes.

To summarize the above discussion we note that the planned baseline attitude determination system and the baseline navigation system have inadequate performance for the purpose of evaluation of the accuracy of individual landmark tracking operations. Consequently, there may be a need to significantly upgrade the performance of the presently planned attitude determination system or, alternatively, to supply a higher-accuracy attitude reference dedicated to this specific experiment and also to improve the baseline navigation system. Reference 33 does not indicate all the sources of attitude determination error which should be investigated prior to recommendation of any new attitude-reference package. It may be possible to upgrade the available attitude reference capability, for example, by using a technique of optical reference-transfer from the baseline inertial reference unit to the experiment package to avoid uncertainties associated with mechanical referencing. If a separate dedicated reference is necessary, it might make use of high performance stellar-inertial or stellar references, possibly coupled to the experiment package by optical means. This coupling could reduce attitude errors due to non-rigidity of the vehicle or experiment package.

Likewise, the baseline navigation system of the Shuttle appears to have a performance which is inadequate (by a factor of 3 to 10) to completely evaluate the performance of the present experiment in relation to its goal. However, several alternatives exist for improving ground based navigation. For example, the General Electric Company has been obtaining radio ranging to ATS satellites from Schenectady and other stations with repeatability of measurements to within 50 meters.

Table 14-2. Expected On-Orbit Navigation Accuracies (3 sigma) for 185km Orbital Altitude (reproduced from reference 33)

NAVIGATION SYSTEM	POSITION, Meters (feet) Altitude	Down-track	Cross-track	Root Sum Square	VELOCITY, Meters/Sec (feet/sec) Altitude	Down-track	Cross-track	Root Sum Square
STDN								
LOCAL (END OF TRACK)	130	110	130	222	1.2	0.15	0.6	1.3
	(440)	(370)	(430)	(730)	(3.9)	(0.5)	(2.0)	(4.4)
PROPOGATED ONE REV.	150	260	130	315	1.3	0.15	0.6	1.4
	(470)	(850)	(430)	(1030)	(4.3)	(0.5)	(2.0)	(4.8)
TDRS								
LOCAL (END OF TRACK)	90	430	460	630	0.5	0.11	0.15	0.5
	(300)	(1400)	(1520)	(2070)	(1.6)	(0.35)	(0.5)	(1.7)
PROPOGATED ONE REV.	90	610	460	740	0.7	0.1	0.15	0.7
	(300)	(2010)	(1520)	(2400)	(2.4)	(0.3)	(0.5)	(2.5)

15.0 GROUND SUPPORT OPERATION DURING FLIGHT

Because of the highly autonomous nature of the experiment, there is expected to be relatively little ground-support activity during the flight. However, the crew may use ground information on local viewing conditions in the vicinity of selected landmarks, when it is available, to supplement the information obtained directly from the orbiting ATL. There may be some limited experiment-performance evaluation at the ground experiment-command station based on telemetered data, to verify the on-board experimental procedures. As we noted earlier, the ATL crew will need precision navigation data, to be provided from the ground or from aboard via an up-link communication channel.

16.0 PRE-FLIGHT FUNCTIONS AND CREW TRAINING

Prior to the lift-off of the experiment vehicle it will be necessary to complete these tasks:

- Selection of approximately 50 landmark areas as either primary or secondary landmarks based on the selection criteria defined in Section 7.
- Fabrication of an assembly of matched spatial-frequency filters for each of these landmarks, followed by selection of approximately 500 matched spatial frequency filters to be loaded in to the matched-filter storage and retrival device.
- Performance evaluation of each of the 500 matched filters in a ground-based coherent correlation experiment.
- Complete checkout of each of the experiment system components individually and as a functioning part of the total experimental system.

Pre-flight crew training will include complete familiarization with all components and functional operations of the experimental system. These operations include the nominal mode of landmark recognition and tracking, the mode of operation in which matched spatial frequency filters are to be fabricated on board the ATL vehicle and conversion of the system to and from the filter-making mode. The crew will need to become thoroughly familiar with the focusing and positioning sensitivity of the input images and the matched spatial frequency filters, as well as with the means for correcting the focusing and positioning of these elements. It is expected that much of the crew training can be most effectively performed with a physical simulator, and plans are included in the proposed schedule for simulator training.

17.0 SAFETY

There are no hazards associated with the experiment which cannot be controlled adequately. As in typical laboratory work involving coherent optical processing, possible eye damage due to viewing of laser-illuminated images could conceivably occur if safety precautions were inadequate. This is a hazard which can be controlled by employing such features as attenuation filters in conjunction with eyepieces, etc. It is recommended that such protective measures be incorporated into the design of the experiment package.

18.0 RESULTS AND CONCLUSIONS

We have shown via the current study and previous related studies the feasibility and practicality of incorporating a landmark recognition and tracking experiment based on coherent optical techniques into the ATL. The most attractive approach is one providing a single integrated package incorporated into the ATL, rather than one based on assembly of laboratory components. The experimental package would be fastened to the "ceiling" of the ATL in an area made available by removal of one of the air locks. Off-nadir tracking would be accomplished by means of a two-axis tracking mirror located at the aperture to the telescope.

In addition to the experimental package, there would also be a command, control and display module to facilitate crew interactions with the experiment. The command and control module can be located remotely from the primary experimental package for crew convenience. Although some of the experimental programs such as selection and retrieval of matched filters can be automated, there will be opportunity for the crew to interrupt or modify the program or to run the entire experiment by manual operations. Optionally, an experimental program is anticipated which will have available to it approximately 500 pre-made matched spatial frequency filters. In addition, it is also planned to perform some limited experiments to evaluate the feasibility of making such matched filters on board the vehicle.

As a result of the present investigation we conclude that a realistic experiment can be designed with size, weight, and power requirements which are realistically attainable on the ATL, an experiment suitable for verifying the predicted capability of the technique when it is applied to a range of landmark types under various viewing conditions.

A recommended program leading to the development and execution of the planned flight experiment in 1981 is outlined in Section 19. As described in that section, the actual flight test program will be preceeded by extensive mathematical and physical simulation tests of the landmark-tracking functions. A simulation facility suited for this function will be selected early in the overall program. It is planned that the simulator will also be used for training of the crew in preparation for the planned flignt experiment.

A key recommendation is made for more extensive experimental evaluation of the most promising optical-to-optical interface devices especially the recently developed hybrid field effect liquid crystal device. This evaluation should include spectral sensitivity tests and correlation evaluation with realistically simulated landmarks.

19.0 RECOMMENDATIONS

As a result of this study a recommendation is made to proceed with detailed design of the experimental procedures and an experimental test model. This would include specific selection of all of the hardware components as well as selection some of the specific landmarks which are compatible with the planned orbit. The design should also include more detailed consideration of operational sequencing as well as the man-machine interface. A recommendation is made to evaluate the recently developed liquid crystal field effect device under accurately simulated photometric conditions to determine its suitability as the real time optical-to-optical interface device. Design alternatives to eliminate problems which may be associated with the optical window are also recommended.

Further effort is also recommended in the areas of soft mock-up design and fabrication. A mathematical simulation of the overall navigation system is also recommended so as to enable prediction of the performance of an autonomous navigation system which utilizes landmark tracking.

It is recommended that the design and fabrication of an engineering test model be undertaken and that the model be used with in a physical simulator to evaluate the experimental system and also to train crew operators.

A program plan is provided in Section 20 and includes the design and fabrication of a flight test model. The plan leads to a flight experiment in 1981. Such an in situ flight test is required to evaluate the landmark tracking concept.

20.0 SCHEDULE ESTIMATES

20.1 Experimental Flight Test

An example of a possible development program is outlined here. It is designed to bridge the gap from the present program status to the initial flight test on ATL tentatively scheduled to take place in 1981.

The program as outlined here consists of:

- Initial Design Task
- Mathematical Simulation of Experiment
- Design, fabrication and test of Engineering Model
- Design, fabrication and test of Flight Model in ATL

Initial Design Task

The objective of the initial design task is to pursue the design of a demonstration test model and a plan to use that test model to provide a complete end-to-end demonstration of the concept of using coherent optics for recognition and tracking landmarks. This document is the final report of that task.

Mathematical Simulation of Experiment

The mathematical simulation will evaluate the overall interrelationships of the planned experiment, including the interaction between the astronaut and the experiment equipment. An outline of the mathematical simulation based on discussions between the NASA (LaRC) Shuttle Experiment Office and the General Electric Space Division, is presented below.

The inputs of orbital parameters, spacecraft attitude, and available landmarks would be employed to determine the various outputs required by the astronaut to perform the experiment:

1. Time to next landmark.
2. Will next landmark be in daylight?
3. Time to a specific landmark.
4. Will specific landmark be in daylight?
5. Time to next landmark after specified period to time.
6. Will landmark be in daylight?
7. Nominal look angle to landmark (for any of the above cases).
8. Identify matched filter to select for the measurement.
9. Viewing time of landmark.
10. Summary of prior uses of a particular landmark
    - i number of times used
    - ii sun angles
    - iii cloud-cover state
    - iv viewing angle

11. When will the next target with the following characteristics be available?

    i given sun angle

    ii given viewing angle

    iii given cloud cover

The final outputs of the computer as determined by the landmark measurements would essentially be:

1. Was the correlation obtained?
2. The x and y location of the correlation spot.
3. Measured look angle to landmark
4. Difference between measured and nominal look angles for use in autonomous navigation for improving knowledge of orbital parameters.
5. Prediction of pointing-direction time history as landmark is traversed.
6. Time of measurement.

As a result of errors in the inputs and errors associated with the landmark tracker, there will be errors in the output quantities. Not only will it be important to determine the approximate magnitude of these output errors, but the relationship between the input and tracker-instrument errors. Inasmuch as the input errors (orbital parameters and attitude) can be reasonably well estimated from past work, they can be used as a basis for a practical landmark-tracker instrument design.

These two Tasks of Initial Design and Mathematical Simulation would be followed by 6 major tasks leading up to and including the flight test program in ATL in 1981. These tasks would be scheduled as shown in Figure 20-1.

The planning charts of Figure 20-2 show the scheduling of the subtasks in somewhat more detail.

Task 1 - Design, Fabricate and Bench-Test Demonstration Model

The objective of Task 1 is to complete the design of a test model, produce the model, and provide an initial operational test of the model of the landmark tracking experiment package. This model will be a relatively compact, integrated device which will have a configuration similar to the flight test model to be produced subsequently. However, it will not be designed to completely meet the environmental-performance requirements which will be imposed on the flight test model. This equipment would not be fully space-qualifiable but would, in most other respects, perform all the functions of the subsequent flight-qualifiable equipment. The test model would be used for laboratory and simulator tests and possibly for aircraft flight tests to demonstrate and evaluate the recognition and training functions under a wide range of conditions. It would also be used for some preliminary evaluations and training of the man/machine interface for the experiment.

This task will begin with a 3-month detailed design effort (Subtask 1.1). This effort will result in design drawings of the favored configuration for the Test Model. This task will include a re-definition of performance specifications and selection of key components.

As the design evolves appropriate parts and sub-assemblies will either be ordered from vendors or, alternatively, will be fabricated (subtasks 1.2 and 1.3 respectively).

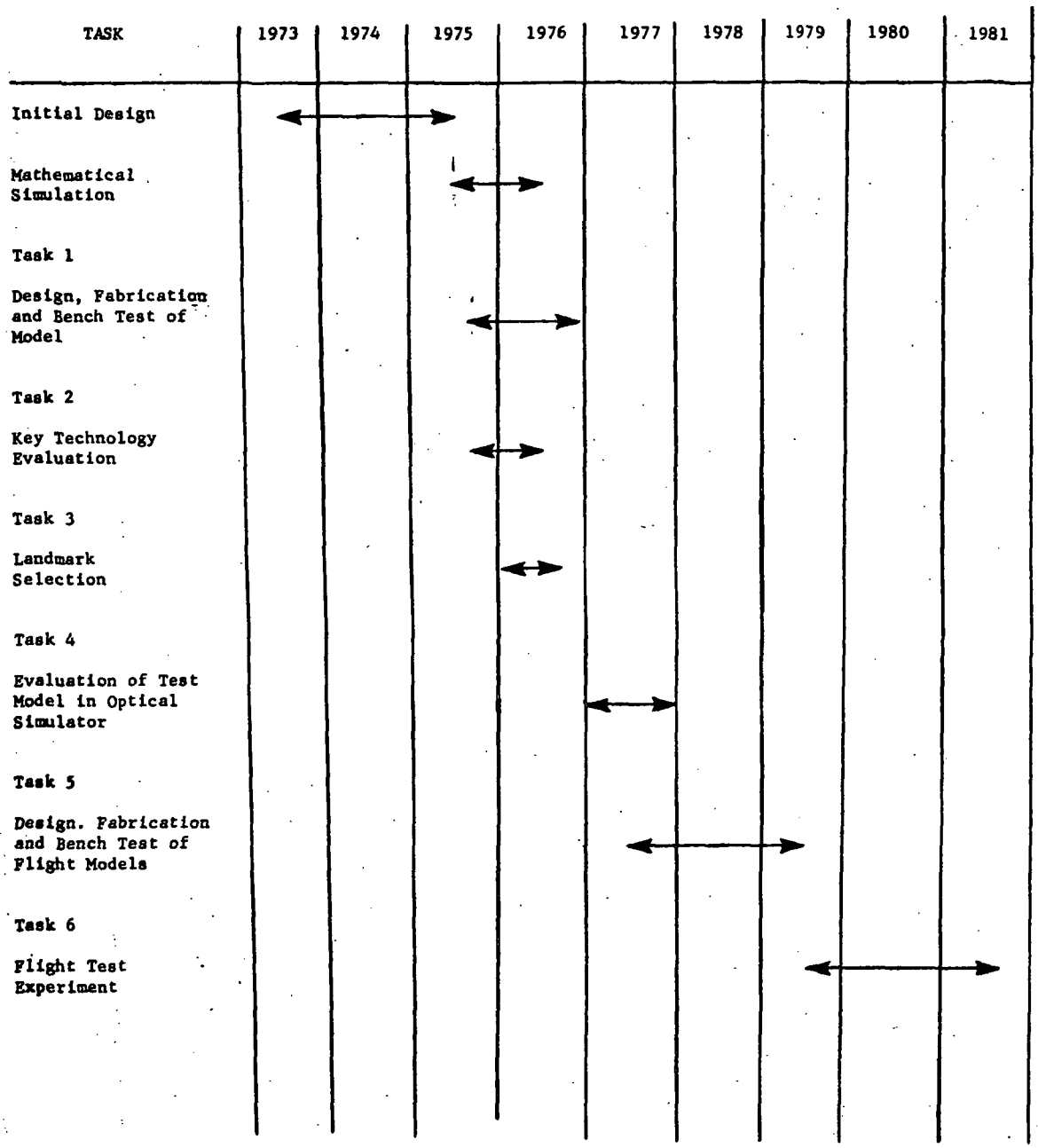

Figure 20-1. Planned Program Schedule

TASK NO.	SUB-TASK NO.	DESCRIPTION OF DETAIL MILESTONES
1		Design, Fabrication and Bench Test Model
	1.1	Detail Design
	1.2	Purchase and Delivery of Components
	1.3	Fabrication of Parts & Subassemblies
	1.4	Assembly
	1.5	Bench Test
	1.6	Debugging
	1.7	Fabrication and Installation of
		"Soft" Mockup
	1.8	Final Bench Test

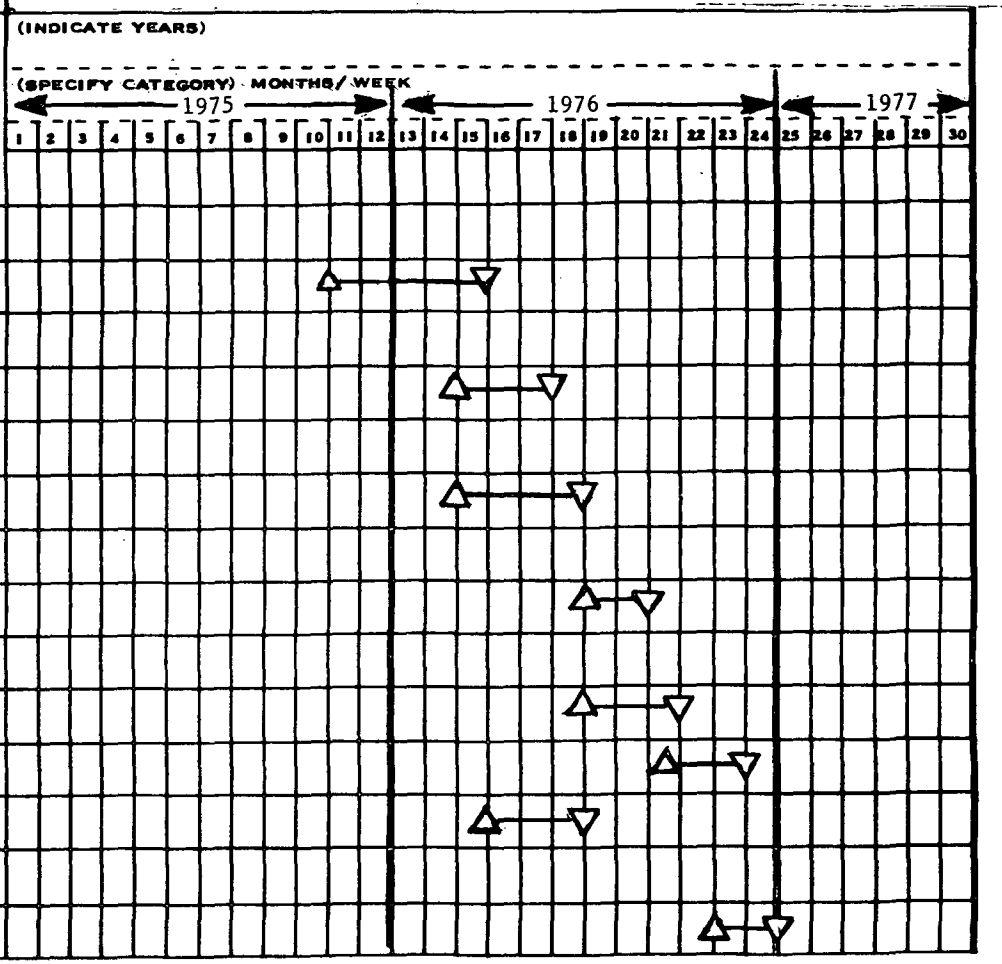

Figure 20-2. Details of Program Schedule (Sheet 1 of 6)

TASK NO.	SUB-TASK NO.	DESCRIPTION OF DETAIL MILESTONES
2		Key Technology Evaluation
	2.1	Optical-to-Optical Interface
	2.2	Spatial Frequency Filter Storage
		and Retrieval Device
	2.3	Electro-Optical Readout Device

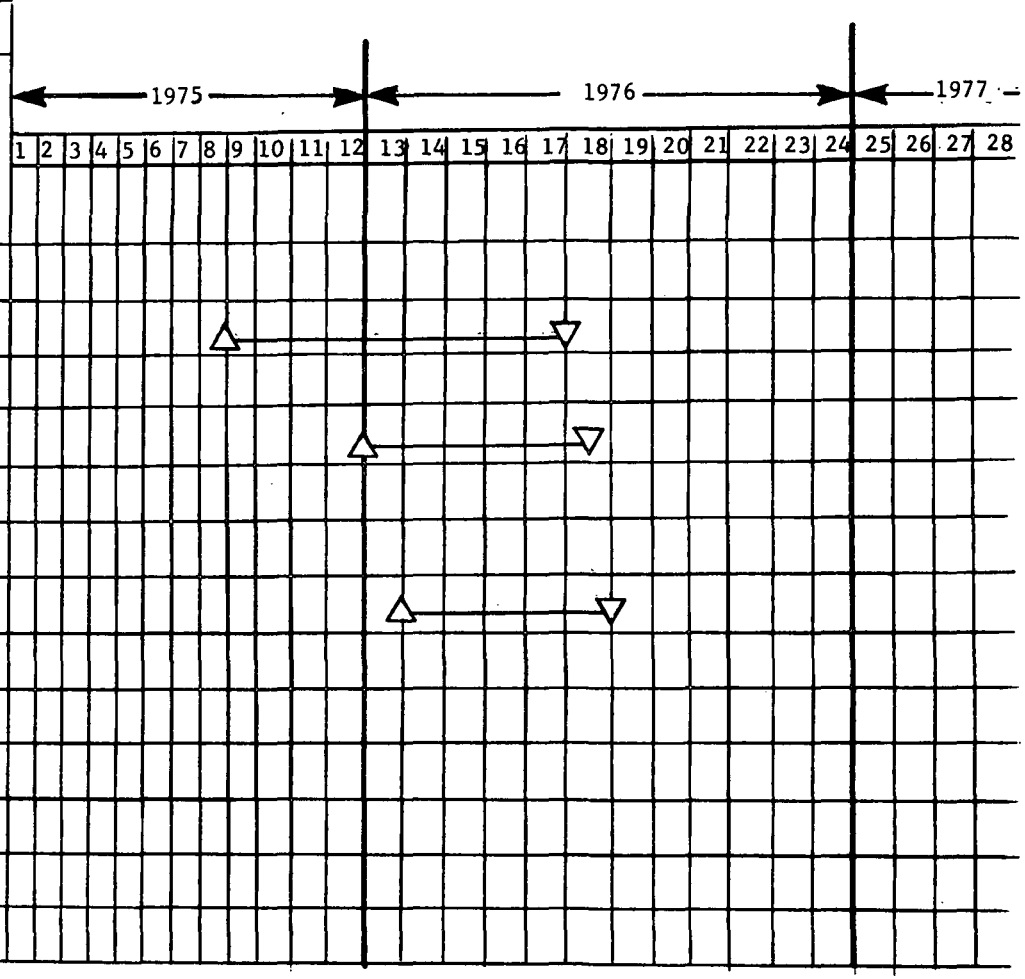

Figure 20-2. Details of Program Schedule (Sheet 2 of 6)

TASK NO.	SUB-TASK NO.	DESCRIPTION OF DETAIL MILESTONES
3		Landmark Selection
	3.1	Selection of Landmarks and Landmark
		Images
	3.2	Fabrication and Initial Tests of
		Matched Filters

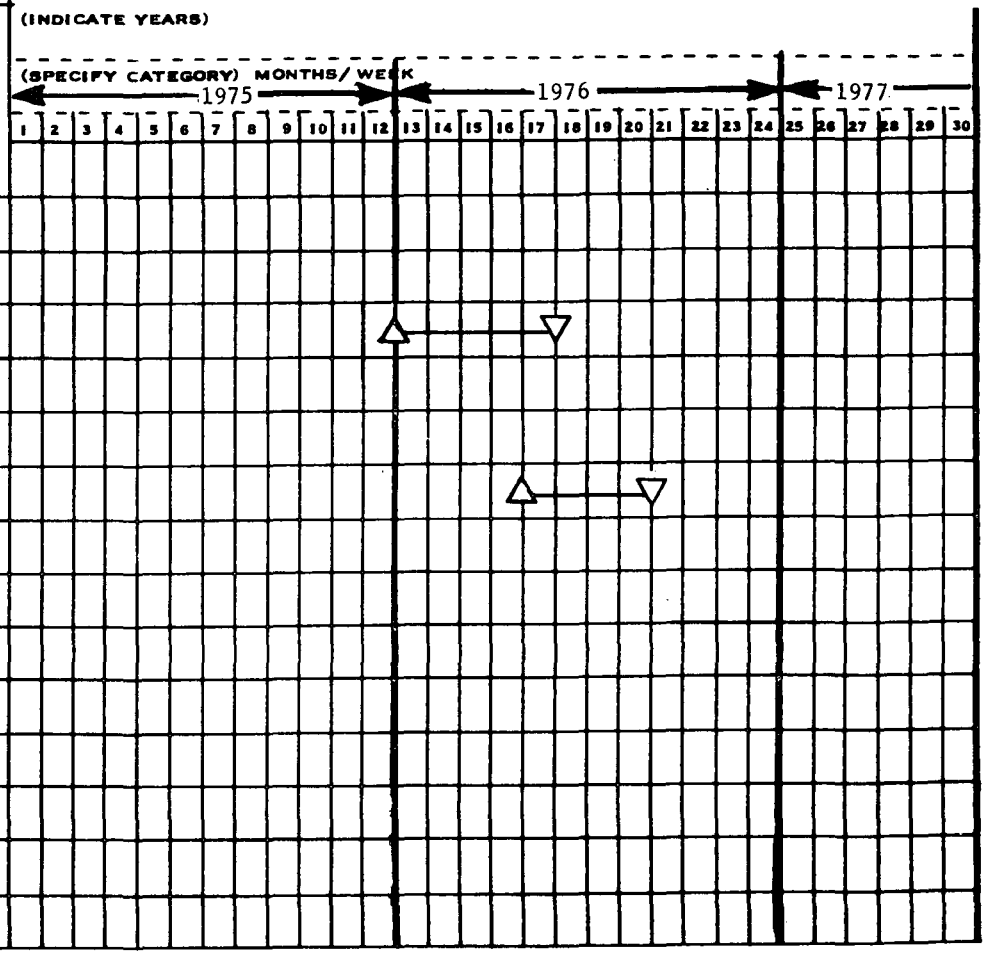

Figure 20-2. Details of Program Schedule (Sheet 3 of 6)

TASK NO.	SUB-TASK NO.	DESCRIPTION OF DETAIL MILESTONES
4		Evaluation of Test Model in Physical Simulator
	4.1	Selection of Simulator
	4.2	Design of Simulation Plan
	4.3	Checkout of Test Model on Simulator
	4.4	Detailed Performance Tests on
		Simulator
	4.5	Modification (as required) of Test
		Model Based on Simulator Tests
	4.6	Man-Machine Test with Astronauts and
		Test Model in Simulator

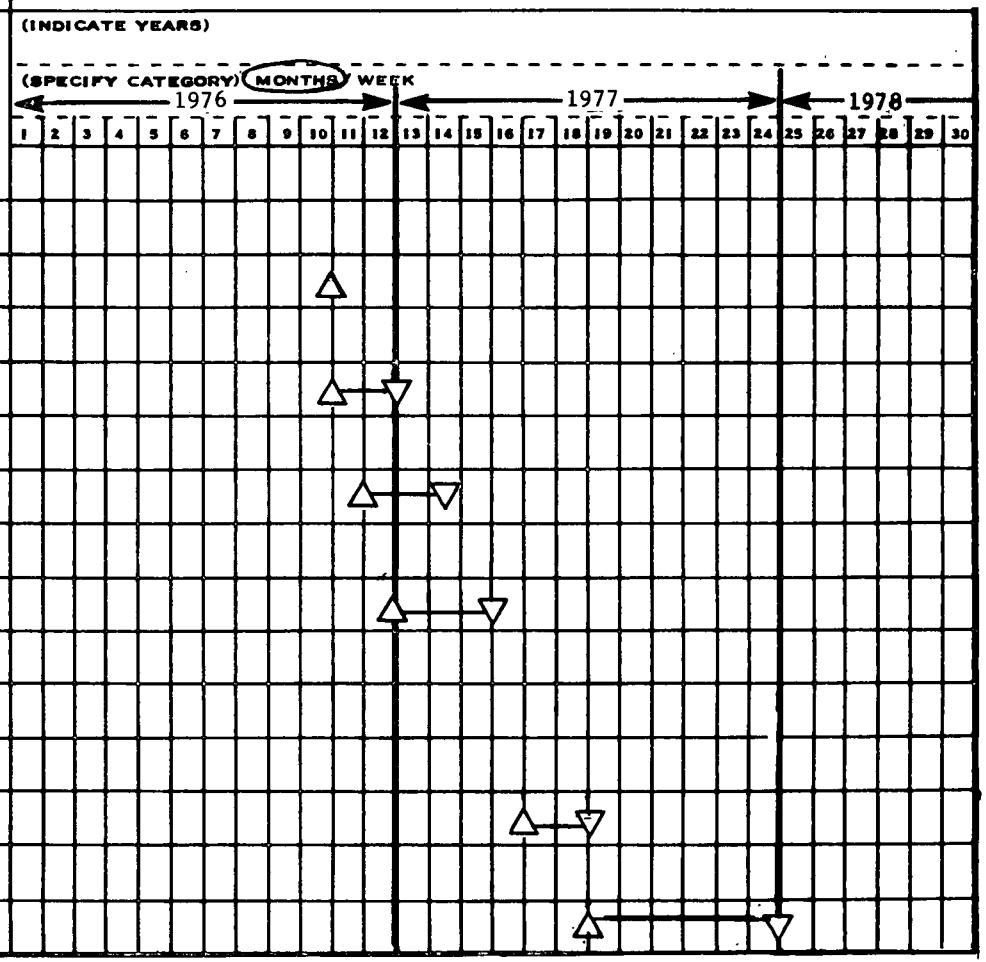

Figure 20-2. Details of Program Schedule (Sheet 4 of 6)

TASK NO.	SUB-TASK NO.	DESCRIPTION OF DETAIL MILESTONES
5		Design, Fabrication and Bench Test of Flight Models
	5.1	Detailed Design
	5.2	Purchase of Components
	5.3	Fabrication of Parts & Subassemblies
	5.4	Assembly
	5.5	Bench Tests
	5.6	De-bugging
	5.7	Final Bench Tests
	5.8	Environmental and Life Tests

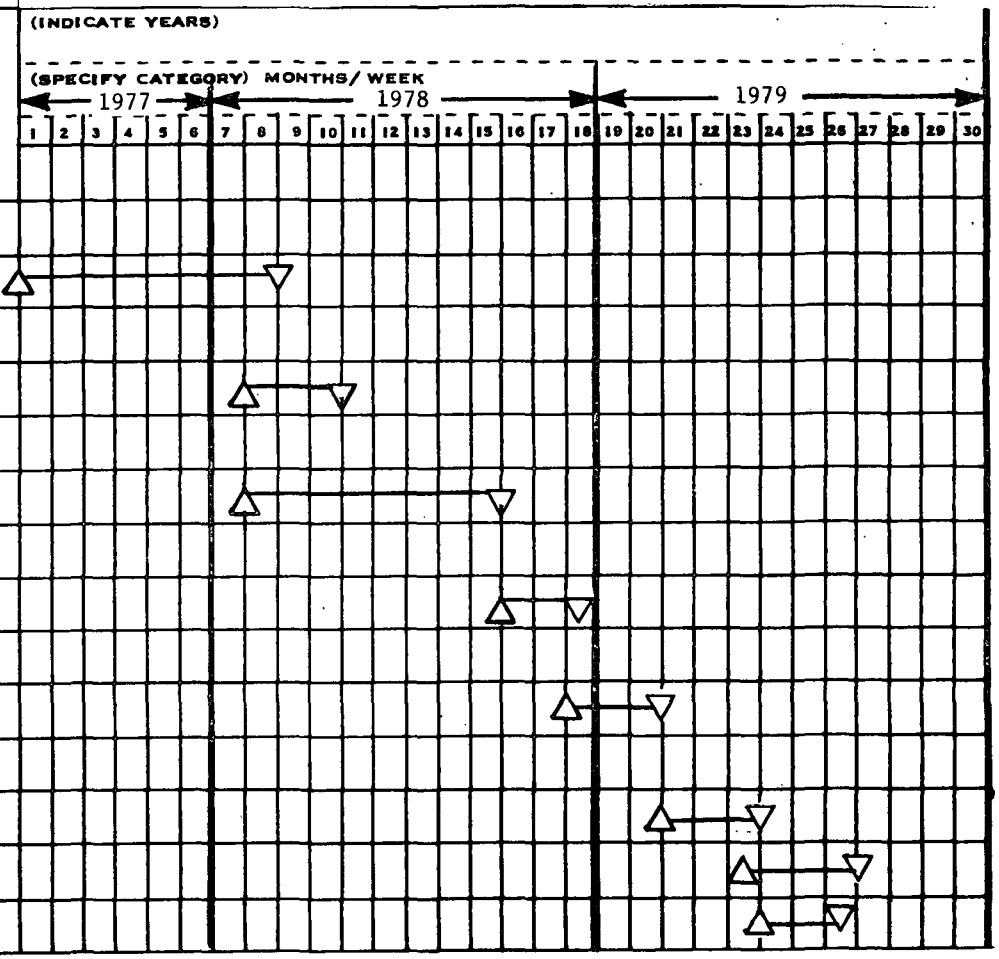

Figure 20-2. Details of Program Schedule (Sheet 5 of 6)

TASK NO.	SUB-TASK NO.	DESCRIPTION OF DETAIL MILESTONES
6		Flight Test Experiment Phase
	6.1	Detailed Flight Test Planning
	6.2	Delivery of 2 Flt.Test Models to NASA
	6.3	Experimental Checkout at NASA
	6.4	Crew Training with Flt. Qual. Model
	6.5	Installation of Experiment in ATL
	6.6	Period of 1st Satellite Space
		Flight Experiments
	6.7	Post-Flight Analysis of Data and
		Procedures

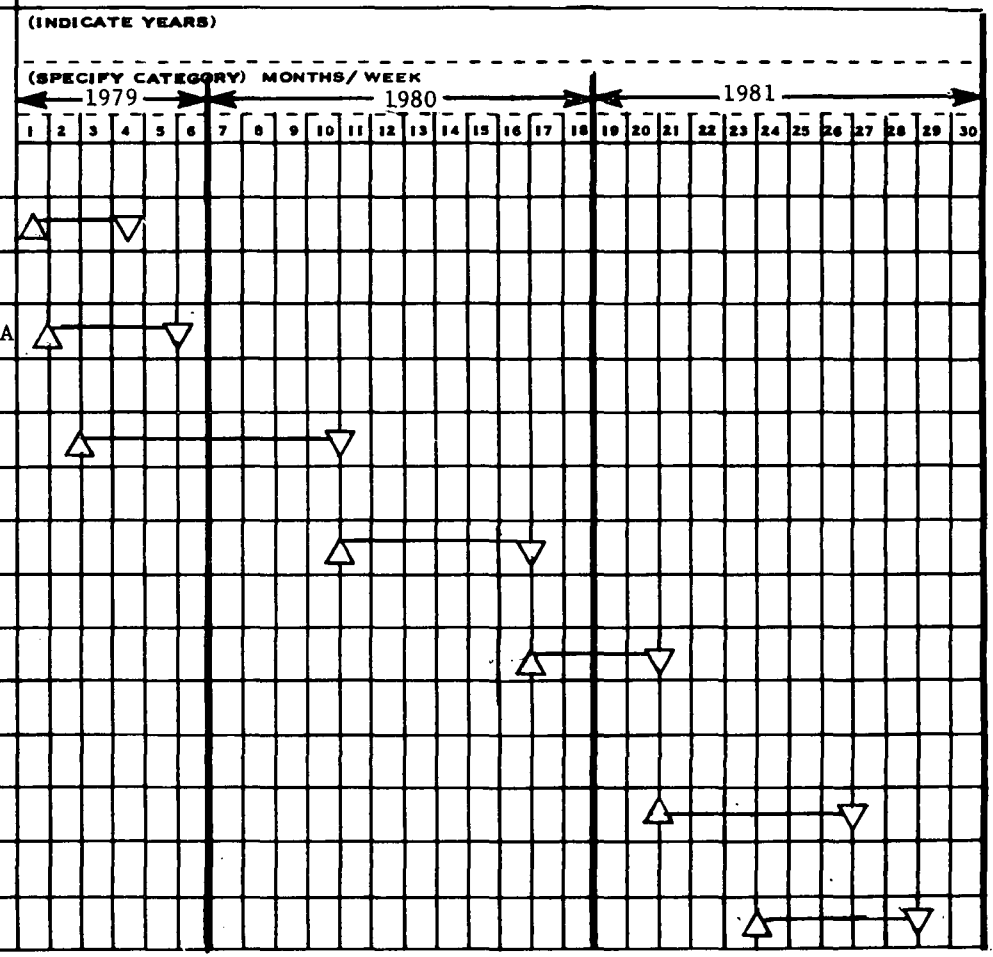

Figure 20-2. Details of Program (Sheet 6 of 6)

After procurement of the components and sub-assemblies, the entire experiment package will be assembled (Subtask 1.4). Then, the entire assembled experiment package will be bench tested to evaluate its primary functions (Subtask 1.5). The device will be de-bugged or modified as may be necessary to meet the operational requirements (Subtask 1.6). After this de-bugging and modification, the system will be given another bench test (Subtask 1.8).

As part of Task 1, a soft physical mock-up will be made (Subtask 1.7) to check out the compatibility of the physical configuration with the interior of the ATL and with the associated equipment.

Task 2 - Key Technology Evaluation

The purpose of this Task is to support Task 1, by evaluation of alternative techniques for performing the key functions: optical-to-optical interface for the candidate input image (Subtask 2.1), spatial frequency filter storage and retrieval (Subtask 2.2) and electro-optical readout of the correlation functions (Subtasks 2.3). It is important that the key optical-to-optical interface device be experimentally evaluated under realistic simulated conditions early in the program.

Task 3 - Landmark Selection

The objective of Task 3 is to select landmarks and to make matched filters for both the simulator and the flight tests. Selection of landmarks (Subtask 3.1) will be based on their availability for realistic ATL missions and also on their favorable distribution relative to the performance of an autonomous navigator. The selection process will also consider various types and sizes of landmarks, as well as probability of viewing degradation as a result of variations in clouds, haze, solar illumination, etc.

Subtask 3.2 will be concerned with the actual fabrication of the matched filters. This will include selection of landmark images from available sources. The matched filters will be compared relative to their performance to allow selection of high-performance filters for use in the subsequent simulation and flight tests.

Task 4 - Demonstration and Evaluation of Demonstration Test Model in Physical Simulator

The objective of Task 4 is to establish the recognition and tracking operation of an integrated experimental package in conjunction with a physical simulator which realistically simulates the dynamics of the orbital viewing conditions.

The initial Subtask 4.1 will confirm the selection of a simulator for these tests, after more fully defining the required characteristics of the simulator.

After the selection of the simulator, a simulation plan will be devised (Subtask 4.2). Then the Test Model will be installed in the simulator and initial check-out of its operation will be made (Subtask 4.3).

After these initial tests the major part of the simulation test program will be performed (Subtask 4.4), involving evaluation of the test model with a range of candidate input images under a variety of realistically simulated viewing conditions. Effects to be considered are variations in illumination level and angle, partial obscuration (or partial truncation) of scene, viewing angle variation, haze and image motion. The result of this evaluation will be a broadly based evaluation of the capability of the test model, configured as an integral device, to function under conditions which more realistically simulate the orbital viewing conditions than would have been possible before.

Subtask 4.5 provides for any modification of the test model that may be indicated as a result of these simulator tests. Tests will continue in the simulator to prove the effectiveness of any modifications which may have been made.

Subtask 4.6 provides an initial opportunity for qualified astronauts to work with the experiment in the form of the test model. It is anticipated that this will provide an opportunity for evaluation of man's role in the man-machine interface under realistic conditions.

Task 5 - Design, Fabrication and Bench Test of Flight Models

Upon successful development of the test model, development of the flight test models would begin. Two identical models would be constructed for purposes of training and back-up, as well as for use in actual experimental flight-test program. These activities would be supported by further evaluation of critical components, selection of landmarks, production of the matched filters as well as by appropriate test-planning functions and detailed cost analysis. The flight test models will be designed to meet all of the environmental and operational-life requirements associated with the ATL flight program. They will also include all the required interface provisions required for their incorporation into the ATL flight vehicle.

This Task includes a detailed design incorporating selected key components (Subtask 5.1), and it includes preparation of detailed drawings for production purposes. The purchase and/or fabrication of components are the functions of Subtasks 5.2 and 5.3. Subtask 5.4 is concerned with the assembly of the flight system, and is followed by a bench testing of both flight test models in Subtask 5.5. As a result of Subtask 5, the equipment will be debugged and modified in any way required to establish its operational performance (Subtask 5.6). This modified equipment will then be subject to further bench tests (Subtask 5.7), as well as environmental and life tests (Subtasks 5.8), in order to establish proof of satisfactory performance prior to the flight-test phase.

Task 6 - Flight-Test Experiment

The primary objective of Task 6 is to successfully conduct the landmark recognition and tracking experiments from satellite orbit on board the ATL. This phase will include detailed flight planning (Subtask 6.1), including details and sequences of events of the flight scenario and the specific functions to be performed by the crew.

After the test of the flight equipment, it will be delivered to NASA for pre-flight check-out and installation in the ATL vehicle. (Subtasks 6.3 and 6.5). During the checkout time the flight qualified equipment will be available for further crew training (Subtask 6.4). Finally, flight tests on-board ATL will be made. (Subtask 6.7), followed by post-flight analysis of data and operational-performance evaluation (Subtask 6.7).

Future Tasks

Upon successful completion of the above-described tasks, the over all program will continue with emphasis on the development and evaluation of a complete autonomous navigation system and other applications of the landmark recognition and tracking technique.

20.2 Material

The major items of material which will be required for each model are:

- Telescope
- HeNe Laser
- Solid State Detector Readout
- Viewing Window
- Object Plane Tracking Mirror and Servo Controls
- Spatial Filters and Storage and Retrieval Component
- Passive Optical Elements of the Coherent System
- Optical-to-Optical Interface Devices
- Solid State Cameras (2) and Monitor
- Supports and Mounts for the Optics
- Command and Control Module
- Housing for the Experiment Package

APPENDIX A

THE APPLICATION OF SPATIAL-FREQUENCY FILTERING TECHNIQUES TO PRECISION AUTONOMOUS SPACE NAVIGATION

This appendix describes an autonomous space navigation system which uses optical spatial filter techniques for automatically recognizing and tracking both known planetary surface features and star fields. The primary navigation constraints utilized are the vector directions to known landmarks measured relative to a stellar reference frame. The technique is applicable to navigation of a wide range of both manned and unmanned spacecraft. It provides high-precision navigation especially for planetary or lunar orbit and also for terminal guidance.

The unique part of the system relates to the spatial-filter method by which the landmarks and the stellar reference directions are recognized and tracked.

Specific features and advantages of the navigation system are:

a. It has greater potential for navigation accuracy than other known autonomous techniques. It can provide primary unsmoothed measured navigation constraints with uncertainties less than 30 meters even in the presence of a high degree of natural obscuration, such as clouds.

b. Recognition by this system eliminates the critical registration problem, a pitfall of conventional "map-matching" techniques.

c. It is completely self-contained and passive and can be adapted to either fully automatic or manually-assisted operation.

d. It can provide recognition and tracking data in either digital or analog form with equal precision for both planetary landmarks and starfields (which can be as low as $\pm$ 10 sec of arc).

e. Laboratory tests on several features of the process have shown signal-to-noise ratios as high as 400:1 for starfields and 250:1 for lunar and planetary features. In most cases, the target area can be as much as 90% obscured and still allow reliable tracking.

f. The use of a light-sensitive fast-response imaging medium permits real-time navigation.

Navigational Concept. - A brief review of some navigational concepts may be helpful. If the angle between a known star reference direction and a landmark having known planetocentric coordinates is measured on board a spacecraft, the spacecraft is known to be located somewhere on a conical locus having the landmark at its vertex. Simultaneous measurement of the angles between two star references and a landmark would correspond to the locus of two intersecting cones or two radial intersecting lines. In practical navigation it is simpler to take measurements between star references and landmarks at successive known times to provide all necessary data.

The data from a continuing sequence of landmark trackings is processed by recursive statistical techniques, such as a Kalman filter, to provide updated estimates of the vehicle's present and future position and velocity state. This approach makes the usually realistic assumption that the vehicle's state estimate can be adequately described in terms of a linearized departure from a nominal vehicle ephemeris. Since the general statistical approach is similar to that described for other space navigation systems, this report covers only the techniques for automatically obtaining constraints by means of spatial filters.

In the present method, obtaining the vector direction of a landmark relative to a stellar frame involves automatic recognition and tracking of both planetary landmarks and stellar reference fields by spatial filter techniques. Since it is desirable to use the same equipment for both functions, a short-period reference is used for determining the orientation of the recognition and tracking system while it is performing, in sequence, these functions of landmark and starfield tracking. This relative angular measurement can be most effectively implemented by means of an intermediate short-period inertial reference.

Usually the computer would have initial approximate state data (based on prior measurements or launch data) which is to be updated. This data should be adequate to permit recognition-filter selection. It will be the function of the optical recognition system to identify the landmark and to provide a recognition signal indicating the location of the landmark in the camera's field-of-view. The direction of the telescopic camera optical axis will, in turn, be obtained by the short-period inertial references mounted on a common frame with the telescopic camera.

In practice, we start with a photographic transparency of the desired information or landmark. When we place this in an appropriate optical system we obtain a modified diffraction image or frequency transformation, which can be photographically recorded. This recording is a spatial filter. It is also possible to produce a diffraction spectrum of the filter and return to the original image. This process of "reconstruction" is possible because the Fourier transform of a transform is the original subject. Thus both the physical apparatus and the mathematical description for obtaining transformations back and forth between the two optical image domains are seen: the conventional image domain and the domain of spatial frequencies. Ideally, all the information of a given scene can be described in either domain.

Those more familiar with electrical or time-varying signals are aware of the advantages of matched filtering to separate and or recognize signals in a background of noise. In the optical analogy, the two-dimensional optical signals are converted to frequencies by the diffraction system and passed through the two-dimensional spatial filter. The correct frequencies pass almost unattenuated while other frequencies are largely suppressed. The transmitted frequencies are then reconstructed to form a normal image which becomes the signal. The leakage of other frequencies reconstruct to produce a "noise" background.

One advantage of pattern recognition in the frequency domain is that an object can be recognized anywhere in the field of view with no requirement for image over-laying or registration. Further, the technique can be mechanized to accommodate rotational misalignment and varying image sizes encountered at different ranges. The spatial filter also provides very exact position information for the landmark in the field of view, which is needed for a precision navigation system.

In all these transformation, recognition and tracking operations it is necessary to operate with a transparency of the image. This transparency can be either a conventional amplitude varying device with opacity variations which produce amplitude modulation of the light, or a surface-deformation or other type of phase varying material which produces phase modulation of the light. Recently developed materials can permit real time operation of the system.

Figure A-1 shows the basic optical layout of a recognition and tracking system. There are three optical "domains":

a) A conventional image domain where the input transparency is located.

b) A frequency domain where the appropriate spatial frequency filter is placed.

c) A second conventional image domain in the output plane where the recognition image appears. Due to the special way the spatial filter (matched filter) was made, the recognition image in every case is a round spot of light rather than an image of the object.

An essential feature of the system is that the position of the image in the frequency domain is independent of the x-y location of the object in the input plane, making it possible for an object to be recognized anywhere in the field. On the other hand, the recognition image position is directly related to that of the object and can be used to determine the location of the landmark.

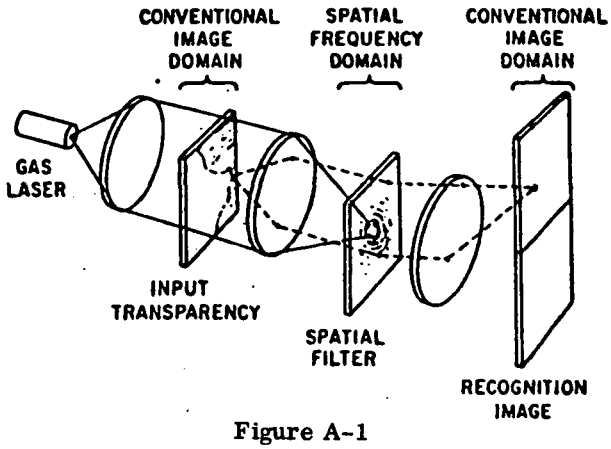

Figure A-1

Making the Spatial Filter - Consider the means for making a spatial filter for an object to be recognized and tracked. One method is the "two-beam" process, (Ref. 34) diagrammed in Figure A-2, which uses a second or reference beam of coherent light to introduce interference fringes; these fringes act as grating-like elements in the filter causing the recognition image to appear as a star-like spot of light off the axis of the optical system.

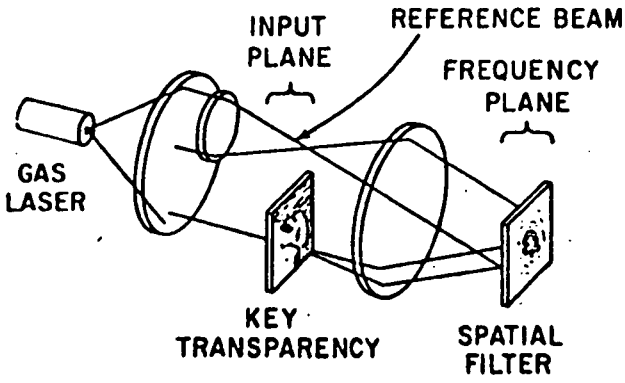

Figure A-2

Experimental Results of Earth Landmark Recognition and Tracking. - A number of features of the proposed system have been tested in the laboratory. General Electric Co. Simulated landmark tracking experiments were conducted via photographs obtained from GEMINI GT-4 and GT-5 flights. The experiments were made with transparencies derived from prints obtained from the United States National Aeronautics and Space Administration and in particular, those showing areas of Arabia, the Nile Valley and Lower California.

Selection of Landmark. - In one series of experiments an input image was used which shows a portion of the high-contrast coast line at the end of the Arabian peninsula. During recognition experiments this landmark gave very good results, although equally good results were obtained by using either much smaller or larger landmarks. Choice of a small valley area within an inconspicuous desert area provided particularly good recognition.

These tests, conducted on several different photographs including some of poorer quality, showed that a conspicuous landmark is not necessary. Any land area containing distinctive detail is satisfactory.

Artificial Generation of Landmark Image. - Tests showed it also possible to use drawings or maps of landmarks as a basis for making spatial filters to recognize areas in these photographs. In general, however, the signal-to-noise ratios obtained were lower than those obtained when a portion of a photograph was used, due to inaccuracy of drawings and omission of details.

Effect of Obscuration on Recognition. - According to present estimates, the earth surface is covered by clouds 70 percent of the time. It was difficult to obtain additional high altitude photographs of areas with different amounts of cloud cover; so cloud cover was simulated by adding cotton wool "clouds" to the photographs. It was found that up to 90 percent of the area of a very good landmark could be covered by clouds with the recognition of the landmark. It was confirmed by tests that if a portion of the landmark appears at the edge of the field-of-view, the landmark will be recognized.

Effect of Obscuration on Tracking. - Several tests were made to determine if partial obscuration of the landmark by clouds or other cover would deviate the "aiming point" or cause a loss of tracking accuracy. In every case the uncertainty was under one part in 1000 of the field-of-view. This corresponds, for example, to uncertainties of less than 11 seconds of arc for a three-degree field-of-view camera system.

Effect of Rotational Misalignment. - A series of tests were conducted to determine the error tolerance permissible in the rotation of the filter in relation to the landmark. Some results can be summarized by stating that if the landmark area is small, relative to the field of view, the tolerance can be large, up to 20 degrees, and if the landmark area is very large, relative to the field of view, the tolerance may be as small as one minute of arc. This variable sensitivity can be as asset. Mechanical means have been developed to rotate the image and peak the output signal to allow additional navigational data to be obtained from vehicle orientation.

Effect of Size Mismatch. - The spatial filter must be made for a landmark at some particular size. If the size as seen by the camera on board the spacecraft is different due to change in altitude or slant range, recognition may not be obtained. A series of tests were made to determine the error tolerance and the reresults were very similar to the rotational tolerance. Size differences up to 15 percent were acceptable for small landmarks, while for very large landmark areas, the tolerance may be less than one percent.

Mechanical means have also been developed for varying the effective size of the image that will cover size variations up to a factor of ten. This sensitivity could also be used to calculate additional navigational data such as altitude or slant range.

Lunar Landmark Tracking. - This discussion relates to several possible missions necessitating realistic future requirements for high-precision self-contained navigation near the moon. One of the major questions related to automatic lunar "landmark" tracking is: Can one devise a spatial filter which will provide recognition and tracking over a wide range of solar illumination angles?

Experiments were conducted that used a series of photos of the same area of the moon shown under different solar angles. One area was Mare Vaporium adjacent to the Sea of Tranquility and was obtained from Reference 35.

In each photo the lighting was different and it may be assumed that the libration and nutation were also slightly different, showing the same area in a somewhat different perspective. It is evident from the photos that the various solar angles significantly affect the apparent landmark geometry. Nevertheless, the ability to devise a single spatial filter to recognize the landmark in every case with a signal-to-noise ratio of 30:1 or greater has been experimentally verified.

Obtaining Stellar References. - Experiments have also demonstrated starfield recognition and tracking. In these experiments starfield "recognition areas" were extracted from images of larger starfields. These "recognition areas" were then converted to spatial filters for use in the recognition and tracking operation. Good results were obtained for thinly-populated as well as for richly populated starfields, for fields containing no bright stars, as well as for ones with bright stars, and for fields containing diffuse nebulosity. Several recognition areas were chosen near the North Celestial Pole, in thinly populated regions of Ursa Major and in densely populated regions of Auriga, containing the galactic equator. Spatial filters were made from areas containing as many as 236 stars or as few as seven stars. These experiments were conducted with silver photographic transparencies of the starfields and with photo-deformable transparencies, with equivalent results. Typical signal-to-noise ratios were 400:1 which indicate very good performance.

As in the case of landmarks, the sensitivity to relative rotation of the starfield and the filter can be varied by choosing an appropriate size recognition area, and the tolerance can be as large as several degrees or as small as a minute of arc. The system can be mechanized to take advantage of this sensitivity and obtain complete three-axis reference signals from one starfield.

Because the inertial reference is used only as a short-period reference, gyros need not be of high performance in terms of drift characteristics. The spatial filter technique can be used to monitor and update a gyro inertial frame which serves as the real-time attitude reference. The gyro can be established without the need for a conventional inertial platform by using high-angular-freedom gyros, the bases of which are attached to the optical system.

Aspect Angle Compensation. - The spatial filter for any landmark is typically made from a near nadir image. If the landmark is viewed from a greatly different angle it will appear foreshortened in one direction and sometimes may not be recognized. The sensitivity to aspect angle is a function of the size of the landmark area, and for typical areas, we have measured tolerances in aspect angle up to 20 degrees from zenith. Still larger variations in aspect angle can be accommodated if optical compensation is used. This can take the form of an anamorphic lens or the same effect can be produced by tilting the object transparency normal to the optical axis. Compensation for aspect angles up to 45 degrees has been obtained and presumably larger angles could be accommodated.

Total System Error. - Since experiments have demonstrated that uncertainties in location of the recognition image, due to various obscuration effects, were typically under 1 part in 1000, electro-optical readout resolution (with a demonstrated point readout resolution of one part in 1000) can be expected to be the primary source (exclusive of mapping errors) of uncertainty in obtaining an unsmoothed navigation constraint. Unsmoothed single measurement constraint uncertainties may typically be in the range of 6 to 12 meters for low altitude satellites.

APPENDIX B

A BRIEF OUTLINE OF RELATED GE EFFORT

The concept of using coherent optical techniques for recognizing and tracking landmarks from space was conceived at General Electric in 1964. A continuous research and development program has been pursued by the Company since that time as outlined in Figure B-1.

The initial concept (Item #1 in Figure B-1) originated at the General Electric Research and Development Center. The early company sponsored activities (Items #1 to #3) were concerned with performance as a function of size and type of landmark, as well as the effect of various factors which tend to degrade performance such as partial obscuration, magnification and various angular mismatches. Beginning in 1967 more emphasis was placed on the use of "real time" input media with initial concentration on the use of photoplastic recording material. In 1968 an investigation was initiated under contract to NASA-Electronic Research Center to pursue a broad investigation of various alternative real time imaging material. Photoplastic recording material continued to be attractive. Later work showed that optically excited liquid crystals also has considerable promise for this function.

Subsequent contracts from NASA were pursued as indicated in Figure B-1 in order to pursue preliminary design of the vehicle borne equipment with emphasis on the starfield recognition and tracking application. This effort was in parallel with continued Company sponsored effort directed at emphasizing the landmark tracking function and determining the limitations of the approach.

FIGURE B-1

GE RESEARCH AND DEVELOPMENT ACTIVITY

RELATED TO

COHERENT OPTICS FOR AUTONOMOUS NAVIGATION

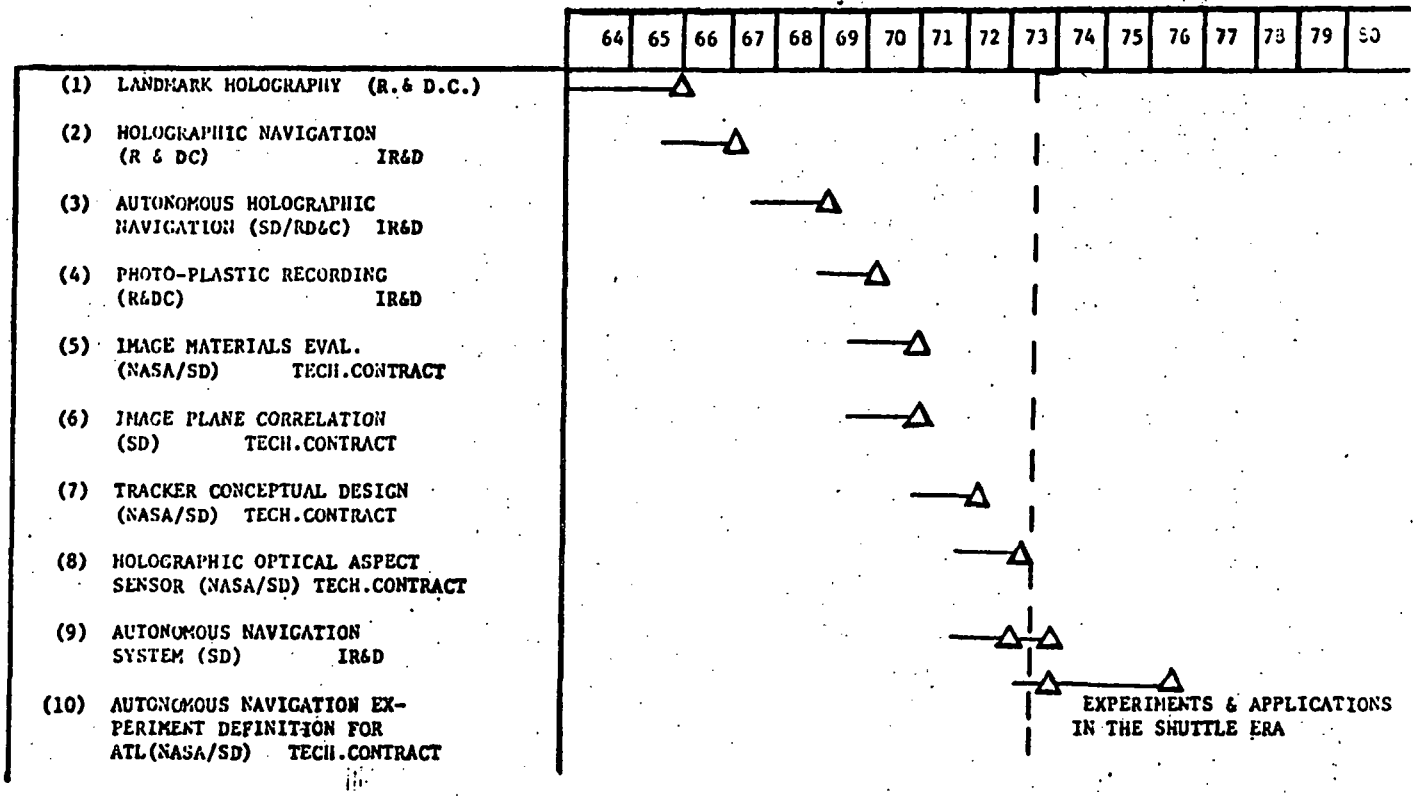

*R. & D.C. indicates GE Research & Development Center (Schenectady).
SD indicates GE Spacecraft Dept. (Valley Forge)

APPENDIX C

REFERENCES

(1) Welch, J. D. and Holeman, J. M., "Autonomous Space Navigation Concepts Utilizing Spatial Filter Techniques, Phase II," GE Report 66-C-199, May 1966.

(2) Holeman, J. M. and Welch, J. D., "Recognition and Tracking of Star Fields by Spatial Filter Techniques," GE Report 66-C-258, Sept. 1966.

(3) Welch, J. D. and Holeman, J. M., "Investigation of Autonomous Space Navigation Concept Utilizing Spatial Filter Techniques," GE Report 66-C-191, Feb. 1966.

(4) U. S. Patent No. 3 636 330 - John M. Holeman and Joseph D. Welch, - "Autonomous Space Navigation Utilizing Holographic Recognition."

(5) Holeman, J. M. and Welch J. D., "The Application of Spatial Filter Techniques to Precision Autonomous Space Navigation," Presented at 17th International Astronautical Federation Meeting, Madrid, October 1966.

(6) Welch, J. D., "Image Media Investigation for Holographic Starfield Mapper," (Final Report for NASA Contract NAS 12-2148), Jan. 1970.

(7) "Study of Shuttle - Compatable Advanced Technology Laboratory (ATL)" by Staff of LaRC Shuttle Experiments Office, NASA TM X-2813, Sept. 1973.

(8) W. L. Brogan, "A Study of Autonomous Orbit Navigation Utilizing Known Land Mark Tracking," Aerospace Corp. Report TOR-1001(2555)-3, Dec. 1966.

(9) Welch, J. D., "Advanced Earth Resources Information System Modeling Investigation," Contract Final Report (NAS 5-23090), General Electric Co., Aug. 1973.

(10) Margerum, J. D., Nimoy, J., Wong S. Y., "Reversible Ultraviolet Imaging with Liquid Crystals," Applied Physics Letters, Vol. 17, No. 2, 15 July 1970.

(11) Feinleib, J.; Oliver, D. S.; "Reusable Optical Image Storage and Processing Device"; Applied Optics; Vol. 11, No. 12, Dec. 1972.

(12) Feinleib, J.; "Optical Processing in Real Time", Laser Focus, September 1973.

(13) Urbach, J., and Meier, R. W.' "Thermoplastic Xerographic Holography," Applied Optics, Vol 5, No. 4, Apr. 1966.

(14) Aftergut, S. and Baitfai, J. J., "Sensitization of PPR Film for Improved Photographic Speed." General Electric Research and Development Center Report 70-C-013, 1970.

(15) Thomas, C. E. and Hall, W. D., "Film Study for a Star Correlator," Final Report of NASA Contract NAS 12-22;2, Feb. 1970.

(16) "Non-Aqueous Silver Halide Rapid Access Photography," Final Report Contract No. DA 36-039, AMC-03711E, Bell and Howell Co., Jan. 1965.

(17) Rayl, G. J., Leccese, F., Final Phase I Report - "Advanced Solid State Multispectral Image System," NASA Contract No. NAS 5-21601.

(18) Femly, R. A., "An Expanding Role for the GaAs Laser, "Optical Spectra, Dec. 1971.

(19) Husain-Abidi, A. S., "On-Board Spacecraft Optical Data Processing, "NASA X711-71-259, June 1971.

(20) Gorstein, M., Hollock J., et al., "Two Approaches to Star Mapping Problem for Space Vehicle Attitude Determination," Applied Optics, March 1970.

(21) Holeman, J. M.; Rayl, G. J.; Welch, J. D.; "Research and Design Study of Holographic Optical Aspect System," Final Report, NASA Contract NAS-5-23148, June 1973.

(22) Welch, J. D., "An Investigation and Conceptual Design of a Holographic Star Field and Landmark Tracker," NASA CR-112143, March 31, 1973.

(23) Foley, W. et al, "Optical-Inertial Space Sextant for an Advanced Space Navigation System," Phase A, Final Report, Contract #NAS2-1087, Jan. 1973.

(24) Compton, R. D., "The Solid State Imaging Revolution," Electro-Optics System Design, April 1974.

(25) Elliott, A., Dickson, J. H., "Laboratory Instruments, Their Design and Application," 2nd Edition, Chemical Publishing Co., N. Y. 1960.

(26) VanderLugt, A., "Operational Notation for Analysis and Synthesis of Optical Data-Processing Systems," Proc. of IEEE, Vol. 54, No. 8, 1966, pp. 1055-1063.

(27) "Optical Matched Filtering Applied to Autonomous Space Navigation," GE Report 946-SW-860, 1970.

(28) Parr, J. Thomas; "Quality Rating of Earth Landmarks"; MIT IL. O. and M. Memorandum No. 99, April 1968.

(29) VanderLugt, A., Applied Optics, Vol. 6, No. 7, July 1967.

(30) Gara, I. A.; Abbott, A.; Hendrickson, H.; "Configuration Studies for Autonomous Satellite Navigation," Aerospace Corp., Report TR 0059 (6784)-1, 28 May 1971.

(31) Schut, G. H.; "Photogrammetric Refraction": Photogrammetric Engineering; pp. 79-86, Vol. 35, No. 1, 1969.

(32) Brown, H. E., "A Study of Landmark Tracker Error Sources," GE Internal Report U - 1J22-HEB-270, Sept. 6, 1973.

(33) "Space Shuttle System Payload Accommodations" - Level II Program Definition and Requirements, Vol. XIV/ NAS JSC Report JSC 07700, Vol. XIV/ Rev. B., Dec. 1973.

(34) VanderLugt, A., "Signal Detection by Complex Spatial Filtering," IEEE Transactions on Information Theory, April 1964, p. 139.

(35) Photographic Lunar Atlas, Univ. of Chic. Press, Ed. by G. P. Kuiper.

(36) "A New Real Time Non-Coherent to Coherent Light Image Converter - the Hybrid Field Effect Liquid Crystal Light Valve." J. Grinberg, A. Jacobson, W. Bleha, L. Miller, Z. Fraas, D. Boswell, G. Myer., Opt. Engin., Vol. 14, No. 3, 217-225, May-June 1975.

(37) T. D. Bearc, W. P. Bleha, S. Y. Wong, "Applied Physics Letters," Vol 22, Page 90 (1973).

(38) W. P. Bleha, J. Grinberg, A. D. Jacobson 1973 SID International Symposium of Technical Papers. Vol. IV (N. Y., N. Y.), page 42 (1973).

(39) A. D. Jacobson, et. al., Pattern Recognition, Vol. 5, page 13, (1973).

(40) P. Nisenson, J. Feinback, R. A. Sprague, S. Iwasa. Characterization and Optimization of an Electro-Optic Imaging Device for Real Time Map Profiling. Final Report, U. S. Army Contract, DAAK02-74-C-0029, December 1974.

(41) J. Feinbeck, D. S. Oliver. Reusable Optical Image Storage and Processing Device. Applied Optics, Vol. II, No. 12, December 1972.